University of Mohamed Boudiaf - M'sila

FACULTY OF TECHNOLOGY

DEPARTMENT OF ELECTRONICS

Numéro de série. . . . . .

Numéro d'inscription: D.ESE/3C/01/21

Thesis

Presented for the Degree of

DOCTORAT LMD

Field : Electronics

Specialty: Electronics of the Embedded systems

THEME

DEVELOPMENT AND IMPLEMENTATION OF AN INTELLIGENT SYSTEM FOR PREDICTING ALZHEIMER'S DISEASE

Presented by

Zakaria MOKADEM

Graduated on::

Before the jury composed of:

Full Name	**Grade**	**Institution**	**Title**
LADJAL Mohamed	President	Professor	University of M'sila
DJERIOUI Mohamed	Supervisor	MCA	University of M'sila
ATTALLAH Bilal	Co-Supervisor	Professor	University of M'sila
OUALI Med Assam	Examiner	MCA	University of M'sila
HAMIDIA Mahfoud	Examiner	MCA	University of USTHB
SAOUDI Kamel	Examiner	Professor	University of Bouira
BRIK Youcef	Guest	MCA	University of M'sila

Academic Year : 2024/2025

Acknowledgements

Praise be to the Almighty God who has given me faith, courage, and patience to carry out this work.

I would like to express my deep gratitude to my supervisor, **Pr. DJERIOUI Mohamed** from M'sila University, for the trust he has placed in me. His constant presence, guidance, modesty, advice, and constructive remarks have been invaluable to the progress of this research.

I also wish to thank **Pr. ATTALLAH Bilal** from M'sila University for supervising me. His guidance, availability, patience, and attentive listening have been crucial throughout the completion of this project.

I am grateful to the esteemed members of the jury: **Pr. LADJAL Mohamed, Dr. OUALI Med Assam, Dr. HAMIDIA Mahfoud, Pr. SAOUDI Kamel, and Dr. BRIK Youcef** for accepting to discuss and evaluate my work.

I would like to extend my thanks to everyone who helped improve my work, and to those who offered valuable feedback that contributed to the refinement of this manuscript.

Finally, I express my sincere gratitude to all those who have, in any way, contributed to the development of this research.

O Allah, send your blessings on your noble messenger, his family, and companions, and bless us in our life.

Dedication

I dedicate this work :

To my Mother May they find here the testimony of my deep gratitude and acknowledgment.

To my wife, my children and all member of my family who give love and liveliness.

To all those who have helped me - directly or indirectly - and those who shared with me the emotional moments during the accomplishment of this work and who warmly supported and encouraged throughout my journey.

To all my friends who have always encouraged me, and to whom I wish more success.

Thanks!

Zakaria MOKADEM

ملخص

مرض الزهايمر هو اضطراب عصبي تنكسي تقدمي والسبب الرئيسي للخرف، ويؤثر في المقام الأول على الأفراد الذين تزيد أعمارهم عن 65 عامًا. يعاني المرضى من انخفاض تدريجي في الوظائف الإدراكية، بما في ذلك الذاكرة والحكم والقدرات الوظيفية. يؤكد الانتشار المتزايد لمرض الزهايمر على الحاجة الملحة إلى طرق تشخيص دقيقة وفعالة بمساعدة الكمبيوتر. في حين تركز معظم دراسات تشخيص مرض الزهايمر على بيانات التصوير العصبي، فإن تكلفتها العالية وإمكانية الوصول المحدودة تحد من استخدامها للسكان الحضريين الذين لديهم مرافق طبية متقدمة، مما يؤدي إلى تحيز محتمل في نماذج التعلم الآلي. بالإضافة إلى ذلك، غالبًا ما يتم تجاهل الأعراض السلوكية والنفسية، والتي تعد بالغة الأهمية لتشخيص مرض الزهايمر. لمعالجة هذه الفجوات، تبحث هذه الدراسة في نهجين تشخيصيين بديلين - التقييمات العصبية النفسية وعلامات البروتين البلازمي - باستخدام تقنيات التعلم الآلي.

في النهج الأول، نقوم بتقييم الأداء التنبئي لنماذج التعلم الآلي باستخدام بيانات التقييم العصبي النفسي التي تم جمعها من خلال أدوات تشخيصية منخفضة التكلفة ومن الدرجة الأولى. يتم تطبيق كل من تقنيات التصنيف الثنائي والمتعدد الفئات لتحليل خمسة تقييمات عصبية نفسية للكشف عن مرض الزهايمر. تسلط النتائج الضوء على إمكانات البيانات العصبية النفسية في التشخيص المبكر لمرض الزهايمر وتؤكد على مزايا الأساليب القائمة على التعلم الآلي في اتخاذ القرارات السريرية.

في النهج الثاني، نستكشف المؤشرات الحيوية لبروتين البلازما لتشخيص مرض الزهايمر. نطبق اختيار الميزات العكسية المتسلسلة (SBFS) وتحليل التباين (ANOVA) لاستخراج البروتينات المهمة من مجموعة بيانات مكونة من 146 بروتينًا بلازميًا تم جمعها من 566 فردًا، بما في ذلك مرضى الزهايمر وضوابط صحية. يتم استخدام خمسة نماذج للتعلم الآلي - شجرة القرار، والغابة العشوائية، والأشجار العشوائية للغاية، وتعزيز التدرج الشديد، وتعزيز التكيف - للتصنيف الأولي، متبوعة بـ XGBoost و AdaBoost للتحقق النهائي.

يوضح كلا النهجين جدوى طرق التشخيص منخفضة التكلفة والمتاحة للكشف عن مرض الزهايمر. توفر التقييمات العصبية النفسية رؤى معرفية وسلوكية قيمة، في حين تقدم المؤشرات الحيوية لبروتين البلازما بديلاً غير جراحي واعدًا للتقنيات التقليدية. وتدعم هذه النتائج دمج الأساليب المعتمدة على التعلم الآلي في تشخيص مرض الزهايمر، مما يمهد الطريق لاستراتيجيات فحص قابلة للتطوير وبأسعار معقولة يمكن أن تفيد عددا أكبر من السكان.

كلمات مفتاحية: مرض الزهايمر، تحليل التباين، المؤشرات الحيوية للدم، التصنيف، الخرف، اختيار السمات، التعلم الآلي، التقييم النفسي العصبي، بروتينات البلازما

Abstract

Alzheimer's Disease (AD) is a progressive neurodegenerative disorder and the leading cause of dementia, primarily affecting individuals over the age of 65. Patients experience a gradual decline in cognitive functions, including memory, judgment, and functional abilities. The increasing prevalence of AD underscores the urgent need for accurate and efficient computer-aided diagnosis (CAD) methods. While most AD diagnostic studies focus on neuroimaging data, its high cost and limited accessibility restrict its use to urban populations with advanced medical facilities, introducing potential bias in machine learning (ML) models. Additionally, behavioral and psychological symptoms, which are critical for AD diagnosis, are often overlooked. To address these gaps, this study investigates two alternative diagnostic approaches—neuropsychological assessments and plasma protein biomarkers—using ML techniques.

In the first approach, we evaluate the predictive performance of ML models using neuropsychological assessment data collected through low-cost, first-line diagnostic tools. Both binary and multiclass classification techniques are applied to analyze five neuropsychological assessments for AD detection. The findings highlight the potential of neuropsychological data in early AD diagnosis and emphasize the advantages of ML-based approaches in clinical decision-making.

In the second approach, we explore plasma protein biomarkers for AD diagnosis. We apply Sequential Backward Feature Selection (SBFS) and Analysis of Variance (ANOVA) to extract significant proteins from a dataset of 146 plasma proteins collected from 566 individuals, including both AD patients and healthy controls. Five ML models—Decision Tree, Random Forest, Extremely Randomized Trees, Extreme Gradient Boosting, and Adaptive Boosting—are used for initial classification, followed by XGBoost and AdaBoost for final validation.

Both approaches demonstrate the feasibility of low-cost, accessible diagnostic methods for AD detection. Neuropsychological assessments provide valuable cognitive and behavioral insights, while plasma protein biomarkers offer a promising non-invasive alternative to traditional techniques. These findings support the integration of ML-driven approaches in AD diagnosis, paving the way for scalable and affordable screening strategies that can benefit a broader population.

Key words: *Alzheimer's disease, ANOVA, Blood biomarker, Classification, Dementia, Feature selection, Machine learning, Neuropsychological assessment, Plasma proteins*

Résumé

La maladie d'Alzheimer (MA) est une maladie neurodégénérative progressive et la principale cause de démence, touchant principalement les personnes de plus de 65 ans. Les patients subissent un déclin progressif des fonctions cognitives, notamment de la mémoire, du jugement et des capacités fonctionnelles. La prévalence croissante de la MA souligne le besoin urgent de méthodes de diagnostic assisté par ordinateur (DAO) précises et efficaces. Alors que la plupart des études diagnostiques de la MA se concentrent sur les données de neuroimagerie, son coût élevé et son accessibilité limitée limitent son utilisation aux populations urbaines dotées d'installations médicales avancées, introduisant un biais potentiel dans les modèles d'apprentissage automatique (ML). De plus, les symptômes comportementaux et psychologiques, qui sont essentiels pour le diagnostic de la MA, sont souvent négligés. Pour combler ces lacunes, cette étude examine deux approches diagnostiques alternatives – les évaluations neuropsychologiques et les biomarqueurs de protéines plasmatiques – en utilisant des techniques d'apprentissage automatique.

Dans la première approche, nous évaluons les performances prédictives des modèles d'apprentissage automatique à l'aide de données d'évaluation neuropsychologique collectées à l'aide d'outils de diagnostic de première intention à faible coût. Des techniques de classification binaire et multiclasse sont appliquées pour analyser cinq évaluations neuropsychologiques pour la détection de la MA. Les résultats soulignent le potentiel des données neuropsychologiques dans le diagnostic précoce de la maladie d'Alzheimer et soulignent les avantages des approches basées sur l'apprentissage automatique dans la prise de décision clinique.

Dans la deuxième approche, nous explorons les biomarqueurs de protéines plasmatiques pour le diagnostic de la maladie d'Alzheimer. Nous appliquons la sélection séquentielle des caractéristiques rétrospectives (SBFS) et l'analyse de la variance (ANOVA) pour extraire des protéines significatives d'un ensemble de données de 146 protéines plasmatiques collectées auprès de 566 personnes, dont des patients atteints de la maladie d'Alzheimer et des témoins sains. Cinq modèles d'apprentissage automatique (Decision Tree, Random Forest, Extremely Randomized Trees, Extreme Gradient Boosting et Adaptive Boosting) sont utilisés pour la classification initiale, suivis de XGBoost et AdaBoost pour la validation finale.

Les deux approches démontrent la faisabilité de méthodes de diagnostic peu coûteuses et accessibles pour la détection de la maladie d'Alzheimer. Les évaluations neuropsychologiques fournissent des informations cognitives et comportementales précieuses, tandis que les biomarqueurs de protéines plasmatiques offrent une alternative non invasive prometteuse aux techniques traditionnelles. Ces résultats soutiennent l'intégration d'approches basées sur l'apprentissage automatique dans le diagnostic de la maladie d'Alzheimer, ouvrant la voie à des stratégies de dépistage évolutives et abordables qui peuvent bénéficier à une population plus large.

Mots clés: *Maladie d'Alzheimer, ANOVA, Biomarqueur sanguin, Classification, Démence, Sélection de caractéristiques, Apprentissage automatique, Évaluation neuropsychologique, Protéines plasmatiques*

Contents

List of Figures

List of Tables

List of Abbreviations

AD:	Alzheimer's Disease
AdaBoost:	Adaptive Boosting
ADNI:	Alzheimer's Disease Neuroimaging Initiative
Aβ:	Amyloid Beta
ANOVA:	Analysis of Variance
AI:	Artificial Intelligence
APP:	Amyloid Precursor Protein
BBB:	Blood-Brain Barrier
CAD:	Computer-Aided Diagnosis
CSF:	Cerebrospinal Fluid
CN:	Cognitively Normal
CAE:	Convolutional Autoencoder
CNN:	Convolutional Neural Network
DL:	Deep Learning
DT:	Decision Tree
FAQ:	Functional Activities Questionnaire
FDG:	Fluorodeoxyglucose
fMRI:	Functional Magnetic Resonance Imaging
GLAM:	General-Linear Active Model
GNB:	Gaussian Naïve Bayes
GCDR:	Global Clinical Dementia Rating
GCN:	Graph Convolutional Network
GDS:	Geriatric Depression Scale
HC:	Healthy Control
KNN:	K-Nearest Neighbors
LDA:	Linear Discriminant Analysis

LR:	Logistic Regression
LSTM:	Long Short-Term Memory
MCI:	Mild Cognitive Impairment
MIRIAD:	Minimal Interval Resonance Imaging in Alzheimer's Disease
ML:	Machine Learning
MMSE:	Mini-Mental State Examination
MRI:	Magnetic Resonance Imaging
MLP:	Multi-Layer Perceptron
NFL:	Neurofibrillary Tangles
NPI-Q:	Neuropsychiatric Inventory Questionnaire
OASIS:	Open Access Series of Imaging Studies
PET:	Positron Emission Tomography
PCA:	Principal Component Analysis
ROC:	Receiver Operating Characteristic
ROI:	Region of Interest
RF:	Random Forest
SBFS:	Sequential Backward Feature Selection
SVM:	Support Vector Machine
VGG:	Visual Geometry Group
XGBoost:	Extreme Gradient Boosting

Chapter 1

Introduction

Alzheimer's disease (AD) is a progressive neurodegenerative disorder and the most common cause of dementia in older adults, accounting for 60–80 of all dementia cases. It leads to irreversible loss of brain cells, causing memory loss, cognitive decline, and a progressive inability to perform daily tasks. The disease progresses through different stages, beginning with short-term memory impairment and difficulty completing daily activities, eventually leading to a complete loss of independence, basic motor skills, and responsiveness to the outside world [1].

1.1 Motivations

Despite decades of research, the early and accurate diagnosis of Alzheimer's remains a challenge. Current diagnostic methods, which include clinical assessments, neuroimaging techniques (such as MRI and PET scans), and biomarker analyses, are often costly, time-consuming, and inaccessible in many regions. Furthermore, by the time clinical symptoms are apparent, substantial and often irreversible brain damage has already occurred. This highlights the critical need for tools that can facilitate earlier detection, enabling timely intervention and potentially slowing the disease's progression.

Advancements in artificial intelligence (AI) and machine learning (ML) have opened new possibilities for improving the diagnosis and prediction of complex diseases like Alzheimer's. Intelligent systems can analyze large and complex datasets, including medical images, genetic information, and clinical records, to identify patterns and predict disease onset with high accuracy. These technologies have the potential to overcome limitations associated with traditional diagnostic methods, making them invaluable in the fight against Alzheimer's

disease.

By leveraging AI, this research seeks to create a robust, efficient, and accessible diagnostic tool to analyze patient data, predict disease progression, and support healthcare professionals in making informed decisions. These studies contribute to advancing diagnostic methodologies and align with global efforts to enhance early detection and management of diseases.

In this context, the proposed research explores the potential of integrating AI-based approaches into Alzheimer's disease prediction, addressing existing gaps, and contributing to developing innovative healthcare solutions.

1.2 Problem statement

Alzheimer's disease is one of the most significant public health challenges of the 21st century, affecting millions of individuals globally. The progressive nature of the disease leads to irreversible cognitive and functional decline. Despite advancements in medical research, the early and accurate diagnosis of Alzheimer's remains a persistent challenge.

Traditional diagnostic methods, such as neuroimaging, and biomarker analysis, are often associated with several limitations. These include high costs, limited accessibility, and dependence on specialized expertise. In addition, by the time symptoms manifest and a diagnosis is made, significant neuronal damage is usually experienced, reducing the effectiveness of available treatment options. Therefore, there is a critical need for cost-effective, scalable, and accurate tools that can facilitate the early detection and prediction of AD.

Recent developments in AI and ML offer a promising solution. However, the integration of these technologies into practical diagnostic systems remains underexplored. Many existing AI-based models for Alzheimer's prediction suffer from issues such as inadequate generalization due to limited datasets, a lack of interpretability, and insufficient validation in clinical settings. These limitations hinder their adoption in real-world healthcare environments. This research aims to develop an intelligent system for accurate and efficient AD prediction, addressing the limitations of existing methods. The system will integrate advanced algorithms to analyze diverse datasets including medical images, genetic data, and clinical records—while ensuring interpretability to support healthcare professionals.

This research aims to fill the gap by designing and implementing an intelligent system that leverages AI to predict AD, thereby contributing to early diagnosis, improved patient outcomes, and enhanced healthcare delivery.

1.3 Objectives of the study

To develop and implement an intelligent system capable of accurately predicting AD, leveraging advanced AI and ML techniques to support early diagnosis and improved clinical decision-making.

Specific objectives

1. **To identify and preprocess relevant data for Alzheimer's prediction:**
    - To collect and integrate diverse datasets such as neuropsychological assessment, blood analysis, and neuroimaging.
    - To perform data cleaning, feature extraction, and selection to improve the model input quality.
2. **To design and develop an AI-based predictive model:**
    - To evaluate and select appropriate machine learning algorithms.
    - To build and optimize robust models for AD detection.
3. **To evaluate the performance of the developed system:**
    - Test the system using various metrics such as accuracy, sensitivity, specificity, and F1 score.
    - Compare the performance of the proposed system with existing diagnostic approaches.
4. **To explore the system's potential for early-stage Alzheimer's detection:**
    - Assess the system's ability to predict Alzheimer's in asymptomatic or mild cognitive impairment stages.
    - Highlight its implications for timely interventions and treatment planning.

By achieving these objectives, the studies aim to advance diagnostic tools for AD and contribute to improved patient outcomes and healthcare efficiency.

1.4 Significance of the study

The development and implementation of an intelligent system for predicting Alzheimer's disease hold profound significance in multiple dimensions, addressing medical and technological.

Medical significance

Alzheimer's disease is a leading cause of dementia, significantly impacting patients' quality of life and placing immense stress on caregivers and healthcare systems. Early and accurate detection is crucial for timely intervention, which may slow disease progression and improve patient outcomes. Our studies contribute to advancing diagnostic methodologies by offering a tool that can identify Alzheimer's in its early stages, potentially before significant cognitive decline occurs. Such advancements can support personalized treatment plans and promote better management of the disease.

Technological advancement

Our studies push the boundaries of AI and ML applications in healthcare. By developing an intelligent system capable of analyzing complex and diverse datasets, the research demonstrates the potential of AI in solving real-world medical challenges. The proposed system could also serve as a model for other AI-based healthcare applications, fostering innovation in medical diagnostics and decision support systems.

Accessibility and efficiency

Traditional diagnostic approaches for Alzheimer's disease, such as neuroimaging and biomarker analyses, are often expensive, resource-intensive, and inaccessible to patients in low-resource settings. The proposed intelligent system aims to provide a cost-effective and scalable alternative, enabling wider access to early diagnosis. This could be especially beneficial in underserved regions, helping bridge gaps in healthcare delivery.

Contribution to scientific knowledge

Our studies contribute to the growing body of research on AI in medicine by addressing existing gaps, such as interpretability, generalizability, and usability of predictive models. By demonstrating the integration of diverse datasets and state-of-the-art algorithms, this research offers insights into best practices for developing AI-driven diagnostic tools.

1.5 Organization of the thesis

This thesis is structured into five chapters, each addressing a specific aspect of the development and implementation of an intelligent system for predicting Alzheimer's disease. The organization is as follows:

Chapter 2: Background of Alzheimer's disease

This chapter provides a comprehensive overview of AD, including its historical background, clinical characteristics, and progression. It explores the underlying pathology of AD, focusing on key neurobiological changes such as amyloid-beta plaques, tau tangles, and neurodegeneration. Additionally, it discusses the different biomarkers used for diagnosis, including neuroimaging techniques, cerebrospinal fluid (CSF) markers, and blood-based biomarkers. This chapter serves as a foundation for understanding the complexities of AD and the challenges associated with its early detection and diagnosis.

Chapter 3: Literature review

This chapter provides a comprehensive analysis of existing research on AD, focusing on current diagnostic methods and their limitations. Explores the role of artificial intelligence, machine and Deep learning in medical diagnostics, focusing on their applications in the detection and prediction of AD. Additionally, the chapter identifies critical gaps in the current body of research, highlighting the challenges and limitations of traditional diagnostic approaches. By doing so, it establishes the rationale for developing an AI-based predictive system for the early and more accurate diagnosis of AD.

Chapter 4: Machine learning algorithms for predicting Alzheimer's disease using neuropsychological data

In this chapter, we compared the performance of nine different ML algorithms—including Logistic Regression (LR), Decision Tree (DT), Random Forest (RF), K-Nearest Neighbors (KNN), Support Vector Machine (SVM), Gaussian Naïve Bayes (GNB), Multi-Layer Perceptron (MLP), eXtreme Gradient Boosting (XGBoost), and Gradient Boosting (GB)—for classifying AD. The classification was based on the results of five neuropsychological assessments: the Geriatric Depression Scale (GDSCALE), Mini-Mental State Exam (MMSE), Global Clinical Dementia Rating (GCDR), Functional Activities Questionnaire (FAQ), and

Neuropsychiatric Inventory Questionnaire (NPI-Q). These neuropsychological questionnaires are commonly used to assess different levels of cognition and are frequently utilized in AD diagnosis.

Chapter 5: Identification of plasma proteins associated with Alzheimer's disease

This chapter aims to use computational algorithms to identify a panel of plasma proteins that can serve as biomarkers for AD detection. We introduce a novel plasma protein panel for the accurate diagnosis of AD using Sequential Backward Feature Selection (SBFS) techniques in combination with five ML models: DT, RF, Extremely Randomized Trees (Extra Trees), eXtreme Gradient Boosting (XGBoost), and Adaptive Boosting (AdaBoost).

Chapter 6: Conclusion

Chapter 6 discusses the results of the studies. It includes a comparison of predictive accuracy with traditional diagnostic methods and an analysis of the system's ability to detect AD. Additionally, the chapter provides a discussion of the findings, addressing both the successes and limitations of the intelligent system, as well as its potential impact on clinical practice.

Chapter 2

Background of Alzheimer's Disease

2.1 Introduction

Alzheimer's Disease is a progressive neurodegenerative disorder and the most common cause of dementia worldwide. It is characterized by cognitive decline, memory loss, and behavioral changes that significantly impact the quality of life of patients. Understanding the pathology of AD is crucial for early detection and effective intervention. This chapter provides an overview of the disease, including its historical background, progression, and clinical manifestations. Additionally, it explores the key pathological hallmarks of AD, such as amyloid-beta plaques, tau neurofibrillary tangles, and neurodegeneration, which contribute to cognitive impairment. Furthermore, the chapter discusses the various biomarkers used for diagnosing AD, including neuroimaging techniques, CSF markers, and blood-based biomarkers. By examining these aspects, this chapter lays the foundation for understanding the complexities of Alzheimer's Disease and the need for improved diagnostic strategies.

2.2 Overview of Alzheimer's disease

Alzheimer's disease was first identified in 1906 by the German neurologist and psychiatrist Alois Alzheimer [2], his photograph is presented in Figure **2.1**. The condition was initially documented in a 51-year-old patient, Auguste Deter, whose family sought medical attention in 1901 due to noticeable changes in her personality and behavior. They reported memory loss, speech difficulties, and impaired comprehension. Dr. Alzheimer diagnosed her with a severe form of dementia, characterized by cognitive, linguistic, and behavioral impairments. Over the next five years, he closely monitored her condition, noting symptoms such as speech

difficulties, agitation, and confusion. After her passing in 1906, Dr. Alzheimer conducted an autopsy, revealing significant cerebral cortex shrinkage, fatty deposits in blood vessels, and degeneration of brain cells. He also identified neurofibrillary tangles (NFL) and senile plaques, which later became key pathological markers of AD [3]. The disease was first mentioned in medical literature in 1907 and officially named after Dr. Alzheimer in 1910. Figure **2.2** shows that AD is the leading cause of dementia.

Figure 2.1: Alois Alzheimer [3].

AD is a progressive neurodegenerative disorder and the leading cause of dementia in older adults, resulting in the irreversible loss of brain cells [4].

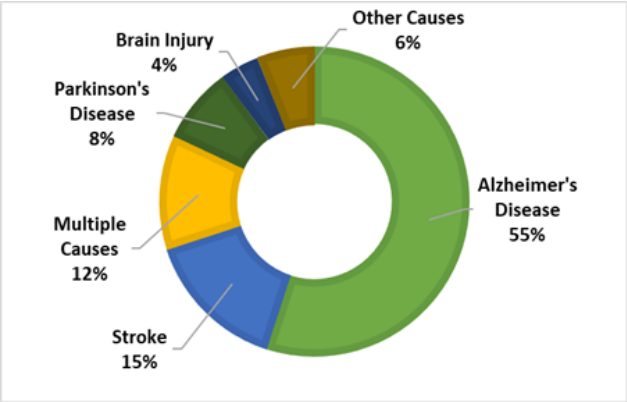

Figure 2.2: Distribution of the causes of dementia [5].

This condition develops gradually over decades, often beginning more than 20 years before noticeable symptoms emerge. The initial phases are marked by memory impairment and disorientation, initially presenting as short-term memory loss and difficulty completing routine tasks. As the disease progresses, individuals struggle to recognize family members and recall personal information, leading to significant behavioral and personality changes. In advanced stages, cognitive decline severely impacts independence, leaving patients entirely reliant on caregivers. Motor functions, such as walking and swallowing, speech abilities are lost, and individuals become unresponsive to their surroundings. In its final phase, patients are bedridden and require continuous care [6, 7].

2.2.1 Pathology of Alzheimer's disease

The hallmark abnormalities in the brains of individuals with AD include neuritic senile plaques and NFL, initially identified by Alois Alzheimer. Additional pathological changes involve neuronal and dendritic loss, neuropil threads, dystrophic neurites, granulovacuolar degeneration, Hirano bodies, cerebrovascular amyloid deposits, and widespread brain atrophy. Notably, similar pathological features are also present in individuals with Down syndrome and, to a lesser extent, in a substantial proportion of cognitively normal elderly individuals. This suggests that some of these individuals may be in the early preclinical stages of AD [8].

In AD, brain atrophy is commonly observed, marked by widened sulci and narrowed gyri. While atrophy tends to be more pronounced in younger patients compared to healthy individuals, the distinction becomes less evident in those aged 70 and older due to considerable overlap in atrophy levels between AD patients and age-matched controls. Consequently, although brain atrophy can be a useful diagnostic marker in younger individuals, it is not a

primary criterion for routine pathological diagnosis. However, in Alzheimer's patients, atrophy is most prominent in the association cortices, resulting in an overall brain size reduction of approximately 8–15% compared to age-matched controls [9].

AD interferes with the three essential processes that maintain neuronal health: communication, metabolism, and repair. This disruption leads to the dysfunction of specific nerve cells in the brain, causing them to lose connections with other neurons and eventually die. The progressive degeneration and loss of these nerve cells result in memory impairment, personality changes, difficulties in performing daily tasks, and other characteristic symptoms of the disease [10]. The brains of AD patients contain an excessive accumulation of two abnormal structures: beta-amyloid plaques and NFL. These abnormalities are particularly prevalent in brain regions associated with memory. Plaques are dense, largely insoluble deposits of protein and cellular debris that accumulate outside and around neurons. Tangles consist of twisted, insoluble fibers that form inside nerve cells. While some plaques and tangles are found in the brains of many older individuals, they are significantly more abundant in AD patients. Although scientists have studied these structures for many years, recent research has provided deeper insights into their composition, formation, and potential role in the progression of AD [4].

2.2.1.1 Amyloid plaques

Amyloid plaques consist of β-amyloid, a protein fragment derived from the amyloid precursor protein (APP). These fragments aggregate and combine with other molecules, neurons, and non-neuronal cells. In AD, plaques primarily form in the hippocampus and regions of the cerebral cortex involved in cognition and decision-making. It remains unclear whether β-amyloid plaques are the direct cause of AD or simply a by-product of the disease process. However, research has established that structural changes in APP can lead to a rare, inherited form of AD [11].

2.2.1.2 From Amyloid precursor protein to β-amyloid

APP is a protein believed to play an important role in supporting neuron growth and survival. APP may also aid in the repair of damaged neurons and promote the growth of neuronal components following brain injury. In AD, an abnormal process leads to the cleavage of APP into smaller fragments, one of which is β-amyloid. These β-amyloid fragments gradually aggregate and form plaques [12].

2.2.1.3 Neurofibrillary tangles

Healthy neurons contain an internal support system, which includes structures known as microtubules. These microtubules function like tracks, facilitating the transport of nutrients and molecules between the cell body and the axon terminals in both directions. The stability of these microtubules is maintained by a protein called tau. In AD, tau undergoes chemical modifications, leading it to bind with other tau molecules and form twisted tangles. As a result, the microtubules break down, disrupting the neuron's transport system. This leads to impaired communication between neurons and, eventually, to the death of the affected cell.

2.2.2 Behaviors and brain changes associated with Alzheimer's disease

The principle cause of AD is still unknown, and it is unclear why age-related changes in the brain become so severe and damaging in those affected. However, significant progress has been made in understanding the progression of the disease and the associated physical and cognitive decline over time. The period from diagnosis to death varies, ranging from as few as three years in individuals diagnosed after the age of 80 to over ten years in younger patients. While the progression of the disease can differ among individuals, the general stages of AD typically follow a similar pattern. AD initially targets the entorhinal cortex, which is closely connected to the hippocampus, a region crucial for the formation of both short-term and long-term memories. Over time, the affected brain regions begin to shrink, with these changes occurring 10 to 20 years prior to any noticeable symptoms. Memory loss typically emerges as the first visible sign, often associated with mild cognitive impairment (MCI), a condition that many researchers consider an intermediate stage between normal aging and AD [5].

As AD advances to the cerebral cortex, memory loss becomes more pronounced, and other cognitive impairments start to emerge. The disease is typically diagnosed during this stage, with symptoms including worsening memory loss, confusion about familiar locations (such as getting lost), difficulty performing daily activities, trouble managing finances and paying bills, poor judgment, and decision-making, reduced spontaneity and motivation, as well as mood and personality changes, including heightened anxiety [13].

At this stage, plaques and tangles start to damage the brain regions involved in memory, language, and reasoning. While physical abilities are typically preserved, individuals begin to have difficulty understanding their environment, and their growing confusion may initially

be mistaken for normal aging. This gradual onset of symptoms can make the recognition of the disease a significant challenge for both patients and their families, often leading to delays in diagnosis and intervention. As AD progresses further within the cerebral cortex, regions responsible for language, thinking, sensory processing, and conscious thought begin to deteriorate. Symptoms progressively worsen and spread, resulting in an increased dependence on caregivers. Behavioral problems, such as agitation and wandering, become more common, making caregiving particularly difficult for families. Key symptoms during this stage include worsening memory loss and confusion, shortened attention span, difficulty recognizing familiar individuals, language impairments (including trouble with reading, writing, and numbers), impaired logical thinking and problem solving abilities, an inability to learn new tasks or adapt to changes, restlessness, anxiety, and emotional distress. Other common issues include hallucinations, paranoia, irritability, loss of impulse control (e.g., inappropriate behavior or undressing in public), and motor difficulties, such as difficulty lifting from a chair.

Disruptions in brain function can result in distressing and seemingly irrational behaviors. For example, a person with AD may refuse to bathe or get dressed, either because they do not understand the request or because they have forgotten how to perform the task. Their frustration and confusion may be expressed through anger. Similarly, an Alzheimer's patient may feel forced to follow a caregiver constantly, driven by fear, as their impaired perception of time and memory makes the world feel unpredictable and threatening. Figure **2.3** illustrates the development of Neurofibrillary Tangles and Amyloid Plaques.

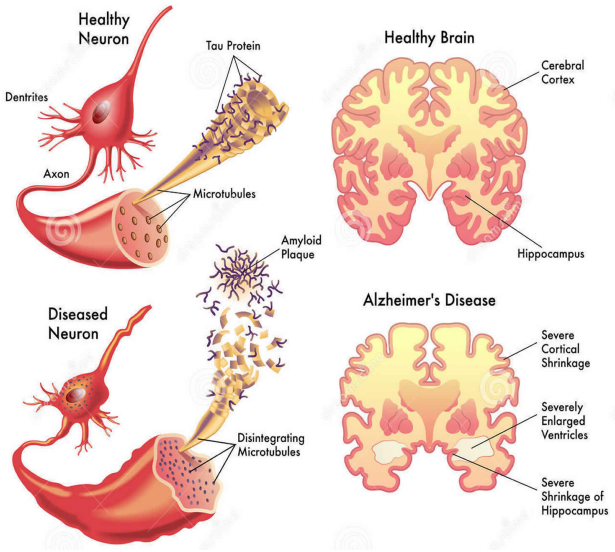

Figure 2.3: Illustration of Brain and Neuron Changes in AD [14].

In the final stage of AD, plaques and tangles have spread throughout the brain, causing significant atrophy. Patients gradually lose the ability to recognize loved ones and communicate, ultimately becoming entirely dependent on caregivers. The sense of self diminishes entirely. Additional symptoms at this stage include severe weight loss, seizures, skin infections, and difficulty with mobility and swallowing [15].

At this stage, patients are typically bedridden and require full-time care. The majority of individuals with AD eventually succumb to complications, such as aspiration pneumonia, which occurs when impaired swallowing causes food or liquids to enter the lungs.

2.2.3 Stages of Alzheimer's disease

Recent studies have identified three stages of AD: the preclinical stage, MCI, and dementia due to AD.

2.2.3.1 Preclinical Alzheimer's disease

At this stage, individuals exhibit detectable changes in the brain, cerebrospinal fluid, and blood biomarkers, indicating the earliest signs of AD. However, they have not yet developed noticeable symptoms such as memory loss. It is also important to note that not everyone with Alzheimer's biomarkers progresses to MCI or dementia, as some biomarkers may remain stable over time.

2.2.3.2 MCI due to Alzheimer's disease

Individuals with MCI exhibit biomarker evidence of brain changes associated with AD, such as increased β-amyloid levels, along with cognitive decline that exceeds normal aging expectations. However, this decline does not substantially impact daily activities [16]. While cognitive changes in MCI may be noticeable to family and close friends, they may not be evident to others. Around 15% to 20% of adults aged 65 and older experience MCI from various causes.

2.2.3.3 Dementia due to Alzheimer's disease

Dementia due to AD is marked by significant memory, thinking, and behavioral impairments that interfere with daily functioning, by signs of brain changes associated with AD. Individuals with dementia appeared a range of symptoms that evolve over the years, corresponding to the progressive damage to nerve cells in different brain regions.

Figure 2.4 illustrates the various brain changes in a patient affected by AD.

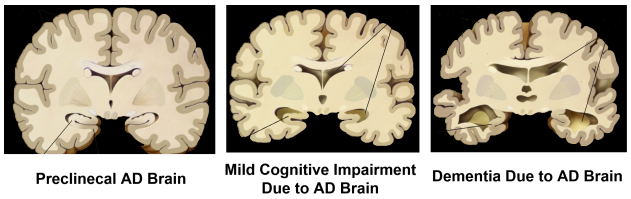

Figure 2.4: Brain changes at different stages of Alzheimer's disease.

2.2.4 Biomarker for diagnosis of Alzheimer's disease

The initial diagnosis of AD relied heavily on cognitive and neuropsychological assessments. However, advancements in neuroimaging, CSF analysis, blood-based tests, and genetic profiling have greatly improved diagnostic accuracy. Understanding these biomarkers can facilitate earlier detection and help optimize treatment strategies.

2.2.4.1 Neuropsychological biomarkers

Neuropsychological assessments are among the first-line diagnostic tools for AD. These tests evaluate a range of cognitive functions, including memory, attention, executive function, language, and visuospatial abilities, which are often affected early in the disease. The decline in cognitive function is a defining characteristic of AD, making these assessments crucial for identifying patients who may be at risk for or already exhibiting signs of the disease.

Several neuropsychological assessments are used to measure the cognition, including:

- **Geriatric Depression Scale (GDS):** This test evaluates symptoms of depression in elderly patients, as depression can sometimes mimic cognitive decline in older adults.
- **Mini-Mental State Examination (MMSE):** This tool measures short- and long-term memory as well as other cognitive functions.
- **Global Clinical Dementia Rating (GCDR):** This scale assesses cognitive and functional abilities to help determine the severity of dementia.
- **Functional Activities Questionnaire (FAQ):** This clinical-report questionnaire measures instrumental activities of daily living (IADLs), providing insights into how dementia affects day-to-day functioning.

- **Neuropsychiatric Inventory Questionnaire (NPI-Q):** This assessment is used to evaluate a range of neuropsychiatric symptoms in individuals with dementia, such as agitation, depression, delusions, hallucinations, and sleep disturbances.

Neuropsychological biomarkers remain an essential component of early diagnosis and clinical evaluation in AD. They provide objective measures of cognitive dysfunction, aiding clinicians in making diagnostic decisions and evaluating disease progression over time [1, 17].

2.2.4.2 Neuroimaging biomarkers

Neuroimaging is essential in diagnosing AD, as it offers visual proof of both structural and functional changes in the brain. Advanced imaging methods enable the detection of early pathological changes, monitor the progression of the disease, and distinguish AD from other neurodegenerative conditions. Three primary imaging techniques—structural MRI (sMRI), functional MRI (fMRI), and Positron Emission Tomography (PET) scans—are commonly used in the diagnosis of AD.

1. **Structural MRI:** sMRI is a powerful tool for assessing brain atrophy, particularly in the hippocampus, a region critical for memory formation. Progressive shrinkage of the hippocampus is a hallmark of AD and serves as an early diagnostic indicator [18].

2. **Functional MRI:** fMRI measures changes in brain activity by detecting blood flow variations. In AD patients, altered connectivity patterns, especially in the default mode network (DMN), provide insights into cognitive decline and disease progression.

3. **PET Scans (Amyloid and Tau Imaging):** PET scans allow for the visualization of amyloid-beta and tau protein accumulation, two key pathological markers of AD. Amyloid PET helps identify plaques, while tau PET imaging detects neurofibrillary tangles, offering critical information for early diagnosis and staging [19].

Figure **2.5** illustrates the neuroimaging modalities for diagnosing AD.

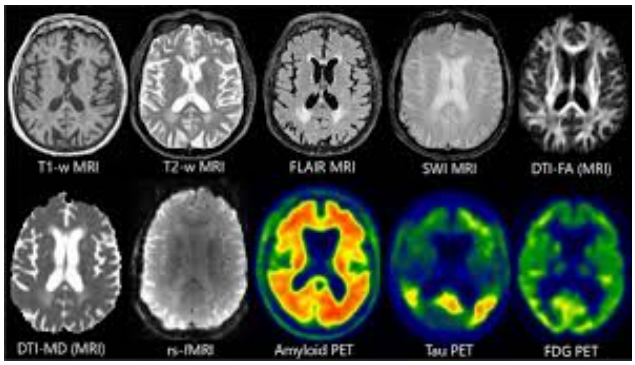

Figure 2.5: Neuroimaging modalities used for diagnosis of AD.

These imaging techniques enhance diagnostic accuracy and are valuable tools in both clinical and research settings. Combining neuroimaging biomarkers with other diagnostic methods improves early detection, monitoring, and treatment development for AD.

2.2.4.3 Cerebrospinal fluid biomarkers

CSF circulates around the brain and spinal cord, which allows it to reflect the biochemical environment of the central nervous system, including the presence of β-amyloid plaques and tau protein tangles.

The ratio of β-amyloid 42 (Aβ42) to β-amyloid 40 (Aβ40) is a key indicator of amyloid accumulation in the brain. Low levels of Aβ42 in CSF are typically seen in individuals with Alzheimer's, reflecting the deposition of amyloid plaques. A decrease in Aβ42 combined with an increase in Aβ40 helps differentiate AD from other neurodegenerative diseases. On the other hand, total tau (T-tau) levels in CSF are elevated in Alzheimer's patients due to neurodegeneration and cell death. Additionally, phosphorylated tau (P-tau), a modified form of tau that forms tangles in the brain, is also elevated in AD. Both T-tau and P-tau serve as indicators of NFL and help assess the severity of the AD [20].

These two CSF biomarkers offer important insights into amyloid and tau pathology, providing biochemical markers of disease progression.

2.2.4.4 Blood-Based biomarkers

Blood-based biomarkers are gaining increasing attention in AD diagnosis due to their non-invasive nature, ease of collection, and potential for large-scale screening. Advances in sensitive detection methods have made it possible to identify key biomarkers in blood that reflect changes occurring in the brain. These biomarkers provide crucial information on β-amyloid

accumulation, tau pathology, neurodegeneration, and neuroinflammation—all hallmarks of AD.

Plasma levels of Aβ and tau are being explored as potential biomarkers for AD. Elevated plasma tau levels, particularly p-tau, correlate with tau pathology in the brain, while plasma amyloid-β levels can reflect amyloid plaque deposition. Neurofilament light chain is a protein released from damaged neurons, and its levels in plasma or serum have been shown to be elevated in AD [21].

Neuroinflammation is a central feature of Alzheimer's pathology, and several inflammatory markers in the blood are being studied for their potential diagnostic value. Proteins such as C-reactive protein (CRP), YKL-40, and interleukins are associated with microglial activation and neuroinflammation, which are prominent in AD. These markers may help assess disease activity and the response to anti-inflammatory treatments.

Blood-based biomarkers offer significant promise in the field of AD diagnosis, providing rapid, low-cost, and minimally invasive methods for identifying the disease in its early stages and monitoring progression over time.

2.2.4.5 Genetic biomarkers

Genetic biomarkers is an important in understanding the genetic basis of AD. Certain genetic variants have been identified as risk factors for AD development, with the APOE ϵ4 allele being the most well known. While genetic testing is not yet a routine part of AD diagnosis, these biomarkers provide critical insights into the susceptibility to Alzheimer's and offer valuable information for understanding individual variations in disease onset and progression [22].

The APOE ϵ4 allele is the strongest genetic risk factor for AD. Individuals who inherit one or more copies of this allele have an increased risk of developing AD, with the risk being greater for those who inherit two copies. The APOE gene encodes a protein involved in lipid metabolism, and the ϵ4 variant is thought to influence amyloid-β aggregation and neuroinflammation, contributing to AD pathology. However, not everyone with the APOE ϵ4 allele will develop AD, indicating that other factors also play a role in disease development. In addition to APOE ϵ4, other genetic mutations are associated with early-onset familial AD [23]. These include mutations in the PSEN1 and PSEN2 genes, which encode components of the gamma-secretase complex involved in amyloid-β production. Mutations in the APP gene, which encodes amyloid precursor protein, also contribute to the development of Alzheimer's by leading to abnormal amyloid-β accumulation. While these mutations are rare, they provide

important clues about the pathophysiology of the disease and the role of amyloid in AD.

Genetic biomarkers, particularly those related to amyloid and tau processing, provide important insights into the genetic underpinnings of AD. They also hold potential for improving personalized medicine approaches by identifying individuals at higher genetic risk, enabling early interventions, and guiding clinical treatment strategies.

2.3 Conclusion

In summary, AD is a complex and progressive neurodegenerative disorder that remains a major global health challenge. This chapter provided an overview of AD, discussing its clinical symptoms, pathological mechanisms, and the biomarkers used for its diagnosis. Despite advancements in understanding AD, early and accurate diagnosis remains difficult due to overlapping symptoms with other forms of dementia and the limitations of current diagnostic tools.

Chapter 3

Literature Review

3.1 Introduction

Alzheimer's disease remains a significant global health concern, driving increasing efforts to enhance its diagnosis and management.

In recent years, there has been a growing focus on developing advanced intelligent systems capable of reliably differentiating individuals with AD and MCI from CN subjects, as well as distinguishing AD from other cognitive dementias that may present similar symptoms [1].

This chapter provides an updated review of the key contributions and emerging trends in the detection and diagnosis of AD using machine and deep learning algorithms. It outlines various techniques used to distinguish different stages of AD and summarizes DL and ML methods and their performance evaluation metrics for AD detection. Additionally, it identifies critical gaps and challenges in the field, underscoring the need for an AI-based predictive system for AD diagnosis.

3.2 Alzheimer's disease databases

3.2.1 Alzheimer's Disease Neuroimaging Initiative Database

The Alzheimer's Disease Neuroimaging Initiative (ADNI) is a large-scale, long-term study aimed at developing clinical, neuropsychological, imaging, genetic, and biochemical biomarkers for the early detection and tracking of AD. The dataset includes MRI (e.g., sMRI, fMRI,...), PET scans (e.g., FDG-PET, Amyloid-PET), neuropsychological assessments (MMSE, GCDR,...), CSF biomarkers (Aβ, Tau), genetic data (APOE genotype, ..), and longitudinal imaging data to monitor disease progression over time [24].

ADNI has evolved through multiple phases, each focusing on different aspects of biomarker development and disease progression.

ADNI-1 (2004-2010) aimed to develop biomarkers as outcome measures for clinical trials, including data on CN, MCI, and AD subjects.

ADNI-GO (2010-2011) introduced early MCI (EMCI) cases to examine biomarkers at earlier stages of the disease.

ADNI-2 (2011-2016) expanded subject groups and imaging techniques while focusing on developing biomarkers as predictors of cognitive decline, incorporating data on CN, EMCI, late MCI (LMCI), and AD.

ADNI-3 (2016-2023) integrates tau PET imaging and functional imaging strategies to enhance clinical trial methodologies, including data on CN, MCI, and AD patients.

ADNI-4, the most recent phase, expands on the study's legacy, striving to enhance the relevance and applicability of ADNI data to North America's diverse population. It supports the development, refinement, standardization, and validation of clinical trial measures and biomarkers for Alzheimer's research. Enrollment for ADNI-4 started in 2023.

3.2.2 Open Access Series of Imaging Studie Database

The Open Access Series of Imaging Studies (OASIS) is a publicly available neuroimaging dataset widely used for research in AD classification, brain aging studies, and deep learning applications in medical imaging. It provides structural MRI scans, along with demographic, clinical, cognitive, and biomarker data, supporting machine learning and deep learning approaches for AD analysis. OASIS consists of both cross-sectional and longitudinal datasets.

OASIS-1 contains T1-weighted MRI scans from 416 individuals aged 18 to 96 years, including cognitively CN and mild to moderate AD subjects. Among them, 100 participants were clinically diagnosed with AD. It provides clinical and demographic data, including MMSE scores and CDR.

OASIS-2 is a longitudinal dataset with 150 subjects aged 60 to 96 years, featuring repeated MRI scans to track brain changes over time, with a focus on cognitive aging and AD progression. Some subjects in this dataset were diagnosed with AD at different points during their participation.

OASIS-3 is a large-scale longitudinal dataset that includes MRI and PET imaging from over 1,000 subjects aged 42 to 95 years. It contains CN, MCI, and AD subjects, with follow-up scans spanning over 30 years. This dataset also provides multimodal biomarkers, including amyloid and tau PET scans, cognitive assessments, and clinical evaluations.

OASIS-4, the newest installment of the OASIS project, focuses on providing free access to neuroimaging datasets for researchers. It includes MRI, clinical, cognitive, and biomarker data from 663 individuals aged 21 to 94, all reporting memory issues [25].

In addition, a subset of OASIS data is available on Kaggle, consisting of 72 subjects diagnosed with mild-to-moderate dementia, extracted from the original dataset. The key features of OASIS include its open access, making it freely available for scientific research, and its longitudinal data, which enables tracking of neurodegenerative changes over time.

3.2.3 Minimal Interval Resonance Imaging in Alzheimer's Disease Database

The Minimal Interval Resonance Imaging in Alzheimer's Disease (MIRIAD) dataset is a publicly available neuroimaging resource designed to facilitate research in AD progression and classification. Developed by University College London (UCL), MIRIAD provides a unique longitudinal dataset with high-frequency MRI scans to track brain atrophy over short time intervals, which is essential for monitoring disease progression and treatment effects. MIRIAD consists of a series of longitudinal volumetric T1-weighted MRI scans from 46 individuals diagnosed with mild to moderate AD and 23 CN controls, totaling 708 MRI scans. Many scans were collected at intervals ranging from 2 weeks to 2 years, conducted by the same radiographer using the same scanner, ensuring consistency in imaging. Unlike other datasets that provide yearly follow-ups, MIRIAD offers short-interval imaging, allowing researchers to observe subtle changes in brain volume over shorter periods [26].

The MIRIAD dataset was specifically designed to investigate the feasibility of using MRI as an outcome measure for clinical trials of Alzheimer's treatments. This makes it particularly valuable for research on longitudinal biomarkers and image analysis, as it provides high-frequency scans to study disease progression in greater detail.

In addition to MRI scans, the dataset includes demographic information such as gender, age, and MMSE scores. MIRIAD is particularly useful for analyzing hippocampal atrophy, a key biomarker of AD progression, and includes expert-annotated hippocampal segmentations, serving as a ground truth for validating computational models.

3.2.4 Australian Imaging, Biomarker, and Lifestyle Flagship Study of Ageing Database

The Australian Imaging, Biomarker, and Lifestyle Flagship Study of Ageing (AIBL) is a large-scale, longitudinal study aimed at identifying biomarkers, imaging markers, and lifestyle factors associated with AD development and progression. Launched in 2006, AIBL is a collaborative initiative between the Commonwealth Scientific and Industrial Research Organisation (CSIRO), Edith Cowan University, the University of Melbourne, the University of Queensland, and several Australian research institutes. It is one of the most comprehensive studies of AD worldwide, providing multimodal data to advance early diagnosis, disease monitoring, and therapeutic interventions.

The AIBL dataset contains MRI, PiB-PET images, and clinical data of more than a thousand participants aged 60 years and older. The dataset includes neuroimaging, genetic, lifestyle, cognitive, and biomarker data collected from a large cohort of participants over extended follow-up periods. It consists of four main groups: CN individuals, Individuals with MCI, AD patients, and Individuals at risk due to genetic or lifestyle factors. AIBL incorporates structural MRI, amyloid PET scans (PiB-PET, Florbetaben, and Flutemetamol PET), CSF biomarkers (Amyloid-beta, Tau, and Phospho-Tau), APOE genotype, and neuropsychological assessments such as the MMSE and the CDR scale. The study also explores lifestyle factors, including diet, sleep, physical activity, and cognitive engagement, to assess their influence on AD risk and progression [27].

AIBL follows participants over multiple years, providing insights into early biomarkers of AD and predictors of cognitive decline. The AIBL dataset is publicly accessible to the research community, enabling collaborations in neuroimaging, genetics, and AI-based medical research.

Among 60 studies collected between 2018 and 2024, 66% utilized the ADNI database, while 22% used the OASIS database.

Figure **3.1** below illustrates the estimated contribution of common AD databases in AD research and Table **3.1** presents a summary of studies categorized by the dataset used for AD diagnosis.

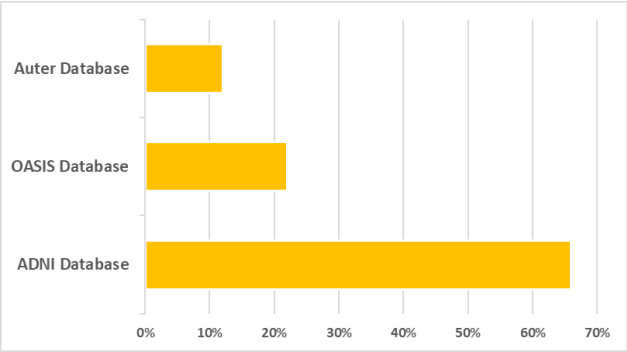

Figure 3.1: Estimated contribution of common AD databases in predicting AD research based on ML (2018–2024).

Table 3.1: Summary of studies categorized by the database used.

Reference	Dataset	Description
[28–48]	ADNI	Alzheimer's Disease Neuroimaging Initiative
[32, 49–54]	OASIS	Open Access Series of Imaging Studies
[55, 56]	MIRIAD	Minimal Interval Resonance Imaging in Alzheimer's Diseas
[57]	AIBL	Australian Imaging, Biomarker, and Lifestyle Flagship Study of Ageing

3.3 Overview of machine and deep learning approaches for AD diagnosis

This section provides a state-of-the-art overview of ML and DL approaches that have been applied to support or improve the accuracy of AD diagnosis. Emphasis is placed on machine and deep learning algorithms, feature selection strategies, and their integration with various types of biomarkers, including neuropsychological assessments, neuroimaging, blood and CSF tests, and genetic information. By reviewing these approaches, we highlight key contributions, current challenges, and existing research gaps.

3.3.1 Neuropsychological-Based AD diagnosis

Neuropsychological assessments play a crucial role in the early detection and diagnosis of AD. These assessments evaluate cognitive functions such as memory, language, attention,

and problem-solving, which are commonly impaired in AD patients. However, most studies do not focus more on analyzing neuropsychological data. Nevertheless, some studies have incorporated it; for example, Francisco J. Martinez-Murcia et al. [40] developed a deep convolutional autoencoder (CAE) for feature extraction, enabling a data-driven decomposition of MRI scans from AD patients. The distribution of the extracted features across neuropsychological data combinations was analyzed and visualized using regression and classification techniques. The imaging-derived markers effectively predicted clinical variables, achieving correlations above 0.6 for neuropsychological evaluation metrics such as MMSE and ADAS11 scores. This approach achieved a classification accuracy exceeding 80% for Alzheimer's disease diagnosis.

Ibrahim Almubark et al. [58] compared the performance of ML models using assessments, a cognitive task, or both. Traditional ML algorithms achieved similar classification performance when using either neuropsychological and/or cognitive data. A multilayer perceptron (MLP) outperformed another algorithms. Specifically, MLP, when trained on a two dataset, achieved 90% sensitivity and 90% specificity. When applied to an independent dataset, the model maintained high specificity (100%), but sensitivity dropped to 66.67%.

Some researchers, including Rohini and Surendran [59], Seshadri et al. [60], and Khan and Zubair [61], proposed a group of supervised ML and DL methods such as Multivariate Linear Regression (MLR), Logistic Regression (LR), Random Forest (RF), and Support Vector Machine (SVM). These methods were applied to a combination of data, including neuropsychological assessments, genetic data, and MRI images, to classify AD patients into distinct stages.

Afreen Khan and Swaleha Zubair [42] developed an ML model using demographic and cognitive data from the ADNI database to create a novel prediction algorithm. Their approach surpassed six machine learning classifier combinations, including LR, Naïve Bayes (NB), SVM, Decision Trees (DT), RF, and XGBoost. In the first experiment, XGBoost, RF, and SVM achieved an accuracy of 89.63%, while in the second experiment, RF alone achieved 93.90% accuracy. The second experiment demonstrated improved classification and overall prediction performance. In the third experiment, which involved hybrid modeling, accuracy increased significantly, with Experiment 1 achieving 90.24% accuracy and Experiment 2 yielding 95.12% accuracy.

Table **3.2** presents a summary of state-of-the-art approaches for AD diagnosis based on neuropsychological data.

Table 3.2: Summary of state-of-the-art approaches for AD diagnosis based on neuropsychological data.

Reference	Method	Data type	Performance
[40]	CAE	MMSE, ADAS11	Acc 80%
[58]	MLP	MMSE, ADAS-Cog, LVF, MoCA, ADAS-Co,NPI,ADL	Sen 90%
[59]	MLR, LR, SVM	MMSE	Acc: 89%, AUC: 0.78
[60]	BiLSTM	MMSE,ADAS	Acc 90.60%
[61]	RF	MMSE, CDR, ASF	Acc 86.84%
[42]	LR, NB, SVM, XGBoost	MMSE, CDR	Acc 93%

3.3.2 Neuroimaging-Based AD diagnosis

Neuroimaging is essential for diagnosing AD by capturing structural and functional brain changes. ML and DL algorithms have been widely applied to MRI, PET, and other imaging modalities to enhance classification accuracy. This section reviews ML and DL approaches that utilize neuroimaging data, for example, Ehsan Hosseini Asl et al. [28] introduced a boosting approach using a 3D-DSA-CNN classifier to predict AD from structural MRI. To enhance feature generalization in detecting AD biomarkers, they applied transfer learning. This involved a three-layered 3D CAE network pre-trained on the CADDementia dataset, combined with the upper layers of a 3D-CNN. Three fully connected layers were added on top of the lower layers to classify 210 subjects from the ADNI dataset. Their findings indicated that hierarchical feature extraction in the hidden layers of the 3D-CNN improved discrimination among AD, MCI, and NC subjects, achieving an accuracy of 99.31% (AD/MCI).

Rieke et al. [62] utilized a 3D convolutional neural network (CNN) with four convolutional layers and two fully connected layers for detecting AD. They applied two occlusion-based visualization methods: occlusion and brain area occlusion, which focus on specific brain regions, and two gradient-based methods: sensitivity analysis and guided backpropagation, which reveal distributed relevance patterns. These techniques help identify problematic areas in brain images associated with the disease.

Shui-Hua Wang et al. [50] proposed a novel DL approach based on transfer learning to detect AD. Brain imaging data were trained and tested using a CNN model consisting of an 8-layer architecture. The proposed model achieved a sensitivity of 97.96%, a specificity of 97.35%, and an accuracy of 97.65%.

Oh et al. [63] employed an unsupervised learning approach using a CAE for AD classification versus CN through dimensionality reduction and the Inception module. They experimented with CNNs trained from scratch, CAE, and ICAE. Additionally, TL was applied to differentiate progressive MCI (pMCI) from stable MCI (sMCI). To identify AD and pMCI classes, they utilized a gradient-based visualization method, specifically the class saliency technique.

Punjabi et al. [64] pre-processed MRI and PET images before applying them to a processing pipeline. Separate CNNs were developed for each imaging modality, as well as a fused model combining both data sources. Diagnosis labels were assigned using categorical cross-entropy as the classification criterion.

Chiyu Feng et al. [65] and Soheil Esmaeilzadeh et al. [29] developed a 3D DL model using MRI and PET for AD diagnosis. The framework proposed by [65] integrates the advantages of 3D-CNN and fully stacked bidirectional long short-term memory (FSBi-LSTM). First, they designed a 3D-CNN architecture to extract deep feature representations from both MRI and PET. Then, they applied FSBi-LSTM to capture hidden spatial information from deep feature maps, further enhancing the model's performance. The method achieved average accuracies of 94.82%, 86.36%, and 65.35% for differentiating AD from normal control (NC), pMCI from NC, and sMCI from NC, respectively.

David S. Cohen et al. [30] utilized DL techniques for multiclass classification of CN, MCI, and AD subjects. They used multi-categorical data, including MRI images, neuropsychological assessment, CSF test, ApoE4 status, and age. Their DL classifier achieved an overall accuracy of 87.197%, while their 1D CNN classifier achieved a similar overall accuracy of 88.275%.

Naimul Mefraz Khan et al. [32] proposed a TL model based on the VGG architecture, leveraging pre-trained weights from large natural image datasets. The model was fine-tuned using layer-wise tuning, where only specific layers were trained on MRI images. Experiments on the ADNI dataset demonstrated that, despite using 10 to 20 times fewer training samples than other methods, their model achieved high classification accuracy: 99.36% for AD vs. NC, 99.20% for AD vs. MCI, and 99.04% for MCI vs. NC.

Saman Sarraf and Ghassem Tofighi [66] proposed a CNN model to classify AD patients. Using the pre-trained architecture (LeNet-5), for classified fMRI data of AD subjects from CN where the accuracy of test data on trained data reached 96.85%.

Yiming Ding et al. [33] developed a DL algorithm to predict the final diagnosis of AD, MCI, or neither, using fluorodeoxyglucose (FDG) PET brain scans. A CNN based on the

InceptionV3 architecture was trained on 90% of the ADNI dataset and tested on the remaining 10%. The algorithm achieved an AUC of 0.98 when evaluated on the independent test set to predict the final clinical diagnosis of AD. It also demonstrated 82% specificity at 100% sensitivity.

Wei Li [34] proposed a DL model called C3D-LSTM, which combines a 3D CNN and an LSTM network. 3D CNNs were used to extract features from a 3D static fMRI images. The extracted feature maps were then fed into the LSTM network to capture the time-varying information in the data. This model leverages the strengths of 3D CNNs for extracting spatial structural information and the advantages of LSTM for processing temporal information. It can directly process 4D fMRI data, fully utilizing both time-varying and structural information for AD detection.

Zhao Fan et al. [35] proposed an SVM model for classifying and predicting different stages of AD based on MRI data. This method aims to assist in the auxiliary diagnosis of the disease. By combining extracted MRI features with the SVM model, more accurate classification and prediction results were achieved. The model demonstrated an impressive classification and prediction accuracy of 100%.

Diego Castillo-Barnes et al. [51] used ML model to analyze three genes in AD. They applied ANOVA and PCA for feature selection and classified subjects with SVM, achieving 72–74% accuracy using PiB PET features. Their findings suggested PSEN1 mutation carriers (PSEN1-MC) form two subgroups, confirmed using k-means clustering. Further classification improved accuracy to 80%, highlighting the heterogeneity of the Dominantly Inherited Alzheimer's Network (DIAN) and the need to treat mutation carriers as distinct groups.

Ahsan Bin Tufail et al. [36] proposed a 2D-CNN to extract features from local brain images. They applied two TL architectures, Inception v3 and Xception, along with a custom CNN incorporating separable convolutional layers to automatically learn generic imaging features for classification. Cross-sectional T1-weighted MRI brain images from the OASIS database were used to ensure consistent size and contrast across different scans.

Atif Mehmood et al. [67] developed a Siamese CNN model, inspired by VGG-16, to classify different stages of dementia. To address the issue of insufficient and imbalanced data, they applied data augmentation techniques. Experiments were conducted on the publicly available OASIS dataset. Using theis approach, they achieved an accuracy of 99.05%.

Farheen Ramzan et al. [68] explored the effectiveness of resting-state functional MRI (rs-fMRI) for multi-class classification of AD and its associated stages, including CN, subjective memory concern (SMC), early-MCI (EMCI), MCI, late-MCI (LMCI), and AD. A longitudinal

cohort of rs-fMRI data from 138 subjects. They investigated DL approaches for AD classification, focusing on the ResNet-18 architecture. By fine-tuning their residual neural network (RNN) model, they achieved improved classification performance for all AD stages, with accuracies of 100% (CN), 96.85% (SMC), 97.38% (EMCI), 97.43% (LMCI), 97.40% (MCI), and 98.01% (AD). In terms of overall performance, their model achieved state-of-the-art results, with an average classification accuracy of 97.92%.

Haibing Guo and Yongjin Zhang [37] introduced the Improved DL Algorithm (IDLA) to analyze brain function using resting-state fMRI (re-fMRI) data. Their method employs an AE network for early AD diagnosis, distinguishing natural aging from disease progression. By integrating biased neural network functionality, IDLA enhances recognition accuracy. It outperformed traditional time-series re-fMRI classifiers, achieving 94.6% sensitivity and 79.8% specificity.

Rashmi Kumari et al. [52] developed a ML approach for AD diagnosis using MRI and a CNN classifier. Their method included noise reduction with a Gaussian filter, image segmentation via Otsu thresholding, edge detection using the Prewitt method, feature extraction with GLCM, and clustering with fuzzy C-means (FCM) before CNN classification. The model achieved 90.25% accuracy and 85.53% sensitivity.

Taeho Jo et al. [69] designed a 3D DL framework using tau PET scans for AD classification. Their 3D CNN model achieved 90.8% accuracy in distinguishing AD from CN individuals through five-fold cross-validation. Additionally, the layer-wise relevance propagation (LRP) model highlighted key brain regions in tau PET images that contributed to classification.

Wei Feng et al. [38] evaluated the performance of 2D-CNN, 3D-CNN, and 3D-CNN-SVM models for AD classification using MRI scans. The 3D-CNN-SVM outperformed the others, achieving 95.74% accuracy in ternary classification (NC, MCI, AD). It also demonstrated superior performance in binary classification, with accuracies of 98.90% (NC vs. MCI), 99.10% (NC vs. AD), and 89.40% (MCI vs. AD). These results highlight the effectiveness of 3D-CNN-SVM in AD diagnosis.

Liu et al. [70] proposed a multi-task CNN designed to automatically extract hippocampus segments and perform disease classification. To enhance feature extraction, they constructed a 3D DenseNet that learns features from 3D patches of hippocampus segments. The extracted features from both the 3D DenseNet and the multi-task CNN for AD classification.

Esther E. Bron et al. [39] compared SVM and CNN models for AD classification using sMRI in a multi-center study. For AD-CN classification with gray matter maps, SVM

achieved an AUC of 0.940, slightly outperforming CNN (0.933). In predicting MCI-to-AD conversion, SVM (AUC 0.756) performed better than CNN (0.742). External validation showed a decline in performance, with SVM and CNN achieving AUCs of 0.896 and 0.876 for AD-CN classification and 0.665 and 0.702 for MCI conversion prediction, respectively.

Fanar E. K. and Al-Khuzaie [53] adopted a DL methodology to differentiate between Alzheimer's patients and healthy individuals using 2D MRI scans. They employed a 2D CNN architecture to optimize deep network weightings. The proposed enhanced network achieved an accuracy of 99.30%.

Qi Li and Mary Qu Yang [41] proposed three ML-based MRI data classifiers to predict AD and identify brain regions contributing to disease development and progression. They developed models based on an SVM, a 3D-VGG, and a 3D-ResNet, respectively, applying a TL strategy. The classification accuracy for distinguishing AD subjects from CN subjects was 90% for SVM, and 95% for both 3D-VGG and 3D-ResNet classifiers.

M. Tanveer et al. [47] proposed a DL architecture named Deep Transfer Ensemble (DTE), trained using TL with the VGG16 model for the classification of AD based on MRI scans. An ensemble of models was trained separately on GM, WM, and CSF datasets. The model achieved an accuracy of 99.05% for the CN vs. AD classification task. For the MCI vs. AD classification, DTE achieved 98.71%.

Nicholas Chedid et al. [71] developed an LR model for a fully automated AD classification process based on resting-state EEG using a low-density channel montage. Their method utilized a fully automated pipeline for data preprocessing and statistically driven feature extraction, resulting in an interpretable machine learning classification model with high accuracy, reaching 81% accuracy.

Ruhul Amin Hazarika et al. [43] utilized a group of DL models (LeNet, AlexNet, VGG-16, VGG-19, Inception-V1, Inception-V2, Inception-v3, ResNet-50, ResNet-101, ResNet50-V2, ResNet152-V2, InceptionResNet, MobileNet, MobileNet-V2, EfficientNet-B0, EfficientNet-B7, Xception, NasNet-A, NasNet-C, and DenseNet-121) for AD classification based on brain MRI images acquired from the ADNI dataset. They modified the DenseNet-121 architecture by replacing the standard convolutional layers with depth-wise convolution layers. The new architecture achieved an average accuracy of 90.22%, demonstrating improved performance.

Andrea Loddo et al. [44] introduced a fully automated deep ensemble approach for dementia-level classification using brain imaging data. Their DL-based framework was designed to detect AD and distinguish dementia stages. The proposed method was trained and evaluated on three MRI datasets and one fMRI dataset with varying features. The model

achieved an average accuracy of 98.51% for binary classification and 98.67% for multiclass classification across the four datasets.

Dong Nguyen et al. [45] proposed an ensemble learning framework that combines DL and ML for AD classification. The DL model was based on 3D-ResNet, while the ML model utilized XGBoost. The framework was applied to brain MRI images, and a 5-fold cross-validation implementation achieved an average AUC of 0.96.

M. Menagadevi et al. [46] proposed an automated prediction system based on a multiscale pooling residual autoencoder (RAE) and SVM for AD detection. The system utilized images from the Kaggle and ADNI datasets. The RAE was used to extract white matter from the brain images, while SVM was used for classification. The model achieved an overall accuracy of 99.77% on the Kaggle dataset and 98.21% on the ADNI dataset for AD classification.

V.P. Subramanyam Rallabandi and Krishnamoorthy Seetharaman [54] developed an Inception-ResNet wrapper model for classifying CN, MCI, and AD using combined MRI and PET scans. They performed 3D tissue segmentation on MRI after skull stripping and fused segmented MR images with PET scans using Fourier and wavelet transforms. The fused dataset was split into training (60%), validation (20%), and testing (20%) for CNN-based classification. The model achieved accuracies of 95.5% (CN vs. MCI), 94.1% (MCI vs. AD), and 95.9% (AD vs. CN).

Romoke Grace Akindele et al. [55] presented a novel hybrid DL framework that integrates both 2D-CNN and 3D-CNN, along with a custom loss function and volumetric data augmentation, to enhance classification performance in AD diagnosis. The results suggest that carefully choosing weighting factors in hybrid predictions is essential for achieving optimal performance. The framework was validated on MRI data from the Kaggle and MIRIAD datasets, achieving accuracies of 98.9% and 99.99%, respectively.

Huan Lao et al. [72] proposed a structural graph CNN method for AD classification based on MRI and PET scans. First, 90 regions of interest (ROIs) from different modal images were used as nodes in the graph to extract positional relationships and specific features of the ROIs, constructing a structural diagram. Then, the model was employed to aggregate the adjacent node features of the structural graph, while a pooling layer was used to obtain graph representations representing different modal image features. Finally, the AD classification diagnosis result was obtained through the softmax layer. Experimental results showed an accuracy of 93.12%, sensitivity of 94.85%, and specificity of 90.42%.

Nitika Goenka et al. [56] employed a DL methodology using T1-weighted MRI images for a binary classification task. They deployed a 3D CNN model and validated it on the

MIRIAD dataset, achieving an accuracy of 97%, surpassing other models. Their study also addressed the challenge of limited datasets for DL models.

Chang-Min Kim and Woobeom Lee [73] developed an ensemble CNN model to classify Alzheimer's stages based on brain shape. They combined a VGG network with a 1D CNN using the Line Segment Feature Analysis (LFA) algorithm, which converts MRI image line segments into feature vectors. These shape-based features were integrated with VGG-extracted features to improve classification accuracy. Evaluated on Kaggle MRI datasets, the model achieved 98.6% accuracy.

Abdul Rehman et al. [48] developed a DL model combining convolution operations, MobileViT-v3, and a Global-Local Attention Module (GLAM) to select both local and global features for AD detection. Using a softened cross-entropy (SCE) function, the model improved sensitivity and specificity by leveraging key diagnostic features. It achieved 92.75% accuracy, 90.80% sensitivity, and 94.14% specificity in classifying MCI and AD.

Chang-Min Kim et al. [74] developed a multimodal model for early Alzheimer's diagnosis, utilizing a depthwise separable convolution block without an activation function to preserve feature integrity. Using multi-model data from ADNI database, including T1-weighted MRI, FDG-PET, Aβ-PET, and tau PET, the model achieved 100% balanced accuracy for AD vs. CN classification and 76% for MCI vs. CN.

Kaya et al. [75] presented an optimized CNNs algorithm for detecting early AD stages from the MRI images using Particle Swarm Optimization (PSO).

Doaa Ahmed Arafa et al [76] proposed a CNN algorithm for AD classification using the MRI images collected by the Kaggle Dataset. The study evaluated two methods: a simple CNN architecture and a fine-tuned VGG16.

Table **3.3** presents summary of state-of-the-art approaches for AD diagnosis based on neuroimaging scans.

Table 3.3: Summary of state-of-the-art approaches for AD diagnosis based on neuroimaging scans.

Ref.	Method	Modality	Performance
[28]	3D-CAE, 3D-CNN	MRI	Acc 99.31%
[62]	3D-CNN	MRI	Acc 77%, AUC 0.78
[29]	3D-CNN	MRI	Acc 94.1%
[50]	3D-CNN	MRI	Sen 97.96%, Spe 97.35% Acc 97.65%
[63]	CAE,CNN	MRI	Acc: 86.60%(AD/CN), 73.95%(AD/MCI)

Ref.	ML Algorithm	Modality	Performance
[64]	CNN	MRI, PET	Acc: 87%(MRI), 85.15%(PET)
[65]	3D-CNN	MRI, PET	Acc: 94.82%(AD/CN), 86.36%(pMCI/NC), 65.35%(sMCI/NC)
[30]	CNN	MRI	Acc 88.75%
[32]	VGG	MRI	Acc: 99.36%(AD/NC), 99.20%(AD/MCI), 99.04%(MCI/NC)
[66]	LeNet5	fMRI	Acc 96.85%
[33]	InceptionV3	FDG-PET	Spe 82%, Sen 100%
[34]	LSTM+3D-CNN	fMRI	Acc:92.11%(AD/MCI), 97.37%(AD/CN), 88.12%(CN/MCI)
[35]	SVM	MRI	Acc 100%
[51]	SVM	PiB PET	Acc 80%
[36]	InceptionV3, Xception	MRI	Acc: 97.92%
[67]	VGG-16	MRI	Acc 99.05%
[68]	ResNet-18	rs-fMRI	Acc 97.88%
[37]	CNN	rs-fMRI	Sen 94.6%,Spe 79.8%
[52]	CNN	MRI	Acc 90.25%
[69]	3D-CNN	tau-PET	Acc 90.8%
[38]	2D-CNN, 3D-CNN, 3DCNN+SVM	MRI	AUC: 99.10%(NC/AD), 98.90%(MCI/NC), 9.40%(MCI/AD)
[70]	CNN	MRI	Acc 88.9%
[39]	SVM, CNN	MRI	AUC: 0.94
[53]	CNN	MRI	Acc 99.30%
[41]	SVM, 3D-VGG, 3D-ResNet	MRI	Acc: 90%(svm), 95%(VGG, ResNet)
[47]	DTE, VGG16	MRI	Acc: 99.05%(VGG), 98.71(DTE)
[71]	LR	EGG	Acc 81%
[43]	DL-Nets	MRI	Acc 90.22%
[44]	DL-Nets	fMRI	Acc: 98.51%(Bin), 98.67(Multi)
[45]	3D-ResNet, XGBoost	MRI	AUC 96%
[46]	RAE+SVM	MRI	Acc 99.77%

Ref.	ML Algorithm	Modality	Performance
[54]	Inception, ResNet	MRI, PET	Acc: 95.5%(CN/MCI), 94.1%(MCI/AD), 95.9%(AD/CN)
[55]	2D-CNN, 3D-CNN	MRI	Acc: 98.9%, 99.99%
[72]	Grph CNN	MRI, PET	Acc: 93.12%
[56]	3D-CNN	MRI	Acc 97%
[73]	VGG	MRI	Acc 98.6%
[48]	MobileViT-v3,	MRI	Acc 92.75%
[74]	CNN	MRI, PET	B-Acc: 100%(AD/CN), 76%(MCI/CN)
[75]	CNN	MRI	Acc 99.53%
[76]	CNN, VGG16	MRI	Acc: 99.53%(CNN), 97.44%(VGG16)

3.3.3 Blood- and CSF-Based AD diagnosis

Blood and CSF tests provide valuable biomarkers for the early detection and diagnosis of AD. ML and DL approaches have been applied to analyze these biomarkers, identifying the significant markers and improving classification accuracy. For example, Thambisetty et al. [77] discovered a panel of 15 plasma proteins that were differentially expressed in AD using the correlation analyses method. while O'Bryant et al. [78] identified a panel with 30 serum proteins with sensitivity of 88%, specificity of 82%, and AUC of 0.91.

Laske et al. [79] used an SVM classifier to identify a panel of three serum markers for AD, achieving 93.8% sensitivity and 80.0% specificity. On the other hand, Llano et al. [80] developed a classifier model and identified four different proteomic signatures with 86.5% sensitivity, 84.2% specificity, and an AUC of 0.85.

Guo et al. [81] applied six algorithms—Linear Discriminant Analysis (LDA), LR, Partial Least Squares (PLS), RF, Nearest Shrunken Centroids (NSC), and SVM—to identify five plasma panels for AD using Statistical Package for the Social Sciences (SPSS) and logistic regression analysis software, achieving 89.36% sensitivity and 79.17% specificity. In addition, Morgan et al. [82] developed a method based on LR to identify a panel of five inflammatory markers in plasma, achieving 84% sensitivity, 70% specificity, and an AUC of 0.79.

Daniel Stamate et al. [83] developed ML models to classify AD and CN individuals using blood metabolites. They applied DL, RF, and XGBoost to metabolite data from 357 subjects (242 CN, 115 AD). The DL and RF models both achieved an AUC of 0.85, while the XGBoost model's AUC was not reported.

Eke et al. [84] and Zhao et al. [85] proposed methods based on SVM and RF machine learning to identify plasma-based biomarkers for early AD detection using feature selection and evaluation modalities. Eke et al. identified a panel of five biomarkers that achieved sensitivity $> 80\%$, specificity $> 70\%$, and an AUC of at least 0.80. Similarly, Zhao et al. identified a panel with 12 serum markers, achieving 90% sensitivity and 66.7% specificity.

Table **3.4** presents a summary of state-of-the-art approaches for AD diagnosis based on blood and CSF tests.

Table 3.4: Summary of state-of-the-art approaches for AD diagnosis based on blood and CSF tests.

Ref.	Method	Data type	Performance
[78]	Statistical method	Serum-protein	Sen 88%, Spe 82%, AUC 0.91.
[79]	SVM	Serum-protein	Sen 93.8%, Spe 80.0%
[80]	ANCOVA	Plasma-protein	Sen 86.5%, Spe 84.2%, AUC of 0.85
[81]	LDA, LR, PLS, RF, NSC, SVM	Plasma-protein	Sen 89.36%, Spe 79.17%
[82]	LR	Plasma-inflammation	Sen 84%, Spe 70%, AUC 0.79
[83]	RF	Blood metabolites	AUC 0.85
[85]	RF	Serum	Sen 90%, Spe 66.7%
[84]	SVM	Plasma-based	Sen 80%, Spe 70%, AUC 0.80

3.3.4 Genetic-Based AD diagnosis

Genetic factors contribute significantly to the development and progression of AD. ML and DL approaches have been increasingly utilized to analyze genetic markers, including APOE genotype and other variants identified through genome-wide association studies (GWAS), to improve early diagnosis and risk assessment. Marwa Mostafa Abd El Hamid et al. [31] developed ML models to identify SNP biomarkers for early AD detection. They applied Sequential Minimal Optimization (SMO), Naïve Bayes (NB), Tree-Augmented Naïve Bayes (TAN), and the K2 learning algorithm to genetic data from ADNI-1 and WGS datasets. Using 500 SNPs selected by a p-value threshold ($p < 0.05$), the NB and K2 models achieved 98% and 98.40% accuracy on ADNI-1 data, and 99.63% and 99.75% on WGS data, respectively.

Karthik Sekaran and Sudha M. [86] analyzed gene expression profiles of AD patients and CN individuals using statistical methods and ML algorithms. Differential gene expression

(DEG) analysis was crucial in selecting the most informative genes. A meta-heuristic global optimization technique, the Rhinoceros Search Algorithm (RSA), was employed to identify 24 novel gene biomarkers—four downregulated and 20 upregulated. Four supervised ML algorithms—SVM, RF, NB, and MLP—were used for classification. The RSA-MLP-NN model achieved 100% accuracy in distinguishing AD-related genes from normal genes, demonstrating its effectiveness. When applied to the reduced dataset, the classifiers achieved accuracies of 87.10% (SVM), 90.32% (NB), 97.66% (RF), and 100% (MLP).

Abhibhav Sharma and Pinki Dey [87] utilized an ensemble of RF and LASSO regression to analyze AD-related microarray data from four brain regions. Their ML approach identified novel genetic biomarkers and developed biologically significant classifiers, achieving an average prediction accuracy of 99%. Key biomarkers included CORO1C, SLC25A46, RAE1, ANKIB1, CRLF3, and PDYN, along with uncharacterized long non-coding RNAs AK057435 and BC037880.

Jessica Binder [88] developed MPxgb(AD), an XGBoost-based model for identifying AD-related genes. The model extracted gene features and was optimized for AD risk prediction. Experimental validation of the top 20 predicted genes highlighted potential AD risk markers, including FRRS1, CTRAM, SCGB3A1, FAM92B/CIBAR2, and TMEFF2. FRRS1 and FAM92B were classified as dark genes, while CTRAM, SCGB3A1, and TMEFF2 were linked to key AD-risk pathways involving TREM2-TYROBP, IL-1β-TNFα, and MTOR-APP, indicating their role in AD pathogenesis.

Nivedhitha Mahendran and Durai Raj Vincent P. M. [89] developed a DL model incorporating an embedded feature selection approach to classify AD patients using DNA methylation data from the GEO Omnibus database. They introduced an Enhanced Deep RNN (EDRNN) and compared its performance to CNN, RNN, and Deep RNN models. Using AdaBoost, they identified key genes associated with 12 CpG sites, including MS4A4A, MYNN, TXNIP, and CORO2B. The EDRNN outperformed the other models, demonstrating superior classification accuracy.

Table **3.5** presents a summary of state-of-the-art approaches for AD diagnosis based on genetic information.

Table 3.5: Summary of state-of-the-art approaches for AD diagnosis based on genetic information.

Reference	ML Algorithm	Data type	Performance
[31]	SMO, NB, TAN, K2	SNP	Acc: 99.63% (NB), 99.75%(K2)
[86]	SVM, RF, NB, MLP	DNA	Acc: 87.10%(SVM), 90.32%(NB), 97.66%(RF), 100%(MLP)
[87]	RF, LASSO	DNA	Acc 99%
[88]	MPxgb	DNA	Genes Identification

3.4 Summary of the literature review

The following table (Table **3.6**) presents a summary of the reviewed literature on ML and DL approaches for Alzheimer's Disease diagnosis. It categorizes studies based on the type of data used, such as neuropsychological assessments, neuroimaging, blood and CSF tests, and genetic information, along with the methodologies and performance outcomes.

Table 3.6: Summary of machine and deep learning techniques for Alzheimer's disease detection.

Ref	**Year**	**Dataset**	**Method**	Modality	Accuracy	AUC	Sensitivity	Specificity
[28]	2018	ADNI	3D-CNN	MRI	94.8%(AD/MCI/NC)	-	-	-
					99.31%(AD/NC)	-	100%	96.63%
					94.2%(MCI/NC)	-	97.15%	91.44%
[49]	2018	OASIS	2D-CNN	MRI	93.18%	-	-	-
[50]	2018	OASIS	2D-CNN	MRI	97.65%		97.96%	97.35%
[29]	2018	ADNI	3D-CNN	MRI	94.1%	-	-	-
					94.82%(CN/AD)	-	-	-
[65]	2019	ADNI	3D-CNN+	MRI+PET	86.36%(CNvspMCI)	-	-	-
			FSBi-LSTM					
					65.35%(CNvssMCI)	-	-	-
			DL			0.85	-	-
[83]	2019	EMIF-AD	RF	Blood metabolic	-	-	0.88	-
			XGBoost			0.85	-	-
[30]	2019	ADNI	ANN	MRI+CSF+APOE4	87.19%(AD/MCI)	-	-	-
			1D-CNN		88.27%	-	-	-
[86]	2019	GSE1297	SVM	Genetic	87.10%	-	-	-
			NB		90.32%	-	-	-
			RF		97.66%	-	-	-
			MLP-NN		100%	-	-	-
[31]	2019	ADNI	NB	Genetic	99.63%	-	-	-
			K2		99.75%	-	-	-
[32]	2019	ADNI	Vgg19	MRI	95.19%(AD/CN/MCI)	-	-	-

Ref	**Year**	**Dataset**	**Method**	Modality	Accuracy	AUC	Sensitivity	Specificity
					99.36%(AD/CN)	-	-	-
					99.20%(AD/MCI)	-	-	-
					99.04%(CN/MCI)	-	-	-
[33]	2019	ADNI	InceptionV3	FDG-PET	-	0.98	-	-
[34]	2020	ADNI	C3d-LSTM	fMRI	92.11%(AD/MCI)	-	-	-
					97.37%(AD/CN)	-	-	-
					88.12%(CN/MCI)	-	-	-
					89.47%(AD/CN/MCI)	-	-	-
[35]	2020	ADNI	SVM	MRI	100%	-	-	-
[58]	2020	Georgetown University	MLP	Neuro- psychological data	-	-	90%	90%
[51]	2020	OASIS	SCNN	MRI	99.05%	-	-	-
[36]	2020	ADNI	ResNet18	fMRI	97.92%	-	-	-
[37]	2020	ADNI	AE+SVM	fMRI	-	-	94.6%	79.8%
[52]	2020	OASIS	CNN	MRI	90.25%	-	85.53%	-
[69]	2020	ADNI	3DCNN	TauPET	90.08%	-	-	-
[38]	2020	ADNI	3D-CNN	MRI	89.76%	-	-	-
			3D-CNN-SVM		95.74%	-	-	-
			2D-CNN		82.57%	-	-	-
[87]	2021	NCBI-GEO	Genetic	-	99%	-	-	-
[39]	2021	ADNI	2D-CNN	MRI	-	0.933	-	-
			SVM			0.94	-	-

Ref	**Year**	**Dataset**	**Method**	Modality	Accuracy	AUC	Sensitivity	Specificity
[53]	2021	OASIS	2D-CNN	MRI	99.305%	-	-	-
[40]	2021	ADNI	CAE	MRI	80%	-	-	-
[41]	2021	ADNI	SVM VGGNET ResNet	MRI	90% 95% 95%	- - -	- - -	- - -
[42]	2022	ADNI	LR+NB+SVM+DT+RF+XGBoost	Psychological data	95.12%	-	-	-
[71]	2022	Local Data	LR	EEG	81%	-	-	-
[43]	2022	ADNI	DenseNet-121	MRI	90.22%	-	-	-
[44]	2022	OASIS, ADNI, KAGGLE	Deep-ensemble Model	MRI and fMRI	98.67%	-	-	-
[45]	2022	ADNI	3D-ResNet +XGBoost	MRI+ Psychological	96%	-	-	-
[46]	2022	ADNI KAGGLE	MSAE+SVM	MRI	99.77% (Kaggle) 98.21% (ADNI)	- -	- -	- -
[47]	2022	ADNI	Deep Transfer Ensemble (DTE)	MRI	99.05%(ADvs CN) 98.71%(MCIvsAD)	- -	- -	- -
[54]	2022	OASIS	Inception-ResNet	MRI+PET	95.5%(MCIvsHC) 94.1%(MCIvsAD) 95.9%(ADvsHC)	- - -	- - -	- - -

Ref	**Year**	**Dataset**	**Method**	Modality	Accuracy	AUC	Sensitivity	Specificity
[55]	2024	KAGGLE MIRIAD	2D-CNN+3D-CNN	MRI	98.9% (KAGGLE) 99.99%(MIRIAD)	- -	- -	- -
[72]	2024		GCN	MRI and FDGPET	93.12%	-	94.85%	90.42%
[56]	2024	MIRIAD	3D-CNN	MRI	97%	-	-	-
[73]	2023	KAGGLE	GGNET+LFA	MRI	96.6%	-	-	-
[48]	2024	ADNI	MobileViT-v3+ GLAM	FDG PET	92.75%(ADvsMCI)	-	90.80%	94.14%
[74]	2024	ADNI	DS-conv, MSC-conv, and SW-conv blocks	MRI+FDG PET+ABPET +TauPET	100%(ADvsCN) 76%(MCIvsCN)	- -	- -	- -

3.5 Research gaps

Most recent studies analyzing data related to AD classification and prediction primarily focus on neuroimaging data, as shown in Figure 3.2, which presents the percentage of each data type from a sample of 60 studies collected between 2018 and 2024. However, collecting such data is not feasible for all Alzheimer's patients due to its high cost and limited accessibility, particularly in certain regions. As a result, studies relying solely on neuroimaging data are often restricted to patients residing in major cities or those with access to advanced medical imaging and analysis facilities. This limitation can introduce significant bias into ML models, favoring these particular patient groups and potentially impacting prediction performance for underrepresented populations.

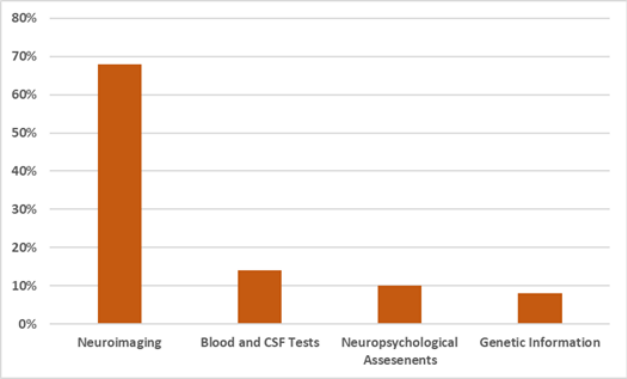

Figure 3.2: Distribution of data types used in AD research.

Moreover, Alzheimer's patients commonly exhibit notable behavioral disturbances and psychological symptoms, which are key features that can assist in diagnosing AD [90]. Nonetheless, many studies have not thoroughly addressed this aspect, with only a few incorporating, at most, one or two neuropsychological assessments. In addition, research on blood and CSF biomarkers associated with AD remains limited.

Our studies seek to address these gaps by analyzing neuropsychological assessments and blood tests, which can be performed using low-cost, first-line diagnostic tools.

3.6 Conclusion

In this chapter, more than 60 research papers published between 2018 and 2024 have been systematically reviewed, discussing their results, identifying research gaps, and analyzing the use of ML and DL in AD prediction. These studies have been examined based on their

use of ML and DL approaches to classify AD using single- and multimodality-based methods. Various biomarkers have been considered, including neuropsychological assessments, neuroimaging data, blood and CSF tests, and genetic information.

Chapter 4

Machine Learning Algorithms for Predicting Alzheimer's Disease Using Neuropsychological Data

4.1 Introduction

Alzheimer's disease is the most common cause of dementia and mainly affects people that have 60 years or older. There are three different stages of AD, early stage, middle stage, and late stage. In the early stage, patients begin to show simple and progressive loss of cognition and memory, with symptoms such as mild forgetfulness and problems with concentration. In the middle stage, as the disease progresses, patients experience trouble remembering events, learning new things, and planning complicated events. In the late stage, patients lose some physical abilities, such as walking, sitting, eating, and speaking [91, 92].

Several machine learning Algorithms in the medical field have been used to analyze medical data and identify patterns that can accurately predict diseases. ML can assist in solving diagnostic challenges across various medical domains and is extensively utilized for disease detection [93]. In this chapter, we compared the performance of nine different ML algorithms including logistic regression, decision tree, random forest, K-Nearest Neighbors, Support Vector Machine, Gaussian Naïve Bayes, Multi-Layer Perceptron, eXtreme Gradient Boost and Gradient Boosting on the classification of AD based on the results of five neuropsychological assessments: Geriatric Depression Scale, Mini-Mental State Exam, Global Clinical Dementia Rating, Functional Activities Questionnaire and Neuropsychiatric Inventory Questionnaire. These neuropsychological questionnaires are commonly used to assess different levels of cog-

nition and they are frequently used for AD diagnosis.

This study aims to propose a robust ML model that accurately predicts AD, helping patients receive timely clinical intervention and avoid delays in diagnosis. Moreover, our work provides valuable insights into the use of ML algorithms as tools for diagnosing AD at a minimal cost. The following list includes some notable contributions:

- To propose methods for addressing the issue of misdiagnosis caused by variability in neuropsychological assessment results, which typically focus on specific brain functions.
- To compare the performance of various types of ML algorithms, including parametric, non-parametric, linear, nonlinear, and ensemble techniques, in predicting AD.
- To develop robust ML models capable of accurately predicting AD.

4.2 Materials and methods

In this section, we describe the procedures and tools used in this work. The dataset is thoroughly detailed, the methods—including nine ML algorithms—are explained, and the performance metrics are presented.

4.2.1 Dataset description

The neuropsychological data used in this study is acquired from the Alzheimer's Disease Neuroimaging Initiative database ADNI [24]. The main objective of ADNI has been to evaluate whether the integration of MRI, PET, biological markers, and neuropsychological assessments can effectively measure the development of the early stage of AD [94]. ADNI provides unlimited access to the database and encourages researchers to use its data to understand the development of AD.

In this work, data collected during ADNI Phase 1 (ADNI-1) were used. The initial dataset contained numerous empty and redundant fields that could affect the classification performance. The dataset was cleaned by removing the non-essential and empty columns. The classes, which were represented by non-numerical values, were transformed into numerical ones to ensure consistency in data processing. The final dataset consisted of 1761 samples, categorized into three groups: 616 Cognitively Normal (CN), 878 Mild Cognitive Impairment (MCI), and 267 Alzheimer's disease (AD). The dataset included five neuropsychological assessments —GDSCALE, MMSE, GCDR, FAQ, and NPI-Q—collected at different time inter-

vals. The age and gender information are included in the dataset. Figure 4.1 illustrates the gender distribution of the subjects, while Table 4.1 presents the demographic information.

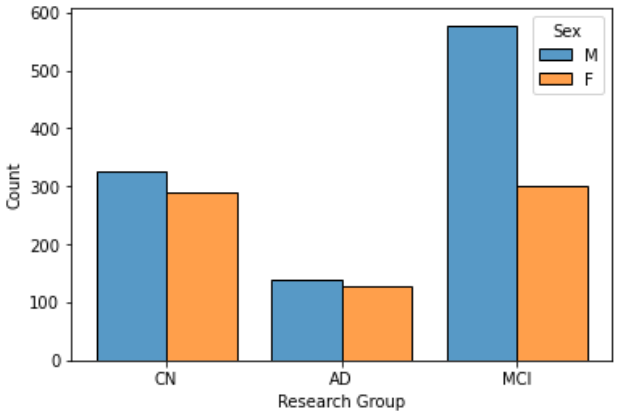

Figure 4.1: Gender distribution of the subjects

Table 4.1: Demographic information of the subjects

Clinical Group	Male	Female	Age (Mean ± Std)
CN	326	290	77.96 ± 6.8
MCI	578	300	76.72 ± 7.0
AD	140	127	77.07 ± 7.6

Table 4.2 provides comprehensive information about the five neuropsychological assessments used, including their purposes and scoring methods.

Table 4.2: Overview of neuropsychological assessments used

Neuropsychological Assessment	Description
GDSCALE	It was used to evaluate the symptoms of depression in elderly patients based on 15 questions.
MMSE	It is an assessment based on a questionnaire used to test cognitive decline. The scale ranges from 0 to 30.
GCDR	It is designed to measure the advancement of Dementia and the progression of dementia, particularly in patients with MCI. The scale for this assessment ranges from 0 to 18.
FAQ	It is used to assess the ability of the patient to perform the usual daily activities independently. The scale ranges from 0 to 30.
NPI-Q	It assesses a range of neuropsychiatric symptoms, including agitation, aggression, anxiety, apathy, depression, disinhibition, irritability, and sleep disturbance. The scale ranges from 0 to 12.

4.2.2 Machine learning classifiers

4.2.2.1 Logistic regression

LR is a linear discriminative method used to solve classification and regression problems. It is primarily employed for binary classification tasks, such as diagnosing a disease based on test results. The LR classifier achieves good accuracy when dealing with linearly separable classes and can be extended to multiclass classification problems. It classifies new samples by measuring the probability of belonging to each class and selecting the class with the highest probability [95]. Unlike linear regression, which predicts continuous values, logistic regression applies the sigmoid function to transform numerical outputs into probabilities. The sigmoid function is defined as:

$$\sigma(z) = \frac{1}{1 + e^{-z}} \tag{4.1}$$

where z is a **linear combination** of the input features and their corresponding weights:

$$z = w_0 + w_1 x_1 + w_2 x_2 + \cdots + w_n x_n \tag{4.2}$$

The sigmoid function maps any real-valued number into a range between 0 and 1, making it ideal for binary classification. The classification decision is based on a threshold (typically 0.5):

- If $\sigma(z) \geq 0.5$, the instance is classified as **1** (e.g., disease present).
- If $\sigma(z) < 0.5$, the instance is classified as **0** (e.g., no disease).

Logistic regression provides a probabilistic framework for classification, meaning it not only makes predictions but also quantifies confidence in the result. This makes it a widely used technique in medical diagnosis, fraud detection, sentiment analysis, and various machine learning applications [96].

4.2.2.2 Decision tree

DT is a hierarchical supervised ML algorithm used for classification and regression tasks. It consists of decision rules that are applied to partition the dataset feature space into subspecies of one class. Building a DT classifier is based on recursively partitioning the feature space of the training set to obtain an optimal set of decision rules that provide the best classification. The node at which the tree begins in a DT is called the" root node", and the node at which the tree ends is called the " leaf node ". An internal node typically branches off into two directions or more, every non-terminal node (i.e., not-leaf node) represents a test node for features, and each branch represents an outcome of the test [97].

Figure 4.2 presents the elements of the decision tree classifier.

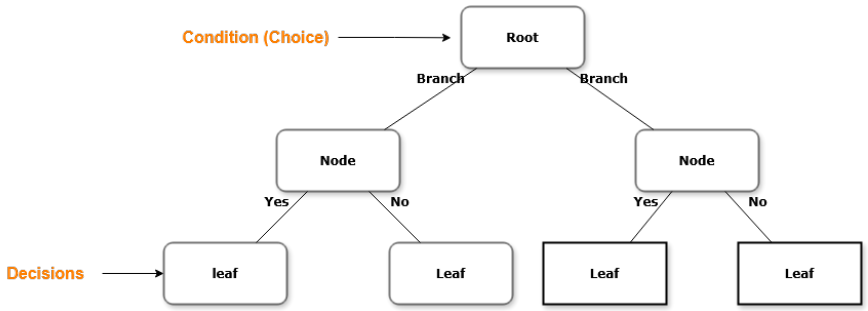

Figure 4.2: Elements of decision tree classifier.

4.2.2.3 Random forest

RF is an ensemble learning algorithm that uses multiple DTs and combines them to improve prediction performance. RF classifier constructs each DT in the ensemble using a bootstrapped sample of the training dataset, where each sample has an equal chance in selection. Additionally, the ensembles are constructed using a sample of data randomly selected from the training dataset with replacement every time. Each tree in the ensemble acts

as an autonomous classifier to determine the class label of an unlabeled instance using an aggregating technique called majority voting, where each classifier casts one vote for its predicted class label. Then the class label with the most votes is used to classify the unlabeled instance [98, 99].

Figure **4.3** presents the architecture of the random forest classifier.

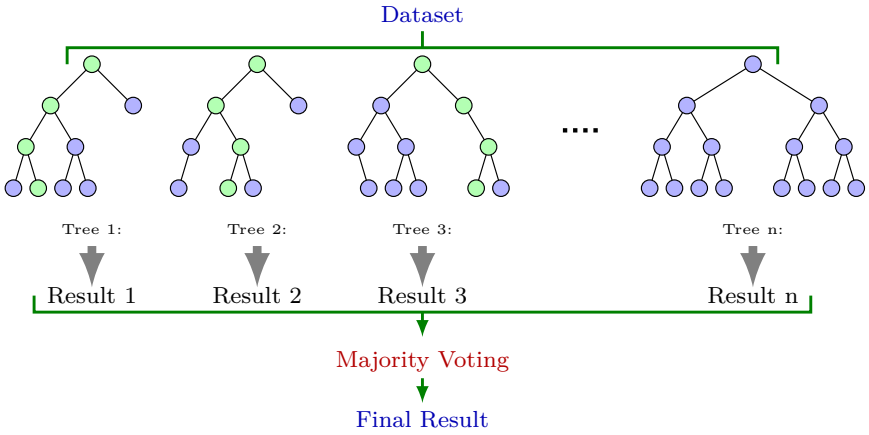

Figure 4.3: Random forest classifier architecture.

4.2.2.4 K-Nearest neighbors

KNN is a cluster analysis technique. However, it is considered the most important and popular classifier. A KNN classifier works by identifying the k closest samples in the training dataset and using them to determine the label of new data based on the majority label among these nearest neighbors [100]. Where k is the number of neighbors based on the similarity in the distance. The optimal value of k chosen is crucial because the small value of k can add noise to the classification process which has an important impact on the classification accuracy, and the big value of k makes computing operations more complex and consumes more time [101]. The Euclidean distance formula is commonly used to calculate the distance between samples [102].

Figure **4.3** illustrates the KNN classification process.

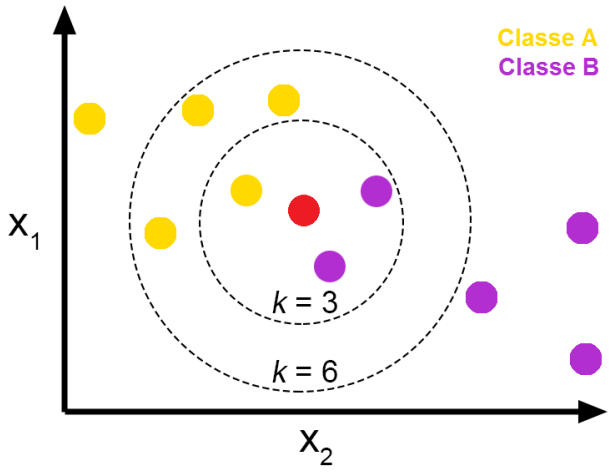

Figure 4.4: Illustration of the K-Nearest neighbors classification.

4.2.2.5 Support vector machine

SVM classifier is a supervised learning technique that aims to create a hyperplane between two classes in a dataset. The hyperplane is positioned in a way that maximizes the distance between the closest labeled instances from each of the classes which permits the classification of new unlabeled instances (i.e., feature vectors) into one of the classes. These closest labeled instances are known as support vectors [103].

when x_i is a feature vectors representation and y_i the classes label of a training compound i. The optimal hyperplane can be defined as: $wx^T + b = 0$, where w is the weight vector, x is the input feature vector, and b is the bias [102]. The w and b would satisfy the following inequalities for all elements of the training set:

$$wx_i^T + b \leq 1, \text{if } y_i = 1$$

$$wx_i^T + b \geq -1, \text{ if } y_i = -1$$

Training an SVM model is aimed to identify the w and b, create a hyperplane that separates the data while maximizing the margin $1/||w||^2$. Figure **4.5** illustrates the SVM classification process.

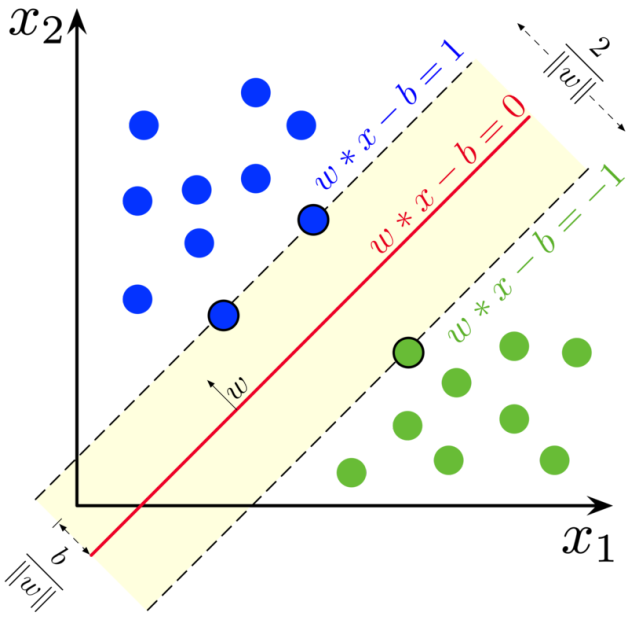

Figure 4.5: Illustration of the hyperplane between two classes in SVM algorithm.

A kernel function can be applied to a nonlinear classification problem to transform the original input feature space into a higher dimensional space. This technique helps to linearly separate the data points by a linear classifier model, which could help to do a fast computation in high dimensional space. The most common kernels are Polynomial, Gaussian, and Radial Basis Function kernels (RBF).

4.2.2.6 Gaussian naïve Bayes

GBN classifier is a probabilistic classifier based on Bayes' theorem. In GNB, each feature in each class is considered an independent variable, and the classification probability for each variable is calculated according to a Gaussian (i.e., Normal) distribution [104]. The classification label is derived from the input using the posterior probability of Bayes' rule.

The posterior probability of Bayesian rule to infer a classification label from input, feature distribution can be defined as the probability of an event X occurring given the probability of another event that has already occurred C and can be expressed as:

$$P(C|X_i) = \frac{P(C).P(X_i|C)}{P(X_i)} \tag{4.3}$$

Where $P(X)$ and $P(C)$ are distributions of the events, X and C, respectively.

For the respective feature set for each class, a mean and standard deviation is calculated

and assume the Likelihood of the features to be Gaussian.The Likelihood is given by:

$$P(X_i|y = y') = \frac{1}{\sigma\sqrt{2\pi}} e^{\left(-\frac{1}{2}\left(\frac{x_i-\mu}{\sigma}\right)^2\right)} \tag{4.4}$$

Where y is a class, x_i is an observation (features), σ is the standard deviation for the selected class, and μ is an associated mean of the class.

Figure 4.6 illustrate the gaussian naïve Bayes classification process.

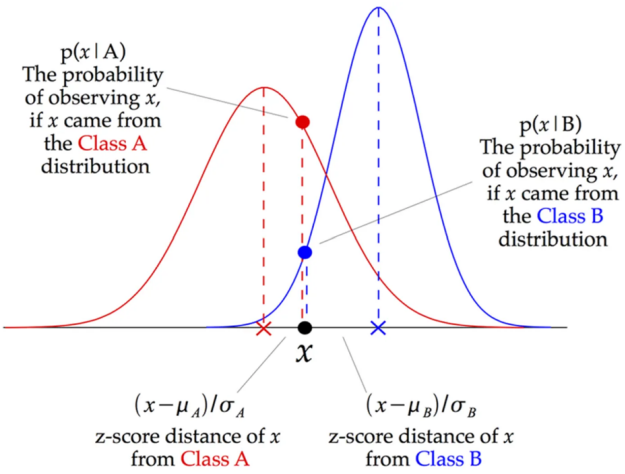

Figure 4.6: Illustration of gaussian naïve Bayes.

4.2.2.7 Multi-layer perceptron

MLP classifier is a type of Artificial Neural Network (ANN). The MLP model is composed of three layers, which are the input layer, the hidden layer, and the output layer [105]. The MLP model processes signals by sequentially computing the output of each layer from the inputs of the preceding layer, propagating the output signal from the input layer to the output layer. During the training process of an MLP model, the error signal —which is the difference between the desired and actual outputs— is propagated backward from the output layer to the inner layers. This backward propagation of the error signal helps optimize the accuracy of the model by repeatedly adjusting the weights and biases until the desired output is achieved. Figure 4.7 presents the connection between the layers in MLP classifier.

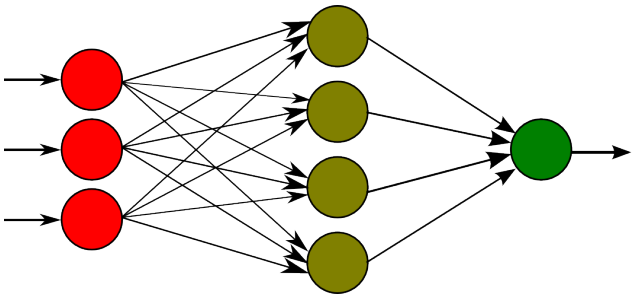

Figure 4.7: Fully connected layers of a multi-Layer perceptron

4.2.2.8 eXtreme gradient boost

XGBoost classifier is an ensemble classifier that uses an iterative process to enhance performance. With this approach, each successive model is trained to correct the errors made by previous models, repeating until further improvement is no longer achievable. This strategy prevents repeated errors across models, strengthening the overall model's accuracy. XGBoost classifier is designed to optimize a specific objective function, which drives it toward more accurate predictions by combining loss and regularization terms. Regularization controls model complexity, reducing overfitting and variance, which helps the model generalize better and results in stable, reliable predictions [106].

4.2.2.9 Gradient boosting

GB classifier follows a stepwise additive model, where weak learners (the Decision Trees models in our case) are added sequentially to the ensemble. Each new learner is trained to correct the errors made by the combined previous models, incrementally improving predictions. The GB algorithm uses gradient descent optimization, adjusting each learner based on the gradient (slope) of the loss function to reduce prediction errors. In this process, each weak learner contributes to minimizing the loss function, which measures the difference between actual and predicted values. By iteratively reducing the residual errors left by previous learners, the ensemble becomes increasingly accurate, as each model minimizes the error across all predictions. However, the iterative nature of adding and adjusting each learner makes this approach computationally expensive [107].

4.2.3 Proposed framework

The nine classifiers (LR, DT, RF, KNN, SVM, GNB, MLP, XGB, and GB) were built by using the models and tools available in scikit-learn based on two steps: The first step involves

training each model individually on each dataset using different hyperparameter configurations to identify the appropriate and optimal hyperparameters. The optimal hyperparameters were selected by the GridSearchCV tuner from the scikit-learn library with 5-fold cross-validation. GridSearchCV uses a predefined set of hyperparameters of the models and exhaustively searches through all possible combinations to find the best combination that produces the highest performance accuracy for each model. The second step involves retraining the models by using the optimal hyperparameters obtained from the first step to confirm the performance results of each algorithm. Finally, the results are compared to select the most robust classifier that achieves the best performance. These two steps were repeated for both modes of classification: binary and multiclass. For the binary classification task, the final dataset was divided into two subsets: CNvsAD and CNvsMCI, while the full dataset, named TriClass, was used for the multiclass classification task. For each classification mode, 80% of each subset was used to train the models, and the remaining 20% was reserved to test the performance of each model. Figure 4.8 illustrates the block diagram of the proposed framework, its main components, and their interactions.

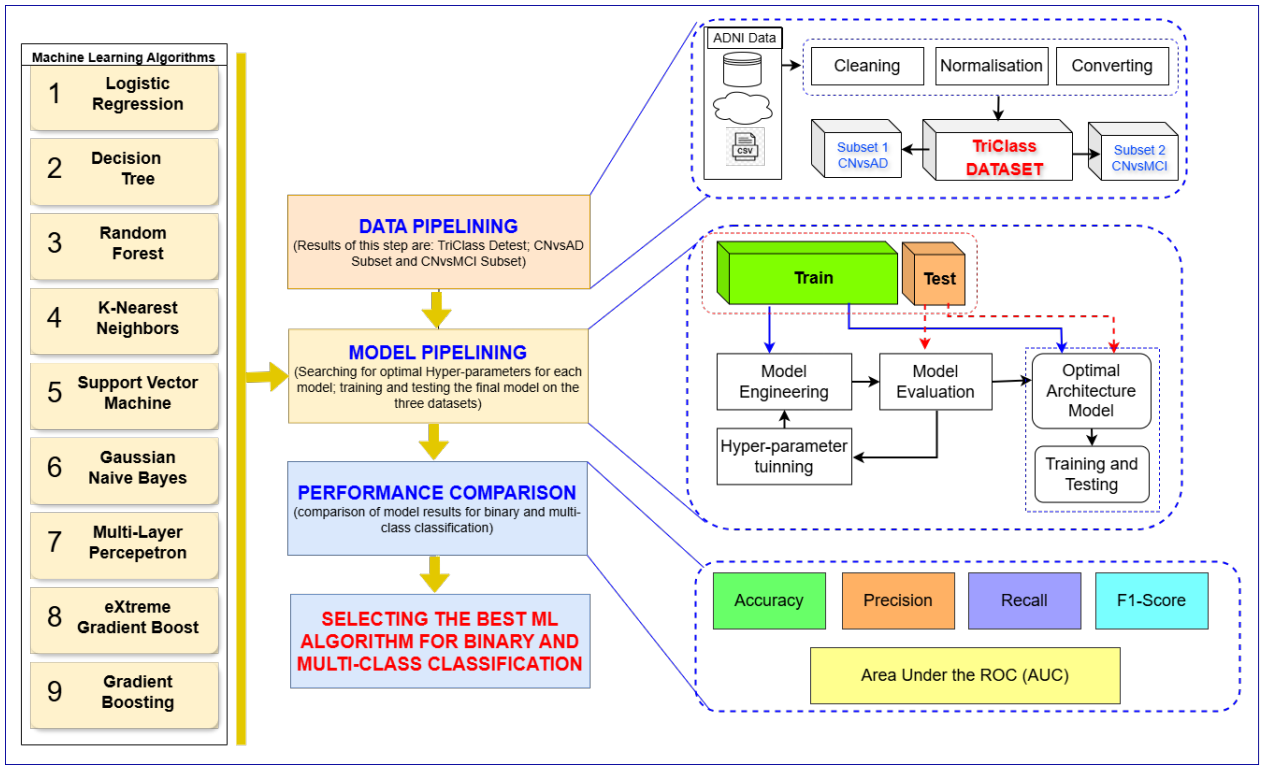

Figure 4.8: Detailed block diagram illustrating the structure of the proposed framework

4.2.3.1 Hyper-parameter optimization

To determine the optimal hyperparameters for the training process we used predefined ranges and trained each model with all possible combinations. The accuracy obtained from training the ML models individually was compared and the hyperparameters that yielded the highest accuracy were selected as the optimal ones. This process was performed for the subsets (CNvsAD and CNvsMCI) for binary classification, and the full dataset (TriClass) used for multiclass classification. The hyperparameter configuration ranges of the models are:

- For the LR model, L1 and L2 Regularization, C parameter, and Solver were tuned.
- For the DT model, we tuned the cost function by utilizing either the Gini index or entropy. Moreover, we adjusted Max-depth, max features, and max-leaf-nodes.
- For the RF model, the Max-depth, max features, max-leaf nodes, and the cost function were tuned.
- For the KNN model, the n-neighbors and distance metrics were adjusted using either Euclidean, Manhattan, or Minkowski metric.
- For the SVM model, we used a different kernel and tuned the value of Gamma and C parameters.
- For the GNB model, we adjusted only Var-smoothing.
- For MLP model, the Hyper-parameters, including the dimensions of the hidden layer, solver, and activation function were tuned.
- For XGBoost model, Max-depth, n-estimators, and the learning-rate hyperparameters were tuned.
- For GB model, we tuned the Max-depth, n-estimators, max-leaf-nodes, and the learning-rate.

4.2.4 Performance metrics

The performance metrics were calculated based on the values of the confusion matrix, which is considered very important for evaluating classification models. The confusion matrix allows to identify the values of True Positives (TP) when the classification model correctly predicts a true target value, False Negatives (FN) when the classification model incorrectly predicts

a false target value, True Negatives (TN) when the classification model correctly predicts a false target value, and False Positives (FP) when the classification model incorrectly predicts a true target value. By using these values from the confusion matrix, the following metrics were calculated for each proposed model:

- **Accuracy:** The accuracy is the ratio of the sum of true cases and the total number of all the cases.

$$Accuracy = (TP + TN)/(TP + TN + FP + FN) \tag{4.5}$$

- **Precision:** The precision is the proportion of the positive cases that were predicted correctly.

$$Precision = TP/(TP + FP) \tag{4.6}$$

- **Recall:** The recall is the proportion of the correctly identified positive cases.

$$Recall = TP/(TP + FN) \tag{4.7}$$

- **F1 Score:** F1 score is calculated as:

$$F1\_Score = (2 \times Precision \times Recall)/(Precision + Recall) \tag{4.8}$$

- **Area Under the ROC (Receiver Operating Characteristic) curve (AUC)**: The AUC is a specific performance metric used to assess the ability of a classification model to distinguish between two classes, ranging from 0 to 1.

4.3 Results

In the following section, we describe the findings obtained in the two steps of the proposed framework, for binary and multiclass classification. We successfully implemented and fitted nine ML models. We split each dataset (CNvsAD, CnvsMCI, and TriClass) into two groups: a training set containing 80% of the total data, which was used to train the ML models, and a testing set containing 20% of the total data, which was used to evaluate the performance of the trained models.

4.3.1 Optimal hyperparameters

The optimal hyperparameters were automatically tuned with the help of the GridSearchCV tuner. Table **4.3** shows the optimal hyperparameters achieved based on the best accuracy.

Table 4.3: Optimal hyperparameters achieved from the first step

ML model	**Optimal hyperparameter**		
	CNvsAD subset	**CNvsMCI subset**	**TriClass dataset**
LR	C=1000; Penality=L1; Solver=liblinear	C=100; Penality=L1; Solver=liblinear	C=1000; Penality=L1; Solver=liblinear
DT	Criterion=gini; max-depth=4; max-leaf=4	Criterion=gini; max-depth=4; max-leaf=2	Criterion=gini; max-depth=4; max-leaf=2

RF	Criterion=gini;
	max-depth=4;
	max-features=auto;
	n-estimators=200
		Criterion=entropy;
		max-depth=9;
		max-features=log2;
		n-estimators=200
			Criterion=gini;
			max-depth=4;
			max-features=auto;
			n-estimators=200

KNN	N-neighbours=20; metric=Manhattan	N-neighbours=7; metric=Manhattan	N-neighbours=14; metric=Manhattan
SVM	C=1000; gamma=1; kernel=RBF	C=1000; gamma=1; kernel=linear	C=1000; gamma=1; kernel=RBF
GNB	Var-smoothing=4.5e-04	var-smoothing=4.9e-06	var-smoothing=3.9e-06

MLP	Learning-rate= adaptive;
	hidden layer=10;
	solver=adam;
	acti. function= tanh
		Learning-rate= adaptive;
		hidden layer=21;
		solver=adam;
		acti. function= sigmoid
			Learning-rate= adaptive;
			hidden layer=40;
			solver=adam;
			acti. function= tanh

XGBoost	Learning-rate=0.001; max-depth=4; n-estimators=200	Learning-rate=0.001; max-depth=2; n-estimators=200	Learning-rate=0.0001; max-depth=4; n-estimators=200

GB	max-depth=2;
	max-leaf=2;
	n-estimators=200
		max-depth=4;
		max-leaf=2;
		n-estimators=200
			max-depth=4;
			max-leaf=2;
			n-estimators=200

4.3.2 Performance comparison

After obtaining the optimal hyperparameters of each model from the first step, we evaluated the overall accuracy of the models by averaging the performance accuracy of each fold of

cross-validation repeated five times. To better visualize the classification performance of proposed models, Figure **4.9** shows the performance accuracy of the ML models performed for the binary classification, while Figure **4.10** presents the model accuracies of multiclass classification.

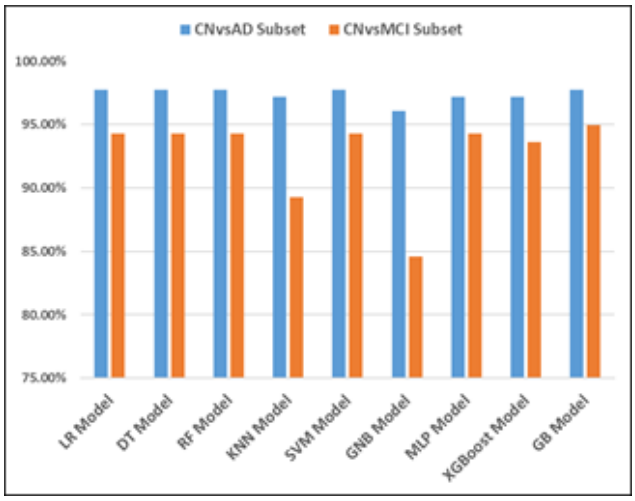

Figure 4.9: Overall accuracies of the nine models trained for binary classification

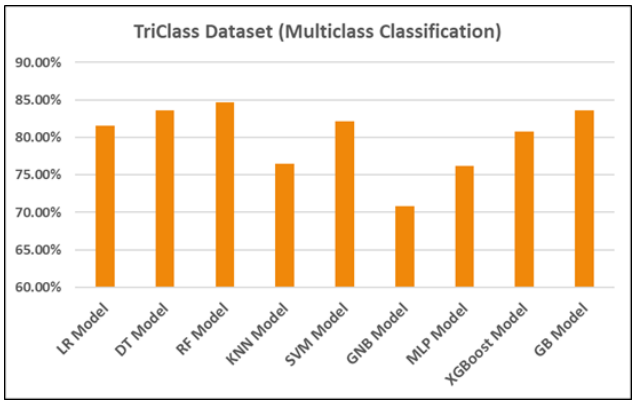

Figure 4.10: Overall accuracies of the nine models trained for multiclass classification

For more details, Tables **4.4** and **4.5** present the performance metrics of the models that use the CNvsAD and CNvsMCI subsets (binary classification). For multiclass classification, Table **4.6** summarizes the performance of the results of the models trained on the TriClass dataset. The tables present several metrics used to evaluate the models' performance, including accuracy, precision, recall, and F1-score.

Table 4.4: Performance metrics of the models trained on ADvsCN subset (binary classification)

Model	Accuracy	Precision	Recall	F1 score
LR	**97.74**%	**95.92**%	**98.48**%	**97.10**%
DT	**97.74**%	**95.92**%	**98.48**%	**97.10**%
RF	**97.74**%	**95.92**%	**98.48**%	**97.10**%
KNN	97.18%	95.00%	98.11%	96.40%
SVM	**97.74**%	**95.92**%	**98.48**%	**97.10**%
GNB	96.05%	93.27%	97.35%	95.03%
MLP	97.18%	95.00%	98.11%	96.40%
XGBoost	97.18%	95.00%	98.11%	96.40%
GB	**97.74**%	**95.92**%	**98.48**%	**97.10**%

Table 4.5: Performance metrics of the models trained on CNvsMCI subset (binary classification)

Model	Accuracy	Precision	Recall	F1 score
LR	94.31%	94.57%	93.67%	94.06%
DT	94.31%	94.74%	93.54%	94.04%
RF	94.31%	94.57%	93.67%	94.06%
KNN	89.30%	88.75%	89.56%	89.05%
SVM	94.31%	94.41%	93.80%	94.08%
GNB	84.62%	84.42%	85.60%	84.45%
MLP	94.31%	94.97%	93.67%	94.06%
XGBoost	93.65%	93.58%	93.23%	93.40%
GB	**94.98**%	**95.45**%	**94.23**%	**94.74**%

Table 4.6: Performance metrics of models trained on TriClass dataset (multiclass classification)

Model	Accuracy	Precision	Recall	F1 score
LR	81.59%	76.18%	74.00%	74.88%
DT	83.57%	79.65%	**78.97**%	79.28%
RF	**84.70**%	**82.11**%	78.65%	**80.06**%
KNN	76.49%	73.21%	72.81%	72.61%
SVM	82.15%	77.74%	72.79%	74.38%
GNB	70.82%	68.10%	69.66%	67.45%
MLP	76.20%	73.95%	74?63%	73.45%
XGBoost	80.74%	79.08%	77.02%	77.96%
GB	83.57%	79.78%	77.39%	78.40%

The experimental results of the performance comparison of LR, DT, RF, KNN, SVM, GNB, MLP, XGBoost, and GB classifiers showed that, for binary classification using the CNvsAD subset, the LR, DT, RF, SVM, and GB models achieved the highest accuracies among all models, with a score of 97.74%. The MLP, XGBoost, and KNN classifiers followed closely behind with accuracy scores of 97.18%. In contrast, the GNB classifier showed the lowest accuracy among all models, with an overall score of only 96.05%. For the CNvsMCI subset, the GB model yielded the highest accuracy, with a score of 94.98%.

In multiclass classification, when using TriClass dataset, the RF classifier achieved the highest accuracy, with a score of 80.70%

4.3.3 Receiver operating characteristic curve

Figures 4.11 and 4.12 show the ROC curves for binary classification for each class pair: CN-AD using the CNvsAD subset, and CN-MCI using the CNvsMCI subset. For the CN-AD classes, most models achieved a high AUC value (AUC = 0.98), indicating that they provide consistent and accurate predictions for these classes, which appear to be linearly separable. While, the LR, DT, RF, SVM, MLP, and GB models achieved an AUC of 0.94 for the CN-MCI classes, suggesting that distinguishing between the CN and MCI classes is more challenging for some models. The GNB model showed poor AUC overall.

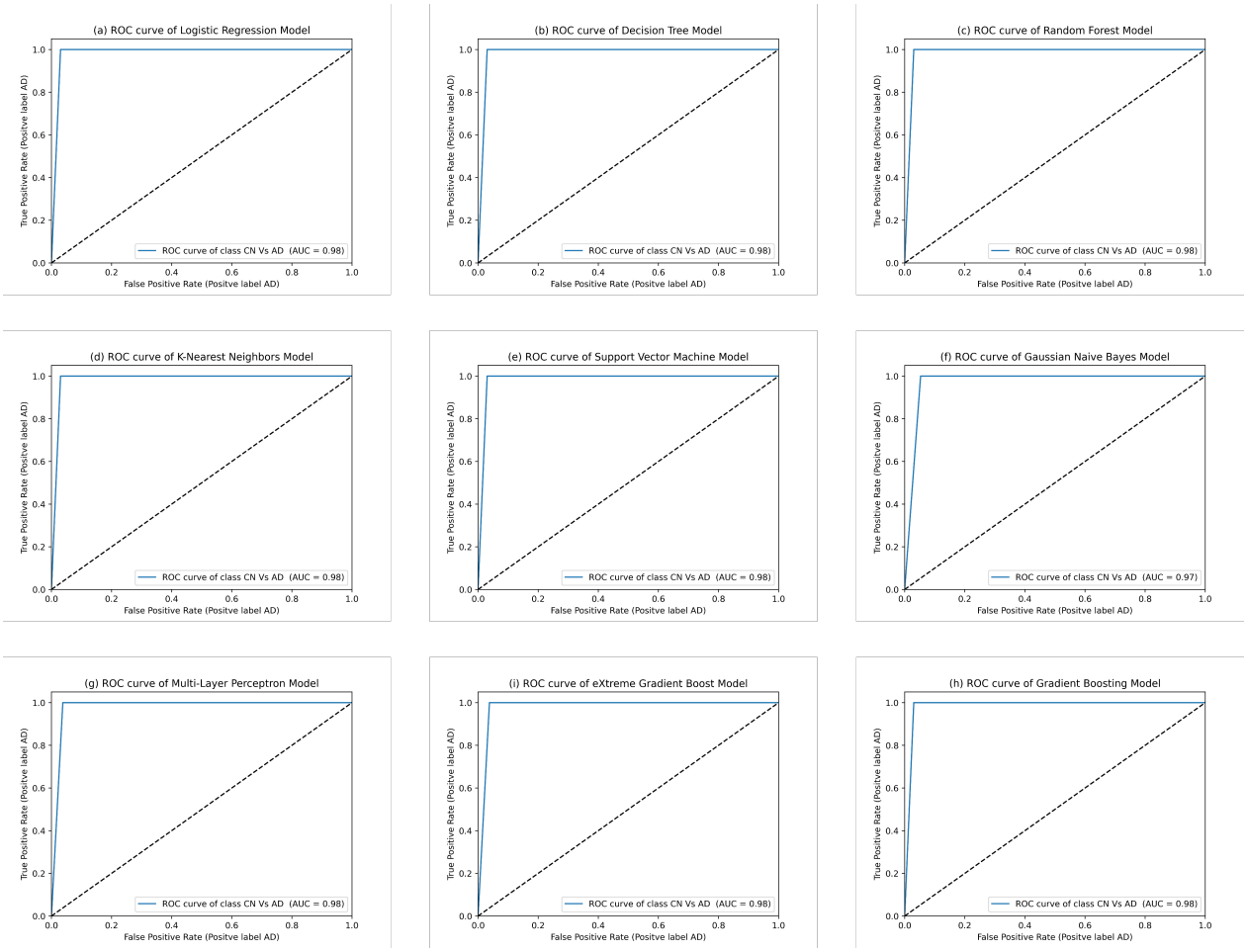

Figure 4.11: ROC curves for pair class CN-AD that trained and tested on CNvsAD subset: *(a) Logistic Regression; (b) Decision Tree; (c) Random Forest; (d) K-Nearest Neighbors; (e) Support Vector Machine; (f) Gaussian Naïve Bayes; (g) multi-layer perceptron; (h) eXtreme Gradient Boost; and (i) Gradient Boosting*

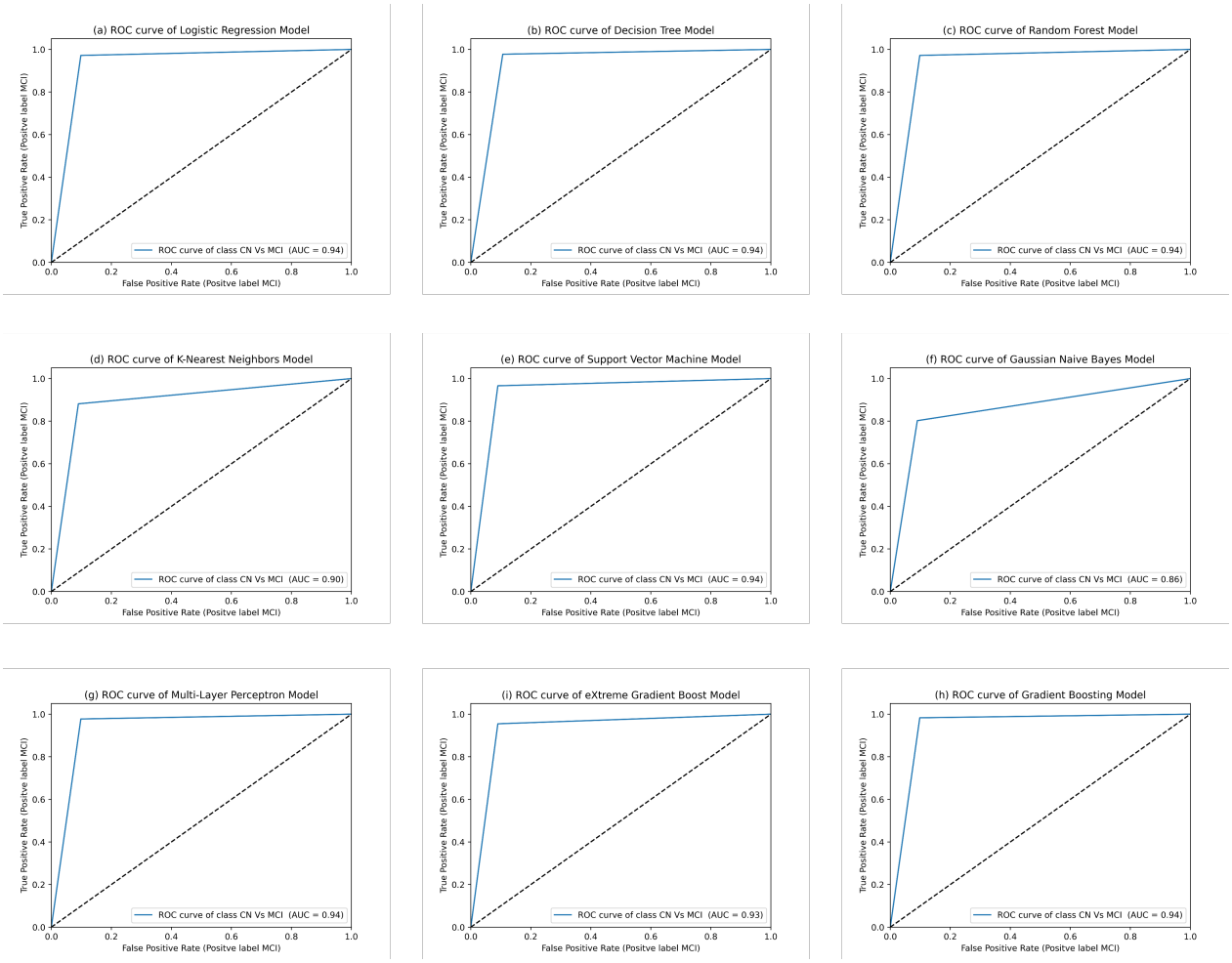

Figure 4.12: ROC curves for pair class CN-MCI that trained and tested on CNvsMCI subset: *(a) Logistic Regression; (b) Decision Tree; (c) Random Forest; (d) K-Nearest Neighbors; (e) Support Vector Machine; (f) Gaussian Naïve Bayes; (g) multi-layer perceptron; (h) eXtreme Gradient Boost; and (i) Gradient Boosting*

The multiclass ROC curves for the three classes were plotted in Figure **4.13** using the prediction from all models using the One-vs-Rest strategy, each class has its own ROC curve. The blue curve is for CN class, the green is for MCI and the red curve is for AD. Based on the plotted data, it is apparent that the CN-Class performs best in the LR, DT, RF, and SVM models, having the highest Area Under the Curve (AUC=0.94), indicating consistent and accurate predictions for this class. The MCI-Class, however, has the highest AUC (0.88) for the RF model. The AD-Class performs best in XGBoost model having an AUC of 0.94, which outperforms all other models.

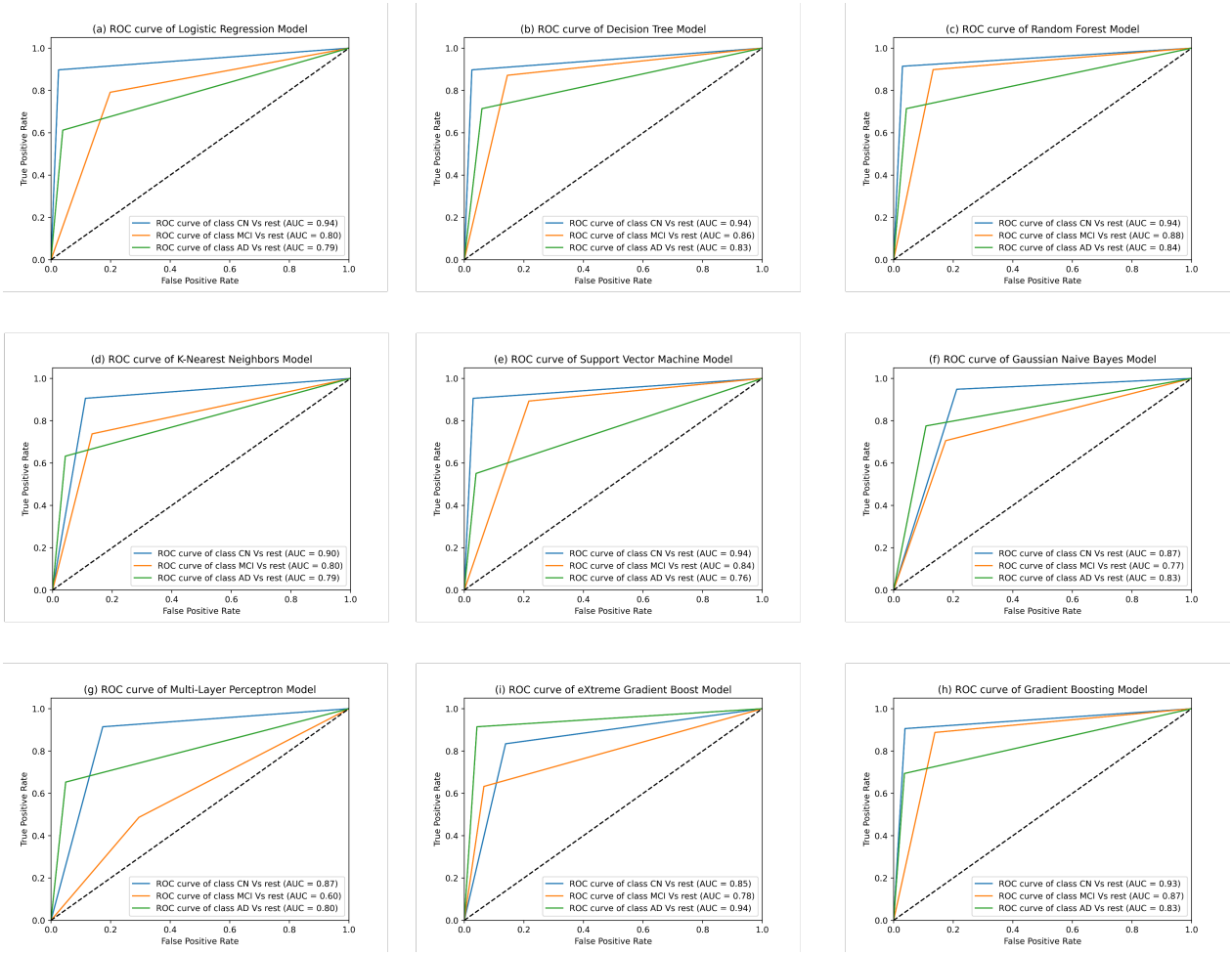

Figure 4.13: ROC curves for multiclass classification that trained and tested on TriClass dataset: *(a) Logistic Regression; (b) Decision Tree; (c) Random Forest; (d) K-Nearest Neighbors; (e) Support Vector Machine; (f) Gaussian Naïve Bayes; (g) multi-layer perceptron; (h) eXtreme Gradient Boost; and (i) Gradient Boosting*

4.4 Discussion

The findings of this study indicate that the performance of any machine learning model is influenced by the correct selection of the ML algorithms and their associated hyperparameters. Therefore, selecting the most appropriate hyperparameters is crucial for achieving optimal performance. Using the GridSearchCV tuner helped to effectively adjust and optimize the hyperparameters of the ML models. The selected hyperparameters included using the regularization techniques (L1 and L2) to address overfitting in the LR model, adjusting the number of weak learners in the XGBosst, GB and RF classifiers to enhance performance and

reduce overfitting, modifying the number of neighbors for the KNN model, and adjusting the kernel and C value for the SVM model. While GridSearchCV is a widely used technique for hyperparameter tuning, it does have some limitations, one of the main drawbacks is that it can be very time-consuming, as it needs to test every possible combination of hyperparameters. This can be a challenge when dealing with large datasets or complex models, requiring significant computational power and time. However, there are alternative optimization techniques available that can help address this issue. For example, RandomizedSearchCV and HalvingGridSearchCV from scikit-learn can test a broader range of hyper-parameter values within the same computation time as GridSearchCV, making them more efficient options for hyperparameter tuning.

Comparison of the results from the nine models revealed that the LR, DT, RF, SVM, and GB models achieved the highest classification accuracies for the CN-AD pair (97.74%), indicating that when data is linearly separable, these ML models perform well, making it difficult to evaluate their individual classification performance. However, when analyzing the results for the second subset (CNvsMCI) in binary classification, a significant gap in model performance emerged. For instance, the GB model achieved the highest accuracy when trained on the CNvsMCI subset (94.98%), and the RF model performed very well when trained on the TriClass dataset, with an accuracy score of 84.70%. This suggests that ensemble learning methods such as GB and RF are highly suitable for the diagnosis of Alzheimer's disease based on neuropsychological assessments. The advantage of ensemble learning algorithms is their ability to improve accuracy by combining multiple models (such as decision trees in our case), often resulting in better performance than individual models. They are more robust to overfitting, especially in high-dimensional data, as they mitigate the impact of errors from individual models using techniques like averaging or voting. Ensemble methods are particularly effective in handling imbalanced and high-dimensional datasets. By reducing both bias and variance, they achieve an optimal balance between these factors, enhancing overall model performance. In contrast, Individual models often rely on specific assumptions about the data distribution or the relationships between features and target variables. For example, LR assumes a linear relationship between input features and the logarithmic probability of the target, while DT may overfit the training data, capturing noise rather than general patterns. These limitations are common among most individual models and can reduce their ability to generalize effectively to new data.

Although the results of this study show that the classification of AD based on neuropsychological markers is promising, it has some limitations. For example, some diseases such

as Schizophrenia and Parkinson's disease can exhibit similar psychological symptoms as AD, which could lead to misdiagnosis. Additionally, the limited sample size affects the results and highlights the need for future research to enhance the dataset by incorporating additional markers, such as brain imaging, and genetic and biological markers. Moreover, using hybrid modeling with various datasets could potentially lead to the development of more robust and accurate models for diagnosing AD.

4.5 Conclusion

This study assessed the effectiveness of nine supervised ML algorithms, including LR, DT, RF, KNN, SVM, GNB, MLP, XGBoost, and GB, for predicting Alzheimer's disease. The aim was to explore the capability of each model to correctly classify individuals with AD using neuropsychological assessments. We used the GridSearchCV function from the scikit-learn library to tune the hyperparameters of each model. Obtaining the optimal hyperparameters allowed us to build nine robust ML models, train them, and compare their classification performance. The results indicated that ensemble learning models, such as Gradient Boosting and Random Forest, demonstrate superior predictive power in Alzheimer's disease classification. These models outperform other algorithms by effectively identifying patterns in complex datasets and making accurate classifications. Their strength lies in handling non-linearly separable data, where the classes cannot be divided by a simple linear boundary, and in multiclass classification tasks, such as categorizing data into CN, MCI, and AD. This makes GB and RF particularly robust and efficient for analyzing neuropsychological data and addressing the challenges of AD diagnosis.

Chapter 5

Identification of Plasma Proteins Associated with Alzheimer's Disease

5.1 Introduction

Alzheimer's disease is a chronic, progressive neurodegenerative disorder that typically affects individuals aged 60 years and older [91, 108]. Generally, AD is characterized by the gradient death of nerve cells, which is caused by the accumulation of extracellular amyloid-β (Aβ) plaques and interneuronal neurofibrillary tangles composed of forms of the Tau-protein [109]. Diagnosing AD is a complicated process that involves a combination of neuropsychological assessments, blood tests, CSF analysis, and neuroimaging. These biomarkers require careful evaluation to exclude the other neurodegenerative disorders that share similar symptoms with AD. However, despite the effectiveness of PET and CSF biomarkers in the clinical diagnostic process for AD, the high cost of PET scans and CSF tests restricts their accessibility and generalizability as diagnostic tools [110]. These limitations could be countered by the use of blood protein biomarkers in AD diagnosis [111]. Blood testing is a well-established part of clinical practice, as it is easy to perform, safe, and does not require additional training for healthcare professionals [112, 113].

Blood is a complex liquid tissue composed of cells and extracellular fluid. It contains a diverse array of molecules, including proteins, nucleic acids, lipids, and other metabolic products, which can be observed in plasma, serum, and cellular compartments [21]. Brain-derived biomarkers are typically present at relatively low concentrations in the blood, due to the blood-brain barrier (BBB), which restricts the free passage of molecules between the central nervous system (CNS) and blood [114]. However, the progressive damage to the BBB

in AD patients may allow some proteomics molecules to pass into the blood, thereby enabling the possibility of diagnosing patients with AD and the progression of the disease based on plasma proteins.

The main objective of this chapter is to use computational algorithms to identify a panel of plasma proteins that can serve as biomarkers for AD detection. This study aims to introduce a novel plasma protein panel for the accurate diagnosis of AD using Sequential Backward Feature Selection (SBFS) techniques utilized with five ML models: DT, RF, Extremely randomized trees (Extra Trees), XGBoost, and Adaptive Boosting (AdaBoost).

Proteins often play a role in biological activities within the body that change during the progression of AD, making them valuable indicators and biomarkers. By computing protein concentrations in the plasma of AD patients, we can identify proteins associated with the disease and develop a practical, cost-effective algorithm for its diagnosis. This study has significant implications: diagnosing AD using the selected protein panel enables timely interventions that can slow disease progression and improve patient outcomes. Furthermore, by focusing on plasma-based biomarkers, the study emphasizes a non-invasive, scalable, and affordable diagnostic method, making AD screening accessible to a broader population.

5.2 Materials and methods

5.2.1 Data description

This study used samples collected by the Alzheimer's Disease Neuroimaging Initiative (ADNI) to qualify multiplex panels in plasma proteomics. ADNI provides unlimited data access and encourages researchers to develop potential methods for analyzing the progression of AD [24]. The data lists 566 subjects, which represent baseline data on the concentration of 146 blood plasma proteins (Presented in Appendix) derived from a cohort of 112 AD patients, 396 MCI patients, and 58 healthy controls (HC). The available neuropsychological assessments in ADNI, such as the MMSE and CDR, were used to categorize the clinical groups. A list of the 146 proteins is provided in the supplementary materials. Table **5.1** presents the demographics of the baseline subjects.

Table 5.1: Demographics of the baseline subjects.

Group	HC	MCI	AD
Nbr baseline	58	396	112
Age	75.3 (62-90)	74.9 (55-90)	75.4 (55-89)
Gender M/F	30/28	256/140	65/47
MMSE	28.9 (25-30)	27.0 (23-30)	23.6 (20-27)

5.3 Machine learning algorithms

5.3.1 Decision tree

DT is a hierarchical supervised machine learning algorithm that employs decision rules to divide the feature space of a dataset into subsets belonging to a single class. It achieves this by recursively partitioning the feature space of the training data to determine an optimal set of decision rules [115].

5.3.2 Random forest

RF is an tree-based ensemble learning algorithm that enhances prediction accuracy by combining multiple decision trees. Each decision tree in the Random Forest is built using a bootstrapped sample of the training data, ensuring that every sample has an equal probability of being chosen. The algorithm selects a random subset of the training data with the replacement for constructing each tree. In the tree-based ensemble, every tree operates as an independent classifier, predicting the class label of an unlabeled instance. The final classification decision is made using a majority voting technique, where the most frequent prediction among the trees determines the output [98, 99].

5.3.3 Extremely randomized trees

The ExtraTrees algorithm is an tree-based ensemble learning method that leverages decision tree principles for both classification and regression tasks. During the tree-building process, Extra Trees randomly selects split points at each node to construct multiple decision trees. Each tree is built using a randomly sampled subset of the data without replacement, ensuring that each tree has unique samples. A random subset of features is selected for each tree from the total feature set. The entire dataset is used to build the trees, enhancing efficiency.

By combining random splits and aggregating the results from multiple trees, Extra Trees reduces computational costs, improves processing speed, and performs effectively on large, high-dimensional datasets.

5.3.4 Extreme gradient boosting

XGBoost is a flexible supervised learning algorithm known for its fast execution and support for parallel computing. XGBoost introduces a regularized model formulation to control overfitting, achieving better performance results. During the boosting process, each new model learns from the errors of previous iterations, creating trees sequentially. Each decision tree is adjusted to address the mistakes of the prior model. This tree ensemble approach enhances the predictive power compared to a single decision tree, enabling boosting to overcome the limitations of poor predictive performance. Additionally, random sampling in the XGBoost model reduces the variance of the final model. It improves prediction accuracy by using only a random subset of the data to fit each new tree [116].

5.3.5 Adaptive boosting

AdaBoost algorithm is an ensemble learning method designed to improve the predictive performance of weak classifiers by combining them into a strong classifier. It works iteratively, adapting to the data at each step. Initially, all training samples are assigned equal weights. A weak classifier is then trained to minimize the classification error on the weighted dataset. After training, the algorithm calculates the error of the classification and assigns it a weight based on its performance. The weights of the training samples are then updated to emphasize those that were misclassified, making them more influential in the next iteration. This process is repeated for a predetermined number of iterations or until the desired accuracy is achieved [117].

5.4 Feature selection techniques

5.4.1 Sequential backward feature selection

Sequential backward feature selection (SBFS) is a feature selection technique that uses a top-down search approach to exclude features iteratively. It begins with the full feature set, involving all the features, and applies the basic Sequential Backward Selection (SBS) method. Features are progressively excluded, and at each iteration, the most significant feature from

the remaining set is conditionally included if it improves the performance of the previous subsets. This process continues until the optimal feature subset is identified. In the first step, the SBFS technique was applied iteratively to train five ML classifiers: DT, RF, Extra Trees, XGBoost, and AdaBoost. The technique evaluated all possible subset combinations of the 146 proteins for each classifier. For each ML model, the accuracy was recorded to identify the subsets of proteins that achieved the best classification performance. By the end, five combinations of significant features, each corresponding to the results of one of the ML algorithms, were improved as the most relevant for Alzheimer's disease classification. Figure 5.1 presents the SBFS diagram.

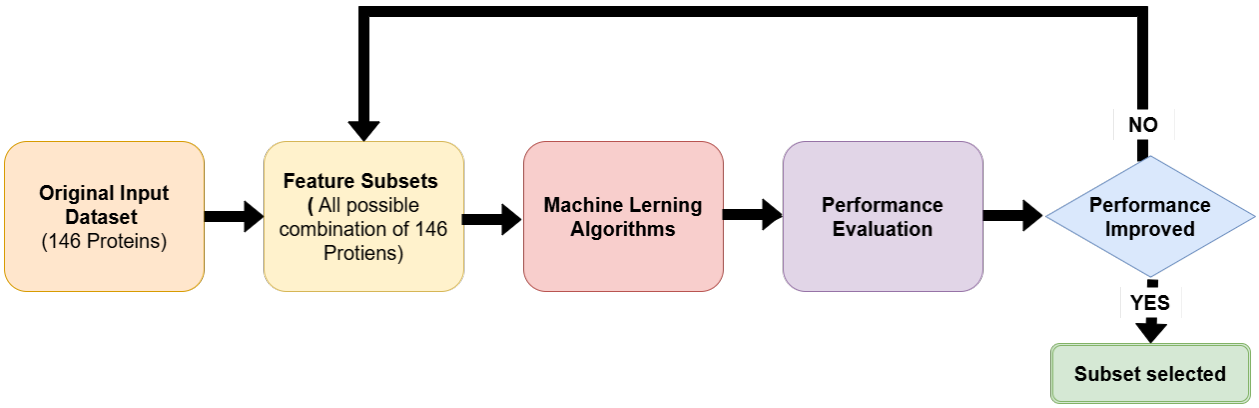

Figure 5.1: Diagram of the sequential backward feature selection technique.

5.4.2 One-way analysis of variance

ANOVA is a statistical technique used to analyze the differences between group means and their associated variances. It helps determine whether at least one group's mean is significantly different from others. ANOVA can help reduce the dimensionality of a dataset by identifying features that have a significant relationship with the target variable. The second step of the framework involved using one-way ANOVA to reduce the size of the panels obtained from the first step of the feature selection by comparing the means and the variances of each protein in two clinical groups, HC and AD. This particular application of ANOVA enabled the exclusion of irrelevant proteins or those not associated with AD from the panels, specifically those with similar concentration values in the two groups. ANOVA provides an F-statistic and a p-value as results. A threshold (p-value=0.05) was applied to determine whether to reject or retain features. Features with non-significant p-values (high p-values) were excluded, as they did not contribute to distinguishing between the classes. While features with significant p-values (low p-values) were retained on the protein panel. The null

hypothesis (H0) states that the means of the two groups (HC and AD) are equal, indicating no statistically significant difference in the tested feature (protein). In such cases, the feature was eliminated from the panel. The alternative hypothesis (H1) states that the means of the two groups are different, indicating a statistically significant difference. These features were kept in the panel. This statistical analysis was applied to all features selected in the first step, enabling the identification of a plasma protein panel for AD prediction. We performed this statistical analysis with all the features that had been selected in the first step.

5.5 Panel validation process

The panel validation process evaluates the robustness, accuracy, and generalizability of the selected plasma protein panel using two ML algorithms: XGBoost and AdaBoost. The dataset was split into training and testing subsets, with 80% allocated for training the models and 20% for testing. To reduce the risk of overfitting and enhance predictive performance, five-fold cross-validation was employed. The effectiveness of the models was assessed using key performance metrics, including sensitivity (the ability to correctly identify AD patients), specificity (the ability to correctly identify healthy controls), accuracy (the overall prediction correctness), and the Area Under the Curve (AUC), which measures the ability of ML models to distinguish between AD and healthy controls. These metrics provided a comprehensive evaluation of the predictive performance achieved with the selected protein panel. The primary goal of the panel validation process is to confirm that the selected plasma protein panel serves as a reliable and accurate tool for early-stage AD diagnosis, highlighting its potential for clinical application. Figure **5.2** illustrates an overall diagram of the framework, which includes the three steps.

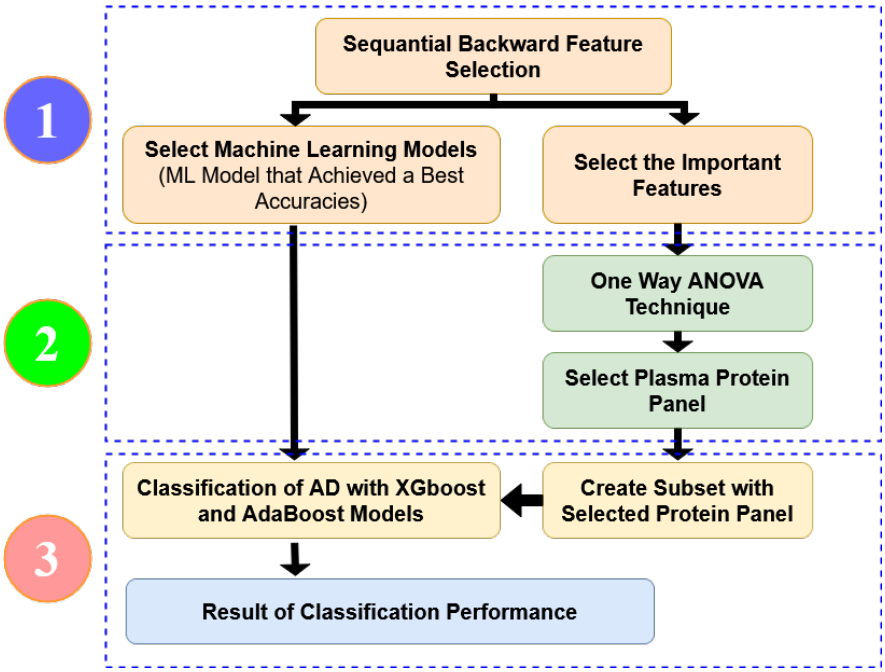

Figure 5.2: Proposed framework diagram.

5.6 Results

This section presents the outcomes of SBFS and ANOVA techniques that applied to the plasma protein dataset in order to identify the most relevant biomarkers for Alzheimer's disease classification.

5.6.1 SBFS technique outcomes

In the first step, the SBFS technique generated subsets (groups of proteins) from the 164 proteins available in the dataset. Each subset was trained and tested using the ML models (DT, RF, Extra Trees, XGBoost, and AdaBoost). Table 5.2 presents the preselected proteins for each ML model along with their achieved accuracies, while Figures 5.3 and 5.4 illustrate the overall results of the SBFS technique, showing the evaluation accuracies as a function of the subset size. The SBFS technique selects the group of proteins that achieves the highest accuracy for each group size. Proteins yielding accuracies greater than 90% are accepted, while those producing results below 90% are eliminated. From the results, the DT and RF classifiers achieved accuracies below 90%. However, the Extra Trees, XGBoost, and AdaBoost models achieved accuracies of 90.58%, 93.52%, and 95.88%, respectively. The selected proteins for the second step constitute the combination of proteins that achieved more

than 90% accuracy in the classification process. This includes all protein groups identified by the Extra Trees, XGBoost, and AdaBoost classifiers. The selected proteins are A1Micro, Apo A-II, BTC, CD5L, Cystatin-C, IL-16, PLGF, Proinsulin-Intact, Proinsulin-Total, PYY, TECK, TN-C, ACE, A-IV, Apo B, Apo E, BMP-6, BNP, IgM, IL-8, MIP-1 alpha, SGOT, Sortilin, AGRP, CA-19-9, FRTN, HGF, IFN-gamma, PPP, RAGE, Transferrin, TTR, and VKDPS.

Table 5.2: Preselected proteins from SBFS for ML models with their best-achieved accuracies

ML Model	**Preselected proteins**	**Accuracy**
Decision tree	Apo A-II, AXL, I-309, IL-16, MDC, PLGF, PPP, PRL, and Sortilin	86.47%
Random forest	Apo A-II, Apo A-IV, Apo B, Apo E, Apo H, Cystatin-C, IL-16, MIGI, MIP-1 alpha, NGL, PLGF, PYY, TIMP-1, and TTR	89.41%
Extra trees	A1Micro, Apo A-II, BTC, CD5L, Cystatin-C, IL-16, PLGF, Proinsulin-Intact, Proinsulin-Total, PYY, TECK, TN-C	90.58%
XGBoost	A1Micro, ACE, Apo A-II, Apo A-IV, Apo B, Apo E, BMP-6, BNP, BTC, CD5L, IGM, IL-16, IL-8, MIP-1 alpha, PYY, SGOT, Sortilin, TN-C.	93.52%
AdBoost	AGRP, Apo A-II, Apo B, Apo E, BMP-6, BNP, BTC, CA-19-9, FRTN, HGF, IL-16, IFN-gamma, PPP, Proinsulin-Total, PYY, RAGE, Transferrin, TTR, VKDP.	95.88%

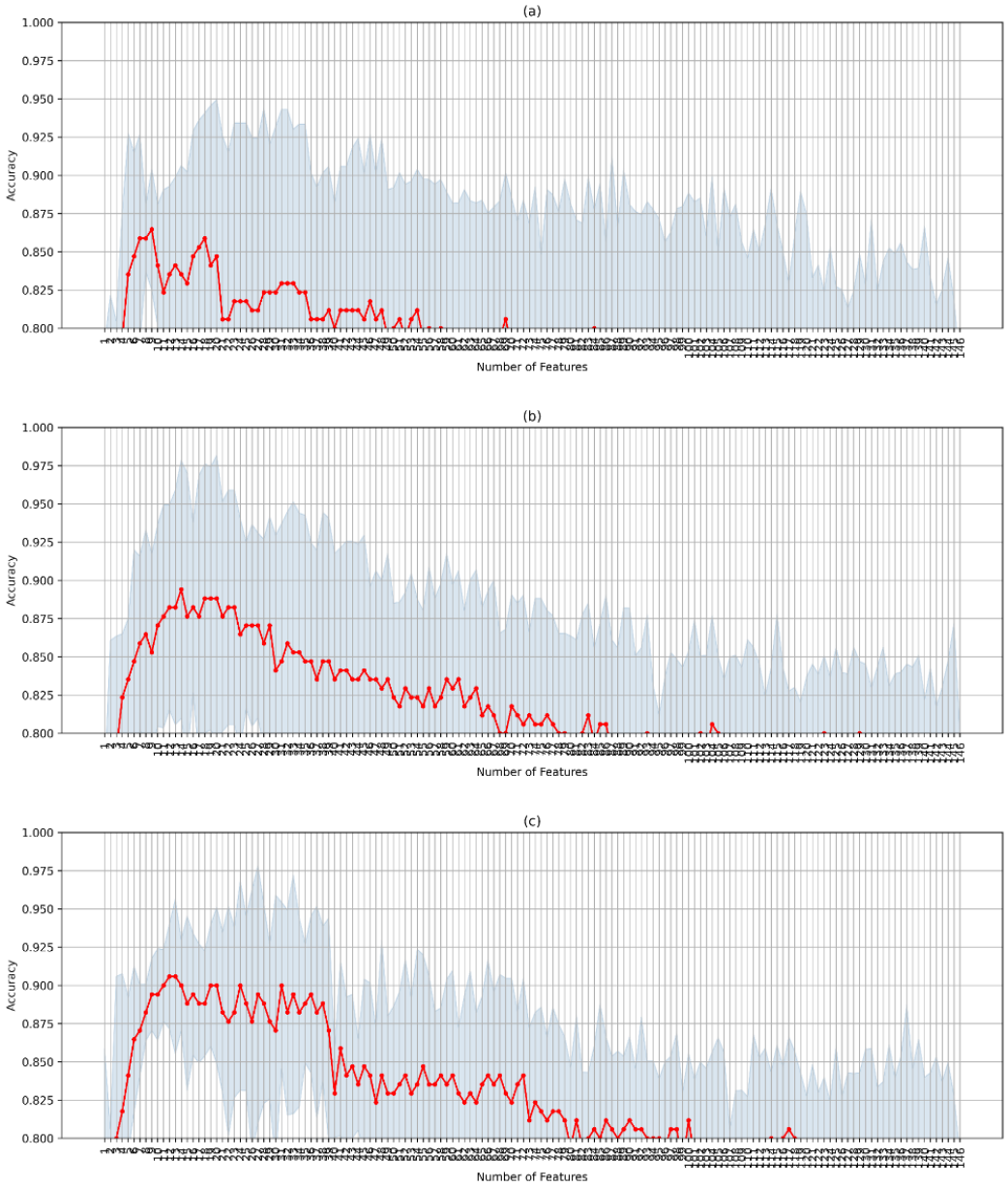

Figure 5.3: Results of SBFS for ADvsHC. Performance accuracy as a function of the subset size for: (a) DT model, (b) RF model, and (c) Extra trees model

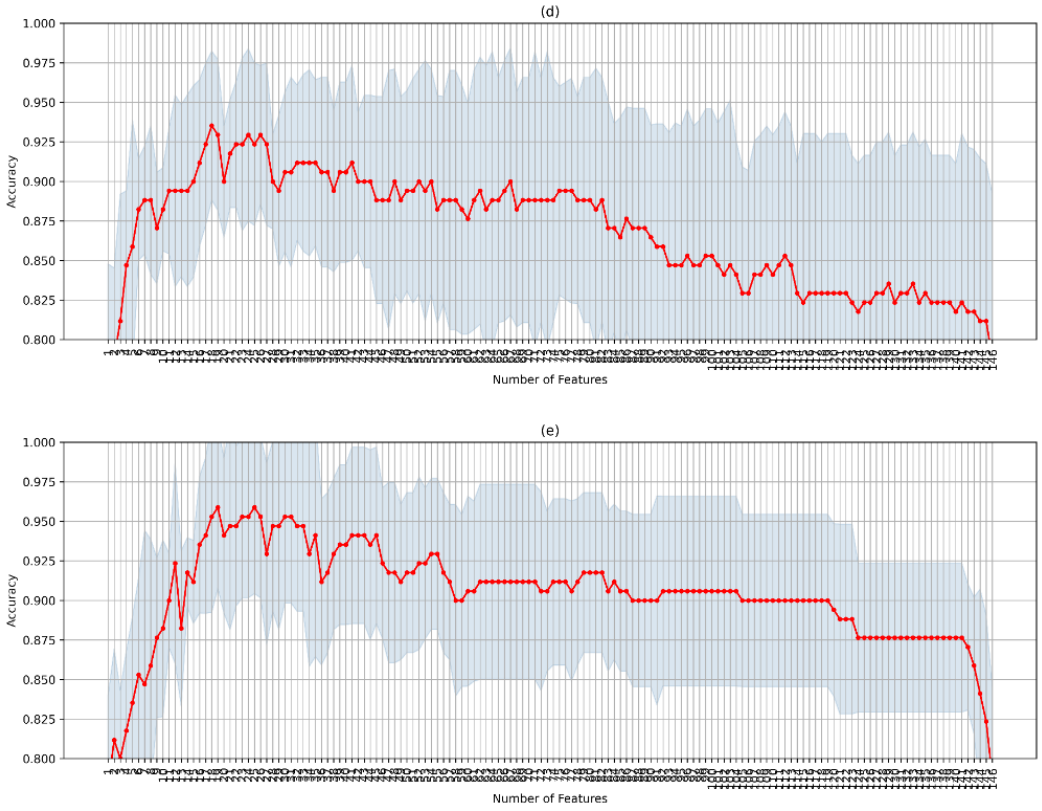

Figure 5.4: Results of SBFS for ADvsHC Performance accuracy as a function of the subset size for: (d) XGboost model and (e) AdaBoost model

5.6.2 ANOVA outcomes

The purpose of the ANOVA test was to determine whether to retain or exclude each preselected protein. For this, the two clinical groups, AD and HC, were separated, and a one-way ANOVA test was performed for each preselected protein. Proteins with high p-values between the classes were excluded, while those with low p-values were retained based on a threshold of (p-value =0.05). This process enabled the exclusion of all proteins with non-significant p-values and the creation of a final plasma protein panel containing only the significant proteins. Table **5.3** presents the result of the one-way ANOVA test. The final plasma protein panel selected consists of five proteins, namely A2Macro, BNP, BTC, PPP, and PYY.

Table 5.3: Panel selected by one-way ANOVA test for proteins that achieved a P-value<0.05

Protein		P-value
A2Macro:	Alpha-2-Macroglobulin	0.016
BNP:	Brain Natriuretic Peptide	0.014
BTC:	Betacellulin	0.013
PPP:	Pancreatic Polypeptide	0.025
PYY:	Peptide YY	0.003

5.6.3 Outcomes of the classification models

We chose two machine learning algorithms, namely XGBoost and AdaBoost, to test and validate the selected protein panel. The performance parameters were measured using 5-fold Cross-validation including accuracy, sensitivity, specificity, and AUC. Both models achieved the same test accuracy of 76.47%, with slightly different values in other performance metrics. Additionally, the XGBoost model yielded an AUC of 0.85, while the AdaBoost model achieved only 0.78. Table **5.4** presents the performance metrics of the two machine learning by using a selected panel. Figure **5.5** shows the receiver operator characteristic (ROC) curves of the XGBoost and AdaBoost models.

Table 5.4: Performance metrics of the XGBoost and AdaBoost models using plasma protein panel selected (A2Macro, BNP, BTC, PPP, and PYY)

Machine learning	Accuracy	Sensitivity	Specificity	AUC
XGBoost	76.47%	81.81%	66.66%	0.85
AdaBoost	76.47%	88.88%	62.50%	0.78

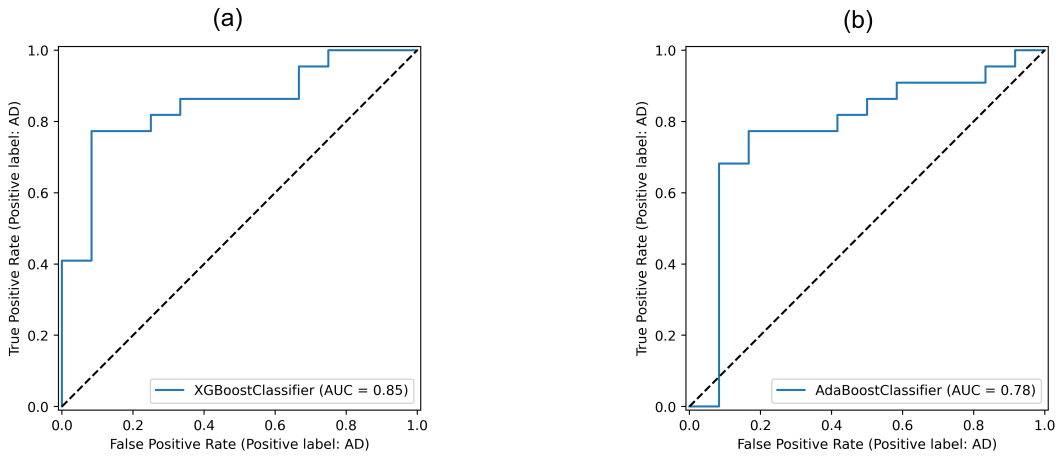

Figure 5.5: Receiver Operator Characteristic (ROC) curves of the classification models using plasma protein panel selected (A2Macro, BNP, BTC, PPP, and PYY). (a) XGBoost model and (b) AdaBoost model

5.7 Discussion

There is a significant need for a fast and cost-effective method to diagnose AD patients. Therefore, our study aimed to identify an optimal panel of blood protein biomarkers that could serve as a first-line diagnostic tool. We proposed a novel non-amyloid and non-tau plasma panel consisting of five proteins: **A2Macro, BNP, BTC, PPP, and PYY**, for AD diagnosis. We used the SBFS technique to train five ML algorithms, followed by one-way ANOVA analysis, to extract five significant proteins for our panel from a dataset containing 146 proteins.

SBFS is a reliable process as it incorporates all possible protein combinations during the training of ML models. However, it requires complex computations and consumes substantial time. Our findings are consistent with several recent studies that aimed to identify blood proteins associated with AD. For instance, A2Macro, BNP, and PYY proteins were identified in the panel proposed by Liano et al. and Eke et al. [80,84], while PPP and BTC proteins were selected in the study conducted by Liano et al. [80]. However, the current study proposes a smaller panel size compared to many panels suggested in previous studies. For example, Eke et al. proposed a panel with six proteins [84], and O'Bryant et al. identified 30 proteins for AD detection [78]. The smaller size of the panel makes it more interpretable and less costly to implement in practical applications, such as machine learning applications. We tested and validated the proposed panel using XGBoost and AdaBoost classifiers. The XGBoost model

achieved an AUC of 0.85, indicating its ability to distinguish AD patients from the control group. While, the AdaBoost classifier achieved a specificity of 88.88%, suggesting that the model is more accurate in the classification of AD group than the HC group. Table **5.5** provides a comparison between our results and the recent related works.

Table 5.5: Comparison of our findings with recent related works

Author	**Algorithm**	**Panel**	**Results**		
			Sensitivity	**Specificity**	**AUC**
[84]	SVM	Apo E, PYY, SGOT, A2M, BNP, EoT3 and RAGE	88.9%	73.80%	0.89
[85]	RF	12 miRNA	90.0%	67.0%	0.77
[83]	XGBoost	20 ranked metabolites	-	-	0.88
	RF		-	-	0.85
	DNN		-	-	0.85
[118]	LR/LASSO	Apo E, AMBP, C3, IL-16, IGFBP2 and Apo D	-	-	0.85
[119]	LASSO	Apo E, CgA, CRP, CCL26, CCL20, Nr-CAM, and PYY	-	-	0.77
Our study [120]	XGBoost	A2Macro, BNP, BTC, PPP, and PYY	81.81%	66.66%	0.85
	AdaBoost		88.88%	62.50%	0.78

It is crucial to interpret our findings while considering certain limitations. Our study focused on AD patients and healthy controls, excluding other AD stages such as early-MCI, MCI, and late-MCI. Therefore, more extensive studies are required, particularly with a larger dataset that includes all these categories of subjects. Additionally, the small size of the available dataset led to higher variance as it did not fully represent the diversity of individuals, potentially limiting the ability to generalize the model to new data.

The main findings of this study confirm that plasma proteins can be used as a biomarker signature for diagnosing AD patients. We identified a panel of five proteins that can be effectively used with machine learning algorithms to predict AD. These findings facilitate the diagnostic process, and we highly recommend using this panel as a first-line diagnostic tool.

5.8 Conclusion

This study focused on exploiting the ML algorithms to identify a robust panel of plasma proteins associated with AD detection. Through the application of two feature selection techniques SBFS followed by one-way ANOVA, we successfully extracted a significant protein panel from a dataset of 146 non-Amyloid-β and non-Tau proteins. The identified panel, consisting of five proteins (A2Macro, BNP, BTC, PPP, and PYY), demonstrated strong potential as reliable biomarkers for AD detection. The validation process, using XGBoost and AdaBoost models, achieved a sensitivity of 88.88%, a specificity of 66.66%, and an AUC of 0.85, further emphasizing the effectiveness of the panel. These results confirm that the proposed plasma protein panel could serve as a non-invasive and cost-effective diagnostic tool for AD, significantly accelerating diagnosis and enabling timely interventions. This study has certain limitations. The dataset used in this research was relatively small, which may limit the generalizability of the findings.

Chapter 6

Conclusion

This chapter discusses the key findings from both studies, make them within the broader field of AD research. It discusses the advantages and challenges of each approach and compares the results with existing literature. Additionally, we examine the study's limitations and propose future research directions that could enhance the robustness and applicability of these methods.

6.1 Discussion of findings

The findings from both studies highlight the effectiveness of ML in diagnosing AD using alternative data sources beyond neuroimaging.

The first study demonstrated that neuropsychological assessments, when processed through well-optimized ML models, provide reliable predictions for AD diagnosis. In particular, ensemble learning methods such as GB and RF exhibited superior performance, emphasizing the importance of combining multiple weak learners to enhance predictive accuracy. These models showed strong classification performance, especially when distinguishing between CN individuals and AD patients, with a slight decrease in accuracy when applied to more challenging cases such as MCI.

The second study identified a novel plasma protein biomarker panel that holds promise as a cost-effective and non-invasive diagnostic tool. The Sequential Backward Feature Selection (SBFS) technique successfully reduced the number of biomarkers while retaining high classification performance. The five-protein panel demonstrated significant predictive power, with XGBoost achieving an AUC of 0.85 and AdaBoost providing high specificity in classifying AD patients. This supports the hypothesis that blood-based biomarkers, when paired with

ML techniques, can serve as an accessible alternative to traditional diagnostic methods.

A comparative analysis of both studies suggests that while neuropsychological assessments offer a behavioral and cognitive perspective on AD, plasma biomarkers provide biological insights that can enhance early detection. The combination of these two approaches, potentially integrated into a hybrid diagnostic model, could lead to a more comprehensive and scalable screening tool for AD.

6.2 Thesis contributions

The findings of presented research contribute to the growing body of research on ML- and DL-based Alzheimer's Disease diagnosis by addressing two key limitations in existing methods: reliance on expensive neuroimaging techniques and the under utilization of behavioral and biological markers.

6.2.1 Theoretical contributions

1. Advancement of ML in AD diagnosis: This research demonstrates that both neuropsychological assessments and plasma protein biomarkers can be effectively leveraged using ML, broadening the scope of non-imaging-based AD diagnostics.

2. Feature selection optimization: The study introduces a structured approach to feature selection in both domains, highlighting the benefits of SBFS in biomarker identification and the impact of hyperparameter tuning in model performance.

3. Comparison of ML classifiers: By evaluating multiple ML models across different data types, this thesis provides insights into the strengths and weaknesses of various classifiers in AD diagnosis.

6.2.2 Practical contributions

1. Development of low-cost, accessible diagnostic approaches – The use of neuropsychological assessments and blood biomarkers makes AD screening more feasible for resource-limited settings, reducing reliance on neuroimaging.

2. Potential for early detection – By identifying behavioral patterns and biological markers linked to AD, this research supports the development of first-line diagnostic tools that can facilitate early intervention.

3. Integration into clinical decision-making – The findings pave the way for the incorporation of ML-driven analysis in healthcare settings, assisting clinicians in making more informed diagnoses with improved accuracy and reliability.

These contributions collectively support the movement toward scalable, AI-assisted diagnostic solutions that could make AD detection more widely available and cost-effective.

6.3 Limitations and future directions

6.3.1 Limitations

Despite its contributions, this research has certain limitations that need to be addressed in future studies:

1. Data constraints:
    - The relatively small dataset size in the plasma biomarker study limits the generalizability of the findings. A larger dataset covering diverse populations is needed for broader validation.
    - The neuropsychological study does not incorporate longitudinal data, restricting its ability to predict disease progression over time.
    - The biomarker study does not include intermediate AD stages such as early-MCI and late-MCI, which are crucial for early intervention.
2. Methodological limitations:
    - Computational complexity – Feature selection using SBFS is computationally expensive, requiring significant processing time. More efficient selection techniques should be explored.
    - Hyperparameter Tuning – While GridSearchCV was effective in optimizing models, alternative tuning methods such as Bayesian optimization could improve efficiency without excessive computational costs.
    - Potential Overfitting – Although regularization techniques were used, there is still a risk of overfitting, particularly when working with high-dimensional data. External validation is necessary to confirm real-world applicability.
3. Clinical and practical considerations

- The ML models have not yet been deployed or tested in clinical environments, making real-world validation a necessary next step.
- Some psychological symptoms of AD overlap with other neurodegenerative diseases, which could lead to misclassification. More research is needed to refine model specificity.

6.3.2 Future directions

To build upon the findings of this research, future work should focus on:

- Incorporating multi-center and longitudinal studies to track disease progression more accurately.
- Integrating multi-modal data (neuropsychological, blood biomarkers, neuroimaging, and genetics) to improve diagnostic robustness.
- Including a more diverse population to enhance model generalizability across different demographic groups.
- Exploring deep learning approaches such as CNNs and transformer models for improved classification accuracy
- Refining feature selection methods to balance computational efficiency and predictive performance.
- Investigating automated hyperparameter optimization techniques to improve ML model selection.
- Conducting pilot studies in healthcare settings to evaluate the usability and impact of ML-driven AD diagnostic models.
- Establishing standardized protocols for plasma biomarker measurement and interpretation to facilitate clinical adoption.
- Addressing ethical and regulatory considerations in AI-driven medical diagnostics to ensure compliance with healthcare standards.

By addressing these limitations and advancing research in these areas, future studies can enhance the effectiveness and accessibility of ML-based AD diagnosis, ultimately improving early detection and patient outcomes.

6.4 Publications

6.4.1 Journals

1. **Title:** A Comparison of Machine Learning Algorithms for Predicting Alzheimer's Disease Using Neuropsychological Data.
   Authors: Zakaria Mokadem, Djerioui Mohamed, Bilal Attallah, Youcef Brik.
   Journal: Science, Engineering and Technology
   Volume: 5
   N°:1
   Pages: 177–191
   Year: 2024
   DOI: https://doi.org/10.54327/set2025/v5.i1.182

2. **Title:** Identification of Plasma Proteins Associated with Alzheimer's Disease Using Feature Selection Techniques and Machine Learning Algorithms.
   Authors: Zakaria Mokadem, Djerioui Mohamed, Bilal Attallah, Youcef Brik.
   Journal: Science, Engineering and Technology
   Volume: 5
   N°:1
   Pages: 192–202
   Year: 2025
   DOI: https://doi.org/10.54327/set2025/v5.i1.189

6.4.2 International conferences

1. **Title:** Machine Learning and Deep Learning Techniques for Alzheimer's Disease Prediction Using CSF and Plasma Biomarkers.
   Authors: AR Zouaoui, H Bentahar, M Djeriuoi, Z Mokadem, HE Bentahar
   Conference: 2023 International Conference on Networking and Advanced Systems (ICNAS)
   Publisher: IEEE
   Pages: 1-6
   Date: 2023/10/21
   DOI: https://doi.org/10.1109/ICNAS59892.2023.10330506

2. **Title:** Random Forest Algorithm for Alzheimer's Disease Prediction.

Authors: Zakaria Mokadem, Djerioui Mohamed, Bilal Attallah, Youcef Brik.
Conference: First International Conference on Artificial Intelligence, Smart Technologies and Communications (AISTC'2025)
Publisher: IEEE
Date: 2025/04/15-14, Chlef, Algeria

6.4.3 National conference

1. **Title:** Blood-based Biomerker Panels for Diagnosis of Alzheimer's Disease.
   Authors: Zakaria Mokadem, Djerioui Mohamed, Bilal Attallah, Youcef Brik.
   Conference: The National Conference on Computer Engineering, Artificial Intelligence and Smart System (NCCIEASS2024)
   Date: 2024/12/12-10, Tamenghasset, Algeria.
   URL: http://dlibrary.univ-boumerdes.dz:8080/bitstream/123456789/15097/1/NCCEAISS-2024_BOOK%20OF%20ABSTRACTS.pdf

6.5 Final summary

Alzheimer's disease remains one of the most pressing neurodegenerative disorders, requiring early and accurate diagnosis to improve patient outcomes. This thesis explored the application of machine learning techniques in diagnosing Alzheimer's disease using two alternative data sources: neuropsychological assessments and plasma protein biomarkers. Given the increasing prevalence of AD and the limitations of traditional neuroimaging-based diagnostic methods, this research aimed to develop accessible, cost-effective, and scalable approaches to support early detection and clinical decision-making.

The first study demonstrated that neuropsychological assessments, when analyzed through well-optimized ML models, provide a reliable tool for AD classification. Ensemble learning models, particularly Gradient Boosting and Random Forest, showed strong performance in distinguishing cognitively normal individuals from AD patients and identifying mild cognitive impairment cases. These findings highlight the potential of cognitive and behavioral assessments in ML-driven diagnostic frameworks.

The second study introduced a novel plasma protein biomarker panel as a non-invasive and cost-effective diagnostic alternative. By employing SBFS and one-way ANOVA, five significant proteins—A2Macro, BNP, BTC, PPP, and PYY—were identified. ML models such as XGBoost and AdaBoost demonstrated high classification accuracy, reinforcing the

feasibility of blood-based biomarkers in AD diagnosis.

Together, these studies emphasize the effectiveness of ML in analyzing diverse data modalities for AD detection. While neuropsychological assessments offer cognitive and behavioral insights, plasma protein biomarkers provide biological indicators of disease progression. A hybrid diagnostic model that integrates both approaches could lead to a more comprehensive and accurate screening framework, addressing the limitations of each method individually.

The findings of this thesis reinforce the importance of ML in AD diagnosis and pave the way for future research on multi-modal diagnostic systems. By leveraging ML-driven techniques, healthcare professionals can improve early detection, enhance patient outcomes, and make AD screening more widely accessible. Ultimately, this research contributes to the development of scalable and cost-effective diagnostic solutions, with the potential to significantly impact the future of AD detection and management.

Bibliography

[1] Zakaria Mokadem, Mohamed Djerioui, Bilal Attallah, and Youcef Brik. A comparison of machine learning algorithms for predicting alzheimer's disease using neuropsychological data. *Science, Engineering and Technology*, 5(1), 2025.

[2] Alzheimer's Association et al. 2018 alzheimer's disease facts and figures. *Alzheimer's & Dementia*, 14(3):367–429, 2018.

[3] Hanns Hippius and Gabriele Neundörfer. The discovery of alzheimer's disease. *Dialogues in clinical neuroscience*, 5(1):101–108, 2003.

[4] Victor L Villemagne, Samantha Burnham, Pierrick Bourgeat, Belinda Brown, Kathryn A Ellis, Olivier Salvado, Cassandra Szoeke, S Lance Macaulay, Ralph Martins, Paul Maruff, et al. Amyloid β deposition, neurodegeneration, and cognitive decline in sporadic alzheimer's disease: a prospective cohort study. *The Lancet Neurology*, 12(4):357–367, 2013.

[5] Mark A Smith. Alzheimer disease. *International review of neurobiology*, 42:1–54, 1998.

[6] Eric M Reiman, Yakeel T Quiroz, Adam S Fleisher, Kewei Chen, Carlos Velez-Pardo, Marlene Jimenez-Del-Rio, Anne M Fagan, Aarti R Shah, Sergio Alvarez, Andrés Arbelaez, et al. Brain imaging and fluid biomarker analysis in young adults at genetic risk for autosomal dominant alzheimer's disease in the presenilin 1 e280a kindred: a case-control study. *The Lancet Neurology*, 11(12):1048–1056, 2012.

[7] Randall J Bateman, Chengjie Xiong, Tammie LS Benzinger, Anne M Fagan, Alison Goate, Nick C Fox, Daniel S Marcus, Nigel J Cairns, Xianyun Xie, Tyler M Blazey, et al. Clinical and biomarker changes in dominantly inherited alzheimer's disease. *New England Journal of Medicine*, 367(9):795–804, 2012.

[8] DW Dickson, E Wu, HA Crystal, LA Matthiace, S-HC Yen, and P Davies. Alzheimer's disease and age-related pathology in diffuse lewy body disease. In *Heterogeneity of Alzheimer's disease*, pages 168–186. Springer, 1992.

[9] Robert D Terry, Arthur Peck, Richard DeTeresa, Ruben Schechter, and Dikran S Horoupian. Some morphometric aspects of the brain in senile dementia of the alzheimer type. *Annals of Neurology: Official Journal of the American Neurological Association and the Child Neurology Society*, 10(2):184–192, 1981.

[10] Joseph L Price, PB Davis, JC Morris, and DL White. The distribution of tangles, plaques and related immunohistochemical markers in healthy aging and alzheimer's disease. *Neurobiology of aging*, 12(4):295–312, 1991.

[11] Philip Seeman and Neil Seeman. Alzheimer's disease: β-amyloid plaque formation in human brain. *Synapse*, 65(12):1289–1297, 2011.

[12] Reisuke H Takahashi, Toshitaka Nagao, and Gunnar K Gouras. Plaque formation and the intraneuronal accumulation of β-amyloid in alzheimer's disease. *Pathology international*, 67(4):185–193, 2017.

[13] Gary L Wenk et al. Neuropathologic changes in alzheimer's disease. *Journal of Clinical Psychiatry*, 64:7–10, 2003.

[14] Howard S Kirshner. Memory loss, alzheimer's disease, and dementia: a practical guide for clinicians, 2022.

[15] Robert D Terry. Alzheimer's disease and the aging brain. *Journal of geriatric psychiatry and neurology*, 19(3):125–128, 2006.

[16] Ronald C Petersen, Oscar Lopez, Melissa J Armstrong, Thomas SD Getchius, Mary Ganguli, David Gloss, Gary S Gronseth, Daniel Marson, Tamara Pringsheim, Gregory S Day, et al. Practice guideline update summary: Mild cognitive impairment: Report of the guideline development, dissemination, and implementation subcommittee of the american academy of neurology. *Neurology*, 90(3):126, 2018.

[17] Robert Perneczky, Stefan Wagenpfeil, Katja Komossa, Timo Grimmer, Janine Diehl, and Alexander Kurz. Mapping scores onto stages: mini-mental state examination and clinical dementia rating. *The American journal of geriatric psychiatry*, 14(2):139–144, 2006.

[18] Prashanthi Vemuri and Clifford R Jack. Role of structural mri in alzheimer's disease. *Alzheimer's research & therapy*, 2:1–10, 2010.

[19] Agneta Nordberg, Juha O Rinne, Ahmadul Kadir, and Bengt Långström. The use of pet in alzheimer disease. *Nature Reviews Neurology*, 6(2):78–87, 2010.

[20] Kaj Blennow and Henrik Zetterberg. Cerebrospinal fluid biomarkers for alzheimer's disease. *Journal of Alzheimer's Disease*, 18(2):413–417, 2009.

[21] Simone Lista, Frank Faltraco, David Prvulovic, and Harald Hampel. Blood and plasma-based proteomic biomarker research in alzheimer's disease. *Progress in neurobiology*, 101:1–17, 2013.

[22] Alberto Serrano-Pozo, Sudeshna Das, and Bradley T Hyman. Apoe and alzheimer's disease: advances in genetics, pathophysiology, and therapeutic approaches. *The Lancet Neurology*, 20(1):68–80, 2021.

[23] Ana-Caroline Raulin, Sydney V Doss, Zachary A Trottier, Tadafumi C Ikezu, Guojun Bu, and Chia-Chen Liu. Apoe in alzheimer's disease: pathophysiology and therapeutic strategies. *Molecular neurodegeneration*, 17(1):72, 2022.

[24] adni. Alzheimer's disease neuroimaging initiative (adni), 2007. Last accessed January 2025.

[25] oasis. Open access series of imaging studies (oasis), 2003. Last accessed 20 january 2025.

[26] miriad. Minimal interval resonance imaging in alzheimer's disease (miriad), 2010. Last accessed January 2025.

[27] aibl. Australian imaging, biomarker, and lifestyle flagship study of ageing (aibl), 2006. Last accessed January 2025.

[28] Ehsan Hosseini-Asl, Georgy Gimel'farb, and Ayman El-Baz. Alzheimer's disease diagnostics by a deeply supervised adaptable 3d convolutional network. *arXiv preprint arXiv:1607.00556*, 2016.

[29] Soheil Esmaeilzadeh, Dimitrios Ioannis Belivanis, Kilian M Pohl, and Ehsan Adeli. End-to-end alzheimer's disease diagnosis and biomarker identification. In *Machine Learning in Medical Imaging: 9th International Workshop, MLMI 2018, Held in Conjunction*

with MICCAI 2018, Granada, Spain, September 16, 2018, Proceedings 9, pages 337–345. Springer, 2018.

[30] David S Cohen, Kristy A Carpenter, Juliet T Jarrell, Xudong Huang, Alzheimer's Disease Neuroimaging Initiative, et al. Deep learning-based classification of multi-categorical alzheimer's disease data. *Current neurobiology*, 10(3):141, 2019.

[31] Marwa Mostafa Abd El Hamid, Mai S Mabrouk, and Yasser MK Omar. Developing an early predictive system for identifying genetic biomarkers associated to alzheimer's disease using machine learning techniques. *Biomedical Engineering: Applications, Basis and Communications*, 31(05):1950040, 2019.

[32] Naimul Mefraz Khan, Nabila Abraham, and Marcia Hon. Transfer learning with intelligent training data selection for prediction of alzheimer's disease. *IEEE Access*, 7:72726–72735, 2019.

[33] Yiming Ding, Jae Ho Sohn, Michael G Kawczynski, Hari Trivedi, Roy Harnish, Nathaniel W Jenkins, Dmytro Lituiev, Timothy P Copeland, Mariam S Aboian, Carina Mari Aparici, et al. A deep learning model to predict a diagnosis of alzheimer disease by using 18f-fdg pet of the brain. *Radiology*, 290(2):456–464, 2019.

[34] Wei Li, Xuefeng Lin, and Xi Chen. Detecting alzheimer's disease based on 4d fmri: An exploration under deep learning framework. *Neurocomputing*, 388:280–287, 2020.

[35] Zhao Fan, Fanyu Xu, Xuedan Qi, Cai Li, and Lili Yao. Classification of alzheimer's disease based on brain mri and machine learning. *Neural Computing and Applications*, 32:1927–1936, 2020.

[36] Ahsan Bin Tufail, Yong-Kui Ma, and Qiu-Na Zhang. Binary classification of alzheimer's disease using smri imaging modality and deep learning. *Journal of digital imaging*, 33(5):1073–1090, 2020.

[37] Haibing Guo and Yongjin Zhang. Resting state fmri and improved deep learning algorithm for earlier detection of alzheimer's disease. *IEEE Access*, 8:115383–115392, 2020.

[38] Wei Feng, Nicholas Van Halm-Lutterodt, Hao Tang, Andrew Mecum, Mohamed Kamal Mesregah, Yuan Ma, Haibin Li, Feng Zhang, Zhiyuan Wu, Erlin Yao, et al. Automated mri-based deep learning model for detection of alzheimer's disease process. *International Journal of Neural Systems*, 30(06):2050032, 2020.

[39] Esther E Bron, Stefan Klein, Janne M Papma, Lize C Jiskoot, Vikram Venkatraghavan, Jara Linders, Pauline Aalten, Peter Paul De Deyn, Geert Jan Biessels, Jurgen AHR Claassen, et al. Cross-cohort generalizability of deep and conventional machine learning for mri-based diagnosis and prediction of alzheimer's disease. *NeuroImage: Clinical*, 31:102712, 2021.

[40] Francisco J Martinez-Murcia, Andres Ortiz, Juan-Manuel Gorriz, Javier Ramirez, and Diego Castillo-Barnes. Studying the manifold structure of alzheimer's disease: a deep learning approach using convolutional autoencoders. *IEEE journal of biomedical and health informatics*, 24(1):17–26, 2019.

[41] Qi Li and Mary Qu Yang. Comparison of machine learning approaches for enhancing alzheimer's disease classification. *PeerJ*, 9:e10549, 2021.

[42] Afreen Khan and Swaleha Zubair. Development of a three tiered cognitive hybrid machine learning algorithm for effective diagnosis of alzheimer's disease. *Journal of King Saud University-Computer and Information Sciences*, 34(10):8000–8018, 2022.

[43] Ruhul Amin Hazarika, Debdatta Kandar, and Arnab Kumar Maji. An experimental analysis of different deep learning based models for alzheimer's disease classification using brain magnetic resonance images. *Journal of King Saud University-Computer and Information Sciences*, 34(10):8576–8598, 2022.

[44] Andrea Loddo, Sara Buttau, and Cecilia Di Ruberto. Deep learning based pipelines for alzheimer's disease diagnosis: a comparative study and a novel deep-ensemble method. *Computers in biology and medicine*, 141:105032, 2022.

[45] Dong Nguyen, Hoang Nguyen, Hong Ong, Hoang Le, Huong Ha, Nguyen Thanh Duc, and Hoan Thanh Ngo. Ensemble learning using traditional machine learning and deep neural network for diagnosis of alzheimer's disease. *IBRO Neuroscience Reports*, 13:255–263, 2022.

[46] M Menagadevi, S Mangai, Nirmala Madian, and D Thiyagarajan. Automated prediction system for alzheimer detection based on deep residual autoencoder and support vector machine. *Optik*, 272:170212, 2023.

[47] Muhammad Tanveer, Ashraf Haroon Rashid, MA Ganaie, Motahar Reza, Imran Razzak, and Kai-Lung Hua. Classification of alzheimer's disease using ensemble of deep

neural networks trained through transfer learning. *IEEE Journal of Biomedical and Health Informatics*, 26(4):1453–1463, 2021.

[48] Abdul Rehman, Myung-Kyu Yi, Abdul Majeed, and Seong Oun Hwang. Early diagnosis of alzheimer's disease using 18f-fdg pet with soften latent representation. *IEEE Access*, 2024.

[49] Jyoti Islam and Yanqing Zhang. Brain mri analysis for alzheimer's disease diagnosis using an ensemble system of deep convolutional neural networks. *Brain informatics*, 5:1–14, 2018.

[50] Shui-Hua Wang, Preetha Phillips, Yuxiu Sui, Bin Liu, Ming Yang, and Hong Cheng. Classification of alzheimer's disease based on eight-layer convolutional neural network with leaky rectified linear unit and max pooling. *Journal of medical systems*, 42:1–11, 2018.

[51] Diego Castillo-Barnes, Li Su, Javier Ramírez, Diego Salas-Gonzalez, Francisco J Martinez-Murcia, Ignacio A Illan, Fermin Segovia, Andres Ortiz, Carlos Cruchaga, Martin R Farlow, et al. Autosomal dominantly inherited alzheimer disease: Analysis of genetic subgroups by machine learning. *Information Fusion*, 58:153–167, 2020.

[52] Rashmi Kumari, Akriti Nigam, and Shashank Pushkar. Machine learning technique for early detection of alzheimer's disease. *Microsystem Technologies*, 26(12):3935–3944, 2020.

[53] Fanar EK Al-Khuzaie, Oguz Bayat, and Adil D Duru. [retracted] diagnosis of alzheimer disease using 2d mri slices by convolutional neural network. *Applied Bionics and Biomechanics*, 2021(1):6690539, 2021.

[54] VP Subramanyam Rallabandi and Krishnamoorthy Seetharaman. Deep learning-based classification of healthy aging controls, mild cognitive impairment and alzheimer's disease using fusion of mri-pet imaging. *Biomedical Signal Processing and Control*, 80:104312, 2023.

[55] Romoke Grace Akindele, Samuel Adebayo, Paul Shekonya Kanda, and Ming Yu. Alzhinet: Traversing from 2dcnn to 3dcnn, towards early detection and diagnosis of alzheimer's disease. *arXiv preprint arXiv:2410.02714*, 2024.

[56] Nitika Goenka, Akhilesh Kumar Sharma, Shamik Tiwari, Nagendra Singh, Vyom Yadav, Srikanth Prabhu, and Krishnaraj Chadaga. A regularized volumetric convnet based alzheimer detection using t1-weighted mri images. *Cogent Engineering*, 11(1):2314872, 2024.

[57] Damiano Archetti, Vikram Venkatraghavan, Béla Weiss, Pierrick Bourgeat, Tibor Auer, Zoltán Vidnyánszky, Stanley Durrleman, Wiesje M van der Flier, Frederik Barkhof, Daniel C Alexander, et al. A machine learning model to harmonize volumetric brain mri data for quantitative neuroradiologic assessment of alzheimer disease. *Radiology: Artificial Intelligence*, 7(1):e240030, 2024.

[58] Ibrahim Almubark, Lin-Ching Chang, Kyle F Shattuck, Thanh Nguyen, Raymond Scott Turner, and Xiong Jiang. A 5-min cognitive task with deep learning accurately detects early alzheimer's disease. *Frontiers in aging neuroscience*, 12:603179, 2020.

[59] M Rohini and D Surendran. Toward alzheimer's disease classification through machine learning. *Soft Computing*, 25(4):2589–2597, 2021.

[60] Nitin Seshadri, Serena McCalla, and Rishi Shah. Early prediction of alzheimer's disease with a multimodal multitask deep learning model. *Journal of Student Research*, 10(1), 2021.

[61] Afreen Khan and Swaleha Zubair. An improved multi-modal based machine learning approach for the prognosis of alzheimer's disease. *Journal of King Saud University-Computer and Information Sciences*, 34(6):2688–2706, 2022.

[62] Johannes Rieke, Fabian Eitel, Martin Weygandt, John-Dylan Haynes, and Kerstin Ritter. Visualizing convolutional networks for mri-based diagnosis of alzheimer's disease. In *Understanding and Interpreting Machine Learning in Medical Image Computing Applications: First International Workshops, MLCN 2018, DLF 2018, and iMIMIC 2018, Held in Conjunction with MICCAI 2018, Granada, Spain, September 16-20, 2018, Proceedings 1*, pages 24–31. Springer, 2018.

[63] Kanghan Oh, Young-Chul Chung, Ko Woon Kim, Woo-Sung Kim, and Il-Seok Oh. Classification and visualization of alzheimer's disease using volumetric convolutional neural network and transfer learning. *Scientific Reports*, 9(1):18150, 2019.

[64] Arjun Punjabi, Adam Martersteck, Yanran Wang, Todd B Parrish, Aggelos K Katsaggelos, and Alzheimer's Disease Neuroimaging Initiative. Neuroimaging modality fusion in alzheimer's classification using convolutional neural networks. *PloS one*, 14(12):e0225759, 2019.

[65] Chiyu Feng, Ahmed Elazab, Peng Yang, Tianfu Wang, Feng Zhou, Huoyou Hu, Xiaohua Xiao, and Baiying Lei. Deep learning framework for alzheimer's disease diagnosis via 3d-cnn and fsbi-lstm. *IEEE Access*, 7:63605–63618, 2019.

[66] Saman Sarraf and Ghassem Tofighi. Classification of alzheimer's disease using fmri data and deep learning convolutional neural networks. *arXiv preprint arXiv:1603.08631*, 2016.

[67] Atif Mehmood, Muazzam Maqsood, Muzaffar Bashir, and Yang Shuyuan. A deep siamese convolution neural network for multi-class classification of alzheimer disease. *Brain sciences*, 10(2):84, 2020.

[68] Farheen Ramzan, Muhammad Usman Ghani Khan, Asim Rehmat, Sajid Iqbal, Tanzila Saba, Amjad Rehman, and Zahid Mehmood. A deep learning approach for automated diagnosis and multi-class classification of alzheimer's disease stages using resting-state fmri and residual neural networks. *Journal of medical systems*, 44:1–16, 2020.

[69] Taeho Jo, Kwangsik Nho, Shannon L Risacher, Andrew J Saykin, and Alzheimer's Neuroimaging Initiative. Deep learning detection of informative features in tau pet for alzheimer's disease classification. *BMC bioinformatics*, 21:1–13, 2020.

[70] Manhua Liu, Fan Li, Hao Yan, Kundong Wang, Yixin Ma, Li Shen, Mingqing Xu, Alzheimer's Disease Neuroimaging Initiative, et al. A multi-model deep convolutional neural network for automatic hippocampus segmentation and classification in alzheimer's disease. *Neuroimage*, 208:116459, 2020.

[71] Nicholas Chedid, Judie Tabbal, Aya Kabbara, Sahar Allouch, and Mahmoud Hassan. The development of an automated machine learning pipeline for the detection of alzheimer's disease. *Scientific Reports*, 12(1):18137, 2022.

[72] Huan Lao, Hongfei Jia, and Zhenhai Chen. Diagnosis of alzheimer's disease based on structural graph convolutional neural networks. In *Proceedings of the ACM Turing Award Celebration Conference-China 2024*, pages 148–152, 2024.

[73] Chang-Min Kim and Woobeom Lee. Classification of alzheimer's disease using ensemble convolutional neural network with lfa algorithm. *IEEE Access*, 2023.

[74] Seung Kyu Kim, Quan Anh Duong, and Jin Kyu Gahm. Multimodal 3d deep learning for early diagnosis of alzheimer's disease. *IEEE Access*, 2024.

[75] Mahir Kaya and Yasemin Çetin-Kaya. A novel deep learning architecture optimization for multiclass classification of alzheimer's disease level. *IEEE Access*, 2024.

[76] Doaa Ahmed Arafa, Hossam El-Din Moustafa, Hesham A Ali, Amr MT Ali-Eldin, and Sabry F Saraya. A deep learning framework for early diagnosis of alzheimer's disease on mri images. *Multimedia Tools and Applications*, 83(2):3767–3799, 2024.

[77] Madhav Thambisetty, Abdul Hye, Catherine Foy, Eileen Daly, Amanda Glover, Allison Cooper, Andrew Simmons, Declan Murphy, and Simon Lovestone. Proteome-based identification of plasma proteins associated with hippocampal metabolism in early alzheimer's disease. *Journal of neurology*, 255:1712–1720, 2008.

[78] Sid E O'Bryant, Guanghua Xiao, Robert Barber, Joan Reisch, James Hall, C Munro Cullum, Rachelle Doody, Thomas Fairchild, Perrie Adams, Kirk Wilhelmsen, et al. A blood-based algorithm for the detection of alzheimer's disease. *Dementia and geriatric cognitive disorders*, 32(1):55–62, 2011.

[79] Christoph Laske, Thomas Leyhe, Elke Stransky, Nadine Hoffmann, Andreas J Fallgatter, and Janko Dietzsch. Identification of a blood-based biomarker panel for classification of alzheimer's disease. *International Journal of Neuropsychopharmacology*, 14(9):1147–1155, 2011.

[80] Daniel A Llano, Viswanath Devanarayan, Adam J Simon, Alzheimer's Disease Neuroimaging Initiative (ADNI, et al. Evaluation of plasma proteomic data for alzheimer disease state classification and for the prediction of progression from mild cognitive impairment to alzheimer disease. *Alzheimer Disease & Associated Disorders*, 27(3):233–243, 2013.

[81] Liang-Hao Guo, Panagiotis Alexopoulos, Stefan Wagenpfeil, Alexander Kurz, Robert Perneczky, Alzheimer's Disease Neuroimaging Initiative, et al. Plasma proteomics for the identification of alzheimer disease. *Alzheimer Disease & Associated Disorders*, 27(4):337–342, 2013.

[82] Angharad R Morgan, Samuel Touchard, Claire Leckey, Caroline O'Hagan, Alejo J Nevado-Holgado, Frederik Barkhof, Lars Bertram, Olivier Blin, Isabelle Bos, Valerija Dobricic, et al. Inflammatory biomarkers in alzheimer's disease plasma. *Alzheimer's & dementia*, 15(6):776–787, 2019.

[83] Daniel Stamate, Min Kim, Petroula Proitsi, Sarah Westwood, Alison Baird, Alejo Nevado-Holgado, Abdul Hye, Isabelle Bos, Stephanie JB Vos, Rik Vandenberghe, et al. A metabolite-based machine learning approach to diagnose alzheimer-type dementia in blood: Results from the european medical information framework for alzheimer disease biomarker discovery cohort. *Alzheimer's & Dementia: Translational Research & Clinical Interventions*, 5(1):933–938, 2019.

[84] Chima S Eke, Emmanuel Jammeh, Xinzhong Li, Camille Carroll, Stephen Pearson, and Emmanuel Ifeachor. Early detection of alzheimer's disease with blood plasma proteins using support vector machines. *IEEE journal of biomedical and health informatics*, 25(1):218–226, 2020.

[85] Xuemei Zhao, John Kang, Vladimir Svetnik, Donald Warden, Gordon Wilcock, A David Smith, Mary J Savage, and Omar F Laterza. A machine learning approach to identify a circulating microrna signature for alzheimer disease. *The journal of applied laboratory medicine*, 5(1):15–28, 2020.

[86] S Karthik and M Sudha. Diagnostic gene biomarker selection for alzheimer's classification using machine learning. *Int. J. Innov. Technol. Explor. Eng*, 8:12, 2019.

[87] Abhibhav Sharma and Pinki Dey. A machine learning approach to unmask novel gene signatures and prediction of alzheimer's disease within different brain regions. *Genomics*, 113(4):1778–1789, 2021.

[88] Jessica Binder, Oleg Ursu, Cristian Bologa, Shanya Jiang, Nicole Maphis, Somayeh Dadras, Devon Chisholm, Jason Weick, Orrin Myers, Praveen Kumar, et al. Machine learning prediction and tau-based screening identifies potential alzheimer's disease genes relevant to immunity. *Communications Biology*, 5(1):125, 2022.

[89] Nivedhitha Mahendran and Durai Raj Vincent PM. A deep learning framework with an embedded-based feature selection approach for the early detection of the alzheimer's disease. *Computers in Biology and Medicine*, 141:105056, 2022.

[90] Franz Müller-Spahn. Behavioral disturbances in dementia. *Dialogues in clinical neuroscience*, 5(1):49–59, 2003.

[91] Reisa A Sperling, Paul S Aisen, Laurel A Beckett, David A Bennett, Suzanne Craft, Anne M Fagan, Takeshi Iwatsubo, Clifford R Jack Jr, Jeffrey Kaye, Thomas J Montine, et al. Toward defining the preclinical stages of alzheimer's disease: Recommendations from the national institute on aging-alzheimer's association workgroups on diagnostic guidelines for alzheimer's disease. *Alzheimer's & dementia*, 7(3):280–292, 2011.

[92] L Bäckman, Sari Jones, A-K Berger, Erika Jonsson Laukka, and BJ Small. Multiple cognitive deficits during the transition to alzheimer's disease. *Journal of internal medicine*, 256(3):195–204, 2004.

[93] I Álvarez Illán, JM Górriz, Javier Ramírez, Diego Salas-Gonzalez, Míriam López, Fermín Segovia, Pablo Padilla, and Carlos García Puntonet. Projecting independent components of spect images for computer aided diagnosis of alzheimer's disease. *Pattern Recognition Letters*, 31(11):1342–1347, 2010.

[94] Tingting Ye, Chen Zu, Biao Jie, Dinggang Shen, Daoqiang Zhang, and Alzheimer's Disease Neuroimaging Initiative. Discriminative multi-task feature selection for multi-modality classification of alzheimer's disease. *Brain imaging and behavior*, 10:739–749, 2016.

[95] Yong Liang, Cheng Liu, Xin-Ze Luan, Kwong-Sak Leung, Tak-Ming Chan, Zong-Ben Xu, and Hai Zhang. Sparse logistic regression with a l 1/2 penalty for gene selection in cancer classification. *BMC bioinformatics*, 14:1–12, 2013.

[96] Rui Wang, Naihua Xiu, and Chao Zhang. Greedy projected gradient-newton method for sparse logistic regression. *IEEE transactions on neural networks and learning systems*, 31(2):527–538, 2019.

[97] Marko Debeljak and Sašo Džeroski. Decision trees in ecological modelling. In *Modelling complex ecological dynamics: An introduction into ecological modelling for students, teachers & scientists*, pages 197–209. Springer, 2011.

[98] Leo Breiman. Random forests. *Machine learning*, 45:5–32, 2001.

[99] Jehad Ali, Rehanullah Khan, Nasir Ahmad, and Imran Maqsood. Random forests and decision trees. *International Journal of Computer Science Issues (IJCSI)*, 9(5):272, 2012.

[100] Rashmi Agrawal. K-nearest neighbor for uncertain data. *International Journal of Computer Applications*, 105(11):13–16, 2014.

[101] Akanksha Singh Thakur and Namrata Sahayam. Speech recognition using euclidean distance. *International Journal of Emerging Technology and Advanced Engineering*, 3(3):587–590, 2013.

[102] William S Noble. What is a support vector machine? *Nature biotechnology*, 24(12):1565–1567, 2006.

[103] Christopher M Bishop and Nasser M Nasrabadi. *Pattern recognition and machine learning*, volume 4. Springer, 2006.

[104] SA Sushma and Keerthan Kumar TG. Comparative study of naive bayes, gaussian naive bayes classifier and decision tree algorithms for prediction of heart diseases. *International Journal for Research in Applied Science and Engineering Technology*, 9(3):475–486, 2021.

[105] Shaohua Wan, Yan Liang, Yin Zhang, and Mohsen Guizani. Deep multi-layer perceptron classifier for behavior analysis to estimate parkinson's disease severity using smartphones. *IEEE Access*, 6:36825–36833, 2018.

[106] Oluwatobi Joshua Afolabi, Gugulethu P Mabuza-Hocquet, Fulufhelo V Nelwamondo, and Babu Sena Paul. The use of u-net lite and extreme gradient boost (xgb) for glaucoma detection. *IEEE access*, 9:47411–47424, 2021.

[107] Candice Bentéjac, Anna Csörgő, and Gonzalo Martínez-Muñoz. A comparative analysis of gradient boosting algorithms. *Artificial Intelligence Review*, 54:1937–1967, 2021.

[108] Chen-Chen Tan, Jin-Tai Yu, and Lan Tan. Biomarkers for preclinical alzheimer's disease. *Journal of Alzheimer's Disease*, 42(4):1051–1069, 2014.

[109] Anil Kumar, Jaskirat Sidhu, Forshing Lui, and Jack W Tsao. Alzheimer disease. In *StatPearls [internet]*. StatPearls Publishing, 2024.

[110] Vincent Planche, Vincent Bouteloup, Isabelle Pellegrin, Jean-Francois Mangin, Bruno Dubois, Pierre-Jean Ousset, Florence Pasquier, Frédéric Blanc, Claire Paquet, Olivier Hanon, et al. Validity and performance of blood biomarkers for alzheimer disease to predict dementia risk in a large clinic-based cohort. *Neurology*, 100(5):e473–e484, 2023.

[111] Simone Lista, Sid E O'Bryant, Kaj Blennow, Bruno Dubois, Jacques Hugon, Henrik Zetterberg, and Harald Hampel. Biomarkers in sporadic and familial alzheimer's disease. *Journal of Alzheimer's Disease*, 47(2):291–317, 2015.

[112] Kim Henriksen, Sid E O'Bryant, Harald Hampel, John Q Trojanowski, Thomas J Montine, Andreas Jeromin, Kaj Blennow, Anders Lönneborg, Tony Wyss-Coray, Holly Soares, et al. The future of blood-based biomarkers for alzheimer's disease. *Alzheimer's & dementia*, 10(1):115–131, 2014.

[113] Philine Schneider, Harald Hampel, and Katharina Buerger. Biological marker candidates of alzheimer's disease in blood, plasma, and serum. *CNS neuroscience & therapeutics*, 15(4):358–374, 2009.

[114] Madhav Thambisetty and Simon Lovestone. Blood-based biomarkers of alzheimer's disease: challenging but feasible. *Biomarkers in medicine*, 4(1):65–79, 2010.

[115] Anthony J Myles, Robert N Feudale, Yang Liu, Nathaniel A Woody, and Steven D Brown. An introduction to decision tree modeling. *Journal of Chemometrics: A Journal of the Chemometrics Society*, 18(6):275–285, 2004.

[116] Antonio Ramón, Ana Maria Torres, Javier Milara, Joaquín Cascón, Pilar Blasco, and Jorge Mateo. extreme gradient boosting-based method to classify patients with covid-19. *Journal of Investigative Medicine*, 70(7):1472–1480, 2022.

[117] De-Cheng Feng, Zhen-Tao Liu, Xiao-Dan Wang, Yin Chen, Jia-Qi Chang, Dong-Fang Wei, and Zhong-Ming Jiang. Machine learning-based compressive strength prediction for concrete: An adaptive boosting approach. *Construction and Building Materials*, 230:117000, 2020.

[118] Habbiburr Rehman, Ting Fang Alvin Ang, Qiushan Tao, Arielle Lauren Espenilla, Rhoda Au, Lindsay A Farrer, Xiaoling Zhang, Wei Qiao Qiu, and Alzheimer's Disease Neuroimaging Initiative. Comparison of commonly measured plasma and cerebrospinal fluid proteins and their significance for the characterization of cognitive impairment status. *Journal of Alzheimer's Disease*, 97(2):621–633, 2024.

[119] Tianchi Zhuang, Yingqi Yang, Haili Ren, Haoxiang Zhang, Chang Gao, Shen Chen, Jiemiao Shen, Minghui Ji, Yan Cui, Alzheimer's Disease Neuroimaging Initiative, et al. Novel plasma protein biomarkers: A time-dependent predictive model for alzheimer's disease. *Archives of Gerontology and Geriatrics*, 129:105650, 2025.

[120] Zakaria Mokadem, Mohamed Djerioui, Bilal Attallah, and Youcef Brik. Identification of plasma proteins associated with alzheimer's disease using feature selection techniques and machine learning algorithms. *Science, Engineering and Technology*, 5(1), 2025.

[121] J. J. Duga, W. H. Fisher, R. W. Buxhaum, A. R. Rosenfield, A. R. Buhr, E. J. Honton, and S. C. McMillan. *The economic effects of fracture in the United States*. NBS Special Publication, USA, 1983.

[122] G. R. Irwin. Onset of fast crack propagation in high strength steel and aluminum alloys. Technical report, Naval Research Laboratories Report 4763, 1956.

[123] G. R. Irwin. Analysis of stresses and strains near the end of a crack traversing a plate. *Journal of Applied Mechanics*, pages 361–364, 1957.

[124] G. R. Irwin. Plastic zone near a crack and fracture toughness. In *Proceedings of Sagamore Research Conference*, 1960.

[125] D. E. Abdelli. *Modélisation par les volumes finis d'un problème de contrôle non destructif de forme complexe*. Magister manuscript, Université Mohamed Kheider de Biskra (Algérie), 2014.

[126] Roger Peyret and Thomas D Taylor. *Computational Methods for Fluid Flow*, chapter 7, 14. Springer-Verlag, New York, 2 edition, 1983.

[127] Rada Mihalcea. Knowledge-based methods for WSD. In Eneko Agirre and Philip Edmonds, editors, *Word Sense Disambiguation: Algorithms and Applications*, pages 107–132. Springer, Dordrecht, the Netherlands, 2006.

[128] Yu Wang, Xi Liu, and Chongchong Yu. Assisted diagnosis of alzheimer's disease based on deep learning and multimodal feature fusion. *Complexity*, 2021(1):6626728, 2021.

[129] KR Kruthika, HD Maheshappa, Alzheimer's Disease Neuroimaging Initiative, et al. Multistage classifier-based approach for alzheimer's disease prediction and retrieval. *Informatics in Medicine Unlocked*, 14:34–42, 2019.

[130] Janani Venugopalan, Li Tong, Hamid Reza Hassanzadeh, and May D Wang. Multimodal deep learning models for early detection of alzheimer's disease stage. *Scientific reports*, 11(1):3254, 2021.

[131] Ruoxuan Cui, Manhua Liu, and Gang Li. Longitudinal analysis for alzheimer's disease diagnosis using rnn. In *2018 IEEE 15th International Symposium on Biomedical Imaging (ISBI 2018)*, pages 1398–1401. IEEE, 2018.

[132] Nguyen Thanh Duc, Seungjun Ryu, Muhammad Naveed Iqbal Qureshi, Min Choi, Kun Ho Lee, and Boreom Lee. 3d-deep learning based automatic diagnosis of alzheimer's disease with joint mmse prediction using resting-state fmri. *Neuroinformatics*, 18:71–86, 2020.

[133] Sandip Ray, Markus Britschgi, Charles Herbert, Yoshiko Takeda-Uchimura, Adam Boxer, Kaj Blennow, Leah F Friedman, Douglas R Galasko, Marek Jutel, Anna Karydas, et al. Classification and prediction of clinical alzheimer's diagnosis based on plasma signaling proteins. *Nature medicine*, 13(11):1359–1362, 2007.

[134] K Kantarci, SD Weigand, SA Przybelski, MM Shiung, Jennifer Lynn Whitwell, S Negash, David S Knopman, Bradley F Boeve, PC O'Brien, Ronald Carl Petersen, et al. Risk of dementia in mci: combined effect of cerebrovascular disease, volumetric mri, and 1h mrs. *Neurology*, 72(17):1519–1525, 2009.

[135] Ahmed Rafik Zouaoui, Heythem Bentahar, Mohamed Djeriuoi, Zakaria Mokadem, and Houssam Eddine Bentahar. Machine learning and deep learning techniques for alzheimer's disease prediction using csf and plasma biomarkers. In *2023 International Conference on Networking and Advanced Systems (ICNAS)*, pages 1–6. IEEE, 2023.

[136] Jerome A Yesavage and Javaid I Sheikh. 9/geriatric depression scale (gds) recent evidence and development of a shorter version. *Clinical gerontologist*, 5(1-2):165–173, 1986.

[137] Sergey Korolev, Amir Safiullin, Mikhail Belyaev, and Yulia Dodonova. Residual and plain convolutional neural networks for 3d brain mri classification. In *2017 IEEE 14th international symposium on biomedical imaging (ISBI 2017)*, pages 835–838. IEEE, 2017.

Appendix

List of plasma proteins

N°	Plasma protiens
1	Alpha-1-Microglobulin (A1Micro) (ug/ml)
2	Alpha-2-Macroglobulin (A2Macro) (mg/mL)
3	Alpha-1-Antichymotrypsin (AACT) (ug/ml)
4	Alpha-1-Antitrypsin (AAT) (mg/mL)
5	Angiotensin-Converting Enzyme (ACE) (ng/ml)
6	Adiponectin (ug/mL)
7	Alpha-Fetoprotein (AFP) (ng/mL)
8	Agouti-Related Protein (AGRP) (pg/mL)
9	Angiopoietin-2 (ANG-2) (ng/mL)
10	Angiotensinogen (ng/mL)
11	Apolipoprotein A-I (Apo A-I) (mg/mL)
12	Apolipoprotein A-II (Apo A-II) (ng/ml)
13	Apolipoprotein A-IV (Apo A-IV) (ug/ml)
14	Apolipoprotein B (Apo B) (ug/ml)
15	Apolipoprotein C-I (Apo C-I) (ng/ml)
16	Apolipoprotein C-III (Apo C-III) (ug/mL)
17	Apolipoprotein D (Apo D) (ug/ml)
18	Apolipoprotein E (Apo E) (ug/ml)
19	Apolipoprotein H (Apo H) (ug/mL)
20	AXL Receptor Tyrosine Kinase (AXL) (ng/mL)
21	Beta-2-Microglobulin (B2M) (ug/mL)
22	Brain-Derived Neurotrophic Factor (BDNF) (ng/mL)

23	B Lymphocyte Chemoattractant (BLC) (pg/ml)
24	Bone Morphogenetic Protein 6 (BMP-6) (ng/mL)
25	Brain Natriuretic Peptide (BNP) (pg/ml)
26	Betacellulin (BTC) (pg/mL)
27	Complement C3 (C3) (mg/mL)
28	Cancer Antigen 19-9 (CA-19-9) (U/mL)
29	Calcitonin (pg/mL)
30	CD 40 antigen (CD40) (ng/mL)
31	CD40 Ligand (CD40-L) (ng/mL)
32	CD5 (CD5L) (ng/ml)
33	Carcinoembryonic Antigen (CEA) (ng/mL)
34	Chromogranin-A (CgA) (ng/mL)
35	Creatine Kinase-MB (CK-MB) (ng/mL)
36	Clusterin (CLU) (ug/ml)
37	Ciliary Neurotrophic Factor (CNTF) (pg/mL)
38	Complement Factor H (ug/ml)
39	Cortisol (Cortisol) (ng/ml)
40	C-peptide (ng/ml)
41	C-Reactive Protein (CRP) (ug/mL)
42	Cystatin-C (ng/ml)
43	Epidermal Growth Factor (EGF) (pg/mL)
44	Epidermal Growth Factor Receptor (EGFR) (ng/mL)
45	Epithelial-Derived Neutrophil-Activating (ng/mL)
46	Eotaxin-1 (pg/mL)
47	Eotaxin-3 (pg/mL)
48	E-Selectin (ng/mL)
49	Fatty Acid-Binding Protein- heart (FABP (ng/mL)
50	Factor VII (ng/mL)
51	FASLG Receptor (FAS) (ng/mL)
52	Fas Ligand (FasL) (pg/mL)
53	Fetuin-A (ug/ml)
54	Fibroblast Growth Factor 4 (FGF-4) (pg/mL)
55	Fibrinogen (mg/mL)
56	Ferritin (FRTN) (ng/mL)

57	Follicle-Stimulating Hormone (FSH) (mIU/mL)
58	Growth Hormone (GH) (ng/mL)
59	Growth-Regulated alpha protein (GRO-alph (pg/mL)
60	Glutathione S-Transferase alpha (GST-alp (ng/ml)
61	Haptoglobin (mg/mL)
62	Heparin-Binding EGF-Like Growth Factor ((pg/mL)
63	Chemokine CC-4 (HCC-4) (ng/mL)
64	Hepatocyte Growth Factor (HGF) (ng/mL)
65	T Lymphocyte-Secreted Protein I-309 (I-3 (pg/mL)
66	Intercellular Adhesion Molecule 1 (ICAM- (ng/mL)
67	Immunoglobulin A (IgA) (mg/mL)
68	Immunoglobulin E (IgE) (ng/mL)
69	Insulin-like Growth Factor-Binding Prote (IGFB)(ng/mL)
70	Immunoglobulin M (IGM) (mg/mL)
71	Interleukin-13 (IL-13) (pg/mL)
72	Interleukin-16 (IL-16) (pg/mL)
73	Interleukin-18 (IL-18) (pg/mL)
74	Interleukin-3 (IL-3) (ng/mL)
75	Interleukin-6 receptor (IL-6r) (ng/mL)
76	Interleukin-8 (IL-8) (pg/mL)
77	Insulin (uIU/mL)
78	Interferon gamma Induced Protein 10 (IFN-Gamma) (IP- (pg/ml)
79	Kidney Injury Molecule-1 (KIM-1) (ng/ml)
80	Leptin (ng/mL)
81	Luteinizing Hormone (LH) (mIU/mL)
82	Apolipoprotein(a) (Lp(a)) (ug/mL)
83	Monocyte Chemotactic Protein 1 (MCP-1) (pg/mL)
84	Monocyte Chemotactic Protein 2 (MCP-2) (pg/ml)
85	Monocyte Chemotactic Protein 3 (MCP-3) (pg/mL)
86	Monocyte Chemotactic Protein 4 (MCP-4) (pg/ml)
87	Macrophage Colony-Stimulating Factor 1 ((ng/mL)
88	Macrophage-Derived Chemokine (MDC) (pg/mL)
89	Macrophage Migration Inhibitory Factor (ng/mL)
90	Monokine Induced by Gamma Interferon (MIGI)(pg/ml)

91	Macrophage Inflammatory Protein-1 alpha (MIP-1 alpha)(pg/mL)
92	Macrophage Inflammatory Protein-1 beta (MIP-1 beta)(pg/mL)
93	Macrophage Inflammatory Protein-3 alpha (MIP-3 alpha) (pg/ml)
94	Matrix Metalloproteinase-1 (MMP-1) (ng/ml)
95	Matrix Metalloproteinase-10 (MMP-10) (ng/ml)
96	Matrix Metalloproteinase-2 (MMP-2) (ng/mL)
97	Matrix Metalloproteinase-7 (MMP-7) (ng/ml)
98	Matrix Metalloproteinase-9 (MMP-9) (ng/mL)
99	Matrix Metalloproteinase-9- total (MMP-9 (ng/ml)
100	Myeloid Progenitor Inhibitory Factor 1 (MPIF) (ng/mL)
101	Myeloperoxidase (MPO) (ng/mL)
102	Myoglobin (ng/mL)
103	Neutrophil Gelatinase-Associated Lipocal (NGL) (ng/ml)
104	Neuronal Cell Adhesion Molecule (Nr-CAM) (ng/mL)
105	Osteopontin (ng/ml)
106	Plasminogen Activator Inhibitor 1 (PAI-1 (ng/mL)
107	Prostatic Acid Phosphatase (PAP) (ng/mL)
108	Pregnancy-Associated Plasma Protein A (P (mIU/mL)
109	Pulmonary and Activation-Regulated Chemo (ng/mL)
110	Platelet-Derived Growth Factor BB (PDGF- (pg/ml)
111	Placenta Growth Factor (PLGF) (pg/ml)
112	Pancreatic Polypeptide (PPP) (pg/ml)
113	Prolactin (PRL) (ng/ml)
114	Proinsulin- Intact (pM)
115	Proinsulin- Total (pM)
116	Peptide YY (PYY) (pg/mL)
117	Receptor for advanced glycosylation end (RAGE)(ng/mL)
118	T-Cell-Specific Protein RANTES (RANTES) (ng/mL)
119	Resistin (ng/ml)
120	Serum Amyloid P-Component (SAP) (ug/mL)
121	Stem Cell Factor (SCF) (pg/mL)
122	Serum Glutamic Oxaloacetic Transaminase(SGOT) (ug/mL)
123	Sex Hormone-Binding Globulin (SHBG) (nmol/L)
124	Superoxide Dismutase 1- Soluble (SOD-1) (ng/mL)

125	Sortilin (ng/mL)
126	Thyroxine-Binding Globulin (TBG) (ug/mL)
127	Thymus-Expressed Chemokine (TECK) (ng/mL)
128	Testosterone- Total (ng/ml)
129	Trefoil Factor 3 (TFF3) (ug/ml)
130	Tamm-Horsfall Urinary Glycoprotein (THP) (ug/ml)
131	Thrombospondin-1 (ng/mL)
132	Tissue Inhibitor of Metalloproteinases 1 (TIMP-1)(ng/mL)
133	Thrombomodulin (TM) (ng/ml)
134	Tenascin-C (TN-C) (ng/mL)
135	Tumor Necrosis Factor alpha (TNF-alpha) (pg/mL)
136	Tumor Necrosis Factor Receptor-Like 2 (T (ng/mL)
137	Thrombopoietin (ng/mL)
138	TNF-Related Apoptosis-Inducing Ligand Re (ng/mL)
139	Serotransferrin (Transferrin) (mg/dl)
140	Thyroid-Stimulating Hormone (TSH) (uIU/mL)
141	Transthyretin (TTR) (mg/dl)
142	Vascular Cell Adhesion Molecule-1 (VCAM- (ng/mL)
143	Vascular Endothelial Growth Factor (VEGF (pg/mL)
144	Vitronectin (ug/ml)
145	Vitamin K-Dependent Protein S (VKDPS) (ug/ml)
146	von Willebrand Factor (vWF) (ug/mL)]